Organizational Capital Destruction and Post-COVID Inflation*

Lukasz A. Drozd
Federal Reserve Bank of Philadelphia
lukasz.drozd@phil.frb.org

Marina M. Tavares
International Monetary Fund
mtavares@imf.org

October 2026

Abstract

Restoring employment rapidly can be costly even while aggregate employment remains below its pre-recession level. Producers must recruit and train relative to the workforces they retained, and uneven depletion concentrates these costs in particular parts of the production network. We argue that this interaction between recovery speed and inherited capacity helps explain why inflation surged after COVID-19 but remained subdued after the Great Recession. Consistent with this friction, predetermined occupational COVID-19 exposure predicts employment contraction and higher supplier prices alongside weaker production, with an input–output decomposition locating much of this initial pressure in a residual beyond measured labor and material costs. When embedded in a nonlinear production-network model—disciplined by microeconomic hiring-cost estimates—and conditional on the inferred demand and productivity paths, workforce rebuilding accounts for about two-thirds of cumulative above-trend inflation in our industry price index through 2022. Unevenness amplifies this effect: redistributing inherited capacity evenly within producer groups reduces the rebuilding contribution by 57 percent. The distribution of workforce losses and the pace of restoration therefore shape the inflation–employment relationship.

JEL Codes: E31, E32, E24, D57, J63, L16
Keywords: Inflation, organizational capital, workforce rebuilding, production networks, hiring costs

*We thank Roc Armenter, Jonas Arias, Giancarlo Corsetti, Domenico Giannone, João Gomes, Urban Jermann, Anna Lipińska, Makoto Nakajima, and Elisa Rubbo for helpful comments and discussions. We are particularly grateful to Pauline Carry for her advice on the empirical strategies. We thank Claire Jellison for research assistance at the early stages of the project. The views expressed herein are those of the authors and do not necessarily represent the views of the IMF, the Federal Reserve Bank of Philadelphia, the Federal Reserve System, or their respective management and Executive Boards.

1 Introduction

After COVID-19, U.S. inflation surged while aggregate employment was still recovering, and much of the initial price increase preceded comparable pressure from measured unit labor costs. Where did inflation come from if not from wage pressure?

This paper proposes an answer: amid an unusually rapid rebound of demand and a labor market overheated by the speed of the recovery, producers had to recruit and train relative to the workforces they retained, and the largely nonwage costs of hiring rose. Because measured labor costs do not fully capture these outlays, the initial price increases appeared empirically in producers' gross margins. The rise and subsequent reversal of measured productivity, associated with the sequence of layoffs and rapid rehiring, prolonged this initial impulse and shifted unit-cost pressure into 2022, the year inflation peaked. Higher energy prices added to inflation that year, while real-estate and other exogenous price shocks contributed beyond the peak. Our empirical section links this underlying pressure to the uneven contraction of 2020, showing that price increases concentrated in the supplier networks most exposed to the pandemic. As our quantitative framework shows, unevenness within producer groups more than doubles the aggregate inflationary contribution of rebuilding costs, with input–output linkages propagating these local cost pressures throughout the economy.

Figure 1 illustrates the speed and unevenness of the COVID-19 recovery, using the Great Recession as a benchmark. While both contractions produced substantial and comparably dispersed employment losses, their recoveries differed sharply. Within just two years, employment gains in industries that initially contracted amounted to roughly 92 percent of their pandemic losses, compared with only 32 percent after the Great Recession (Panel A). Furthermore, the variance of recovery employment growth was about two and a half times as large after COVID-19, driven largely by industries expanding faster than average (Panel B).[1] The subsequent price dynamics point to a major disruption of the production network: the dispersion of price growth across industries rose during reopening and stayed high through the 2022 inflation peak. In comparison, the Great Recession's recovery shows no comparable sustained increase

[1] Contraction-period employment-growth variances are 14.7 and 14.1 for COVID and the Great Recession, respectively, in the same display units. The recovery comparison concerns absolute dispersion, not dispersion relative to the mean expansion rate.

relative to its pre-recession benchmark (Panels C–D). Our reading of these data is that an explanation of the sudden inflation surge requires three key features: a mechanism linking nonwage costs to the speed of recovery; a connection to uneven capacity destruction and network propagation; and an accounting of the boom–bust productivity dynamics that initially cushioned prices from wage growth.

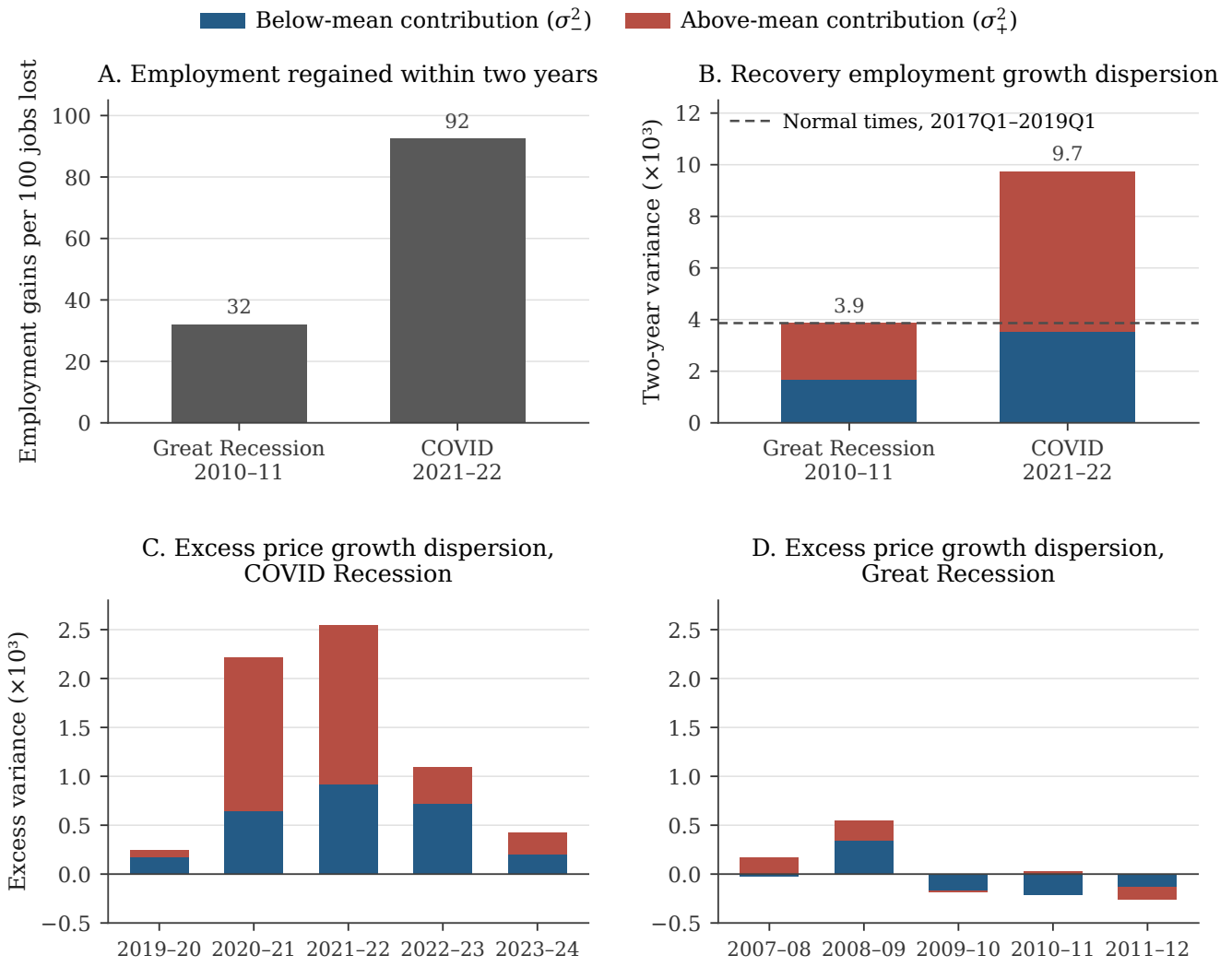

Figure 1: Employment recovery and price dispersion: COVID-19 and the Great Recession.

Notes: Panel A: recovery gains in the industries that contracted, per 100 jobs those industries lost. Panel B: cross-industry variance of two-year log employment growth. The dashed line is the 2017Q1–2019Q1 benchmark. Panels A–B use private-sector employment from the Quarterly Workforce Indicators (QWI) for 817 six-digit industries in 47 states, adjusted for workers on temporary layoff awaiting recall. Losses are measured over 2008Q1–2010Q1 and 2020Q1–2021Q1, and recovery over the following two years. Panels C–D: cross-industry variance of annual growth in BEA gross-output price indexes for the 302 industries that remain after excluding the 16 EXO and 39 commodity-price-linked industries (full list in Online Appendix A.2), relative to the two annual changes before each episode, so zero marks normal-times dispersion. Variances are multiplied by 10^3 after 3 percent winsorization. Blue and red are the contributions of industries below and above the weighted mean. Sources, weights, and sample: Online Appendix A.11.

We build an explanation with these three features. The relevant productive state is the workforce a producer retains when demand returns. A firm can remain below its pre-pandemic employment level

while expanding rapidly beyond the trained team it has available. Recruiting workers, training them, and reorganizing production require resources. These investments become increasingly costly when many workers must be integrated at once, and employment restored today enlarges the workforce available for subsequent production. A gradual recovery can therefore spread adjustment costs over small increments, whereas a rapid rebound can make the restoration of the same eventual workforce expensive.

Aggregate labor-market conditions amplify these costs. Intensive hiring raises recruitment and training requirements, while higher turnover shortens the period over which investments in employment relationships can be recovered. We discipline these largely nonwage costs of workforce restoration using microeconomic estimates of hiring-cost levels, their convexity, and their response to labor-market tightness (Muehlemann and Pfeifer, 2016; Linckh et al., 2025).

Consistent with this friction, predetermined occupational COVID-19 exposure predicts both the depth of the initial employment contraction and the location of subsequent price pressure. The exposure measure combines an external index of occupational COVID-19 exposure with industries' pre-pandemic employment composition and input–output linkages. In an event-study design comparing annualized changes over 2019–2022 with 2017–2019, more exposed supplier networks exhibit higher price growth alongside weaker employment and real output growth. These price increases are measured from 2019, so the finding concerns prices relative to their pre-pandemic levels, rather than merely their rebound from 2020. Supplier exposure is also associated with higher prices charged by the customer industries that rely on these networks, with the clearest evidence among middle and upstream producers. This combination of higher prices and weaker quantities points to a supply drag in the parts of the economy most exposed to pandemic disruption, rather than a purely demand-driven expansion.

An input–output accounting decomposition clarifies where this price pressure appears. It separates measured labor costs, domestic and imported input costs, and a gross-margin residual—the price growth left unexplained by measured costs. The residual has a markup interpretation under the accounting assumptions, but can also reflect unmeasured costs of expanding production. It accounts for most of the initial 2021 inflation surge, contributes modestly in 2022, and recedes in 2023. Early gains in output per worker cushion wage pressure; their subsequent reversal raises unit labor costs and helps sustain inflation even as the wage contribution declines.

Across industries, roughly 60 percent of the exposure-related increase in supplier prices appears in suppliers' margin residuals, while measured labor costs account for little. As these supplier prices feed into customers' costs, the same pressure appears downstream as measured input-cost inflation. The evidence thus locates substantial early price pressure in disrupted supply networks, with much of the pressure at its origin falling outside measured labor and material costs.

To quantify the aggregate implications of these localized pressures, we embed the disciplined hiring costs into a nonlinear production-network model with differently depleted producers. A recall allowance distinguishes retained employment relationships from capacity that must be restored through costly expansion. Producers incur a quadratic additional labor-cost premium when they expand beyond inherited capacity, and rebuilding today enlarges the capacity available tomorrow.[2] Following Chari et al. (2007), we infer demand, productivity, and pricing wedges from the observed sectoral paths, and compare recovery trajectories with and without rebuilding costs.[3]

Conditional on the inferred demand and productivity shifters, workforce rebuilding contributes 4.76 percentage points[4] to cumulative above-trend inflation through 2022—approximately two-thirds of the observed 7.18-point increase in the model's PCE-weighted gross-output price index. This pressure is concentrated early in reopening: the contribution reaches 4.11 points through 2021, exceeding the observed 2.06-point increase because other components offset part of it. The mechanism contributes little additional cumulative inflation after 2022.

The distribution of inherited capacity is central to this result. Equalizing capacity relative to steady-state employment between hit and safe producers within each chain-by-tier group—preserving each group's total capacity and holding cost coefficients fixed—reduces the rebuilding contribution from 4.76 to 2.05 percentage points. The reduction is 57 percent. Convex adjustment, limits to substitution, and network propagation make uneven capacity consequential even with an unchanged cost schedule.

Because marginal costs depend on how fast producers expand beyond the workforces they retained,

[2]The microeconomic evidence disciplines the premium's scale and its response to hiring conditions. The quadratic producer-level schedule remains a maintained specification; Section 4 describes the user-cost conversion and calibration.
[3]Both paths remove recovery-period residual pricing wedges and exogenous price shocks and retain the structural collapse-year pricing wedge. The productivity path is conditioned on, rather than generated endogenously by rebuilding. Section 5.1 defines the comparison.
[4]Throughout, changes are measured in log percentage points (pp).

the inflation–employment relationship depends on the recovery path. The same aggregate employment shortfall can coexist with different retained workforces, local expansion requirements, and hiring conditions, allowing rapid and gradual recoveries to generate different inflation paths without a permanent change in price-setting parameters.

Related literature. Our paper connects workforce capital and costly labor adjustment (Oi, 1962; Prescott and Visscher, 1980; Atkeson and Kehoe, 2005; Merz and Yashiv, 2007) to the empirical accounting of post-COVID inflation. Merz and Yashiv (2007) connect costly labor adjustment to firms' market values, and Muehlemann and Pfeifer (2016), Muehlemann and Strupler Leiser (2018), Aepli et al. (2024), and Linckh et al. (2025) provide microeconomic evidence on hiring and training expenditures and their determinants. It is closest to Ferrante et al. (2023), who show how costly labor reallocation makes a shift in consumption toward goods inflationary in a production network. They estimate adjustment costs using pandemic price and quantity moments. We bring complementary discipline from predetermined pandemic exposure, measured workforce depletion, and external evidence on recruitment and training costs. Our findings also bear on the interpretation of expenditure reallocation: observed spending shifts can reflect responses to disrupted supply as well as changes in preferences. Workforce destruction is therefore a candidate source of some dynamics represented by their demand-reallocation shock.

Comin et al. (2023) show how binding capacity constraints amplify demand pressures and generate inflation. Their capacity paths are exogenous, while the resulting scarcity pressures respond endogenously to demand. We connect capacity to observed workforce losses and allow its restoration to evolve with producers' employment decisions. The cost of rebuilding provides a complementary account of why supply remains expensive as demand recovers: restoring capacity itself raises marginal production costs. Our distributional experiment quantifies how the location of inherited capacity affects inflation through production linkages (Baqaee and Farhi, 2019, 2022; Rubbo, 2023).

Benigno and Eggertsson (2023) and Gitti (2026) share the broader narrative of nonlinear inflation under strained labor-market conditions. Their frameworks distinguish marginal new-hire costs from average payroll and incorporate hiring expenses. Our accounting supplies an additional empirical restriction: measured labor and material costs leave a substantial part of the initial price increase unexplained. The

QWI earnings comparison likewise assigns a limited contribution to observed recent-hire pay movements under our accounting conversion.[5] These findings direct attention to the nonwage component of workforce restoration. We assess its quantitative importance using external hiring-cost evidence and trace how uneven rebuilding requirements transmit price pressure through the production network.

The paper also relates to explanations of post-COVID inflation based on capacity constraints and reallocation, and to theories of a nonlinear Phillips curve. Rubbo (2024) shows that shocks shifting expenditure toward inelastically supplied goods and factors act as endogenous cost-push shocks. Bohr (2024) models firms' precautionary capacity buffers, ample before the pandemic and eroded by it, as the source of both the pre-COVID flatness and the post-COVID steepening of the Phillips curve.[6] Fornaro (2025) studies fiscal stimulus under supply constraints, and Boehm and Pandalai-Nayar (2022) estimate industry supply curves that steepen as producers approach capacity. Schmitt-Grohé and Uribe (2022) trace the nonlinearity to heterogeneous downward nominal wage rigidity, which makes the wage Phillips curve flat in slack territory and steep once inflation rises. Harding et al. (2023) trace it to price setting under a quasi-kinked demand schedule, and Blanco et al. (2024) to state-dependent price adjustment, in which a large cost shock raises the frequency of repricing. Beaudry et al. (2025) find that the evidence for a generic nonlinear Phillips curve is fragile. This is consistent with our mechanism, in which the steepening depends on the recovery path while price-setting parameters stay unchanged.

Our accounting and propagation analysis builds on the production-network literature (Acemoglu et al., 2012; Baqaee and Farhi, 2019, 2022; Rubbo, 2023). Evidence from natural disasters on input specificity and supplier disruptions (Barrot and Sauvagnat, 2016; Carvalho et al., 2021), together with work on firm-to-firm matching (Miyauchi, 2024), motivates the limits to replacing a constrained supplier. We study the inflationary implications of those limits when the damaged asset is workforce capacity. The analysis also complements demand and international-transmission mechanisms (Guerrieri et al., 2022; di Giovanni et al., 2022) and aggregate accounts of the episode. Ball et al. (2022) relate the rise in core inflation to labor-market tightness and to the pass-through of headline price shocks. Bernanke and Blanchard (2025) estimate a dynamic model of wages, prices, and expectations that attributes the initial surge

[5] Online Appendix A.4.3 reports that conversion. It is an accounting comparison, not an estimate of the regional new-hire wage elasticity studied by Gitti (2026).

[6] In our setting, capacity is the workforce a producer retains through the downturn. Its rebuilding cost rises with the pace of hiring, so the steepening depends on how quickly depleted workforces are restored.

mainly to price shocks and supply disruptions and its persistence to labor-market tightness, and Blanchard and Bernanke (2024) extend the analysis to eleven economies. Structural VAR evidence quantifies the contributions of demand and supply shocks (Giannone and Primiceri, 2024) and of pandemic fiscal transfers (Arias et al., 2026) within linear frameworks. Convex rebuilding costs add a state-dependent channel through which these conditions raise prices.[7]

The remainder of the paper is organized as follows. Section 2 presents the empirical evidence. Section 3 develops the model, and Section 4 describes its quantitative discipline. Section 5 reports the aggregate contribution, its implications for recovery dynamics and relative prices, and the role of uneven capacity. Section 6 concludes.

2 Empirical Evidence

This section lays out the key empirical facts and our network-based decomposition of inflation dynamics.

2.1 Data and Measurement

Data sources and sample. We link industry accounts, employment and payroll, occupational composition, import prices, and workplace-exposure measures on a common classification of 357 BEA industries.[8] Sectoral inflation is the annual log change in the BEA gross-output deflator (throughout, we report changes in log percentage points, abbreviated pp). Real and nominal gross output measure industry production rather than final sales. The Quarterly Census of Employment and Wages (QCEW) supplies employment and average payroll per worker. BEA–BLS KLEMS data are used to estimate the labor–input substitution elasticity in the accounting framework.

Our regression sample contains 330 industries. We exclude industries without a measured exposure score and sectors whose prices are predominantly externally determined, administered, or imputed: the paper's exogenous (EXO) blocks covering selected extractive and refining industries, real estate, finance

[7] Related mechanisms include job-ladder dynamics (Moscarini and Postel-Vinay, 2023) and the relationship between marginal costs and activity (Gagliardone et al., 2025). Furlanetto and Lepetit (2024) survey estimates of the Phillips-curve slope.

[8] The 402 industries in the BEA 2017 detail-level supply–use tables (SUTs), in producer prices, are aggregated to 357 to bridge classification changes, particularly the 2022 NAICS revision in retail. Occupational composition comes from the 2019 Occupational Employment and Wage Statistics (OEWS) and import prices from the BLS International Price Program. Online Appendices A.2, A.5, and A.11 document the concordances and sources.

and insurance, and government. These exclusions apply to regression observations, not to the supplier network, in which all 357 industries remain. The unconditional accounting first uses 2017 value-added weights on the regression sample, with and without retail. A separate PCE-weighted measure connects the industry accounts to the quantitative exercise below.

Inflation decomposition and cost tracing. Let Y_i denote industry i's real gross output, P_i its deflator, N_i employment, and W_i average payroll per worker. We measure the margin as the ratio of nominal gross output to variable production costs. This measure captures the part of the output price not accounted for by observed payroll and intermediate-input costs; it is not a measure of net profits. Formally,

$$\mu_i \equiv \frac{P_i Y_i}{C_i(Y_i)}, \qquad C_i(Y_i) \equiv \min_{N_i, M_i} \{W_i N_i + P_i^M M_i\} \quad \text{subject to producing } Y_i. \tag{1}$$

Here M_i is a composite of domestic and imported intermediate inputs, P_i^M its price, and P_i^{IMP} the price of its imported-input bundle. Capital is predetermined. With the Cobb–Douglas technology of Online Appendix A.1, marginal cost then exceeds average variable cost by the fixed factor $1/(1-\alpha_i)$, so the margin and the markup over that benchmark marginal cost have identical log changes. This relationship does not identify the empirical residual with a markup over true marginal cost when some production costs are unmeasured. A nested constant elasticity of substitution (CES) cost structure yields the first-order decomposition

$$\Delta \log P = \underbrace{\Delta \log \mu}_{\Delta\text{MARGIN}} + \underbrace{\underbrace{\text{diag}(b)\Delta \log W}_{\Delta\text{WAGE}} + \underbrace{[-\Delta \log(Y/N)]}_{\Delta\text{PROD}}}_{\Delta\text{ULC}} + \underbrace{A\Delta \log P}_{\Delta\text{MAT}} + \underbrace{A^{\text{IMP}}\Delta \log P^{\text{IMP}}}_{\Delta\text{IMP}}. \tag{2}$$

Time subscripts are suppressed, and all operations on vectors are elementwise unless indicated otherwise. The inflation decomposition in equation (2) is a first-order approximation derived from this nested CES cost-minimization problem. It partitions an industry's price growth into its margin growth, the growth in its unit labor costs (wage growth net of labor productivity), and the cost-share-weighted inflation of its intermediate inputs. In the empirical application, the components add exactly because margin growth is recovered as a residual.

The $I \times I$ industry-by-industry matrix $A = [a_{ii'}]$ and the diagonal matrix A^{IMP} govern the network propagation of these intermediate input costs. Specifically, A captures domestic network propagation by mapping the price changes of upstream domestic suppliers into the measured input-cost inflation of downstream buyers (which we refer to as *supply-chain price inflation*), while A^{IMP} routes exogenous import-price shocks into domestic production costs. To construct these matrices, we rely on the 2017 BEA Make and Use tables. These accounts provide the empirical expenditure share of each commodity in an industry's input bundle, the domestic-versus-imported sourcing split for each commodity, and each industry's market share in producing specific commodities. Rather than assuming mechanical one-to-one pass-through, the matrices scale these input–output linkages by a CES-adjusted pass-through coefficient, $d_i = (1 - s_i^N)(1 - \rho)$. The corresponding wage coefficient is $b_i = 1 - d_i$. An entry $a_{ii'}$ thus represents d_i scaled by the 2017 share of industry i's input purchases consisting of domestic commodities produced by industry i'. This formulation ensures that intermediate input prices pass into unit costs as a function of both the industry's variable labor share, s_i^N, and the elasticity of substitution between labor and materials, ρ. We estimate $\rho = 0.39$ using relative input expenditures and prices in KLEMS; the 95 percent confidence interval is $[0.06, 0.72]$. Complete derivation and details are in Online Appendix A.1.

We recover ΔMARGIN as the exact residual required to balance equation (2) for each industry and year. It measures price growth not accounted for by measured labor and input costs. It can absorb unmeasured expenditures, such as the nonwage costs of recruiting, training, and reorganizing depleted workforces, as well as differences between marginal and average costs, the timing of price adjustment relative to measured costs, and measurement error. The identity locates where inflationary pressure emerges. Relating that pressure to pandemic disruption is the task of the exposure design.

Predetermined pandemic exposure. We measure workplace exposure using the COVID-19 Job-Exposure Matrix (JEM) of Oude Hengel et al. (2022), which scores occupations on six dimensions of contact and mitigation: the number and nature of contacts, contaminated workspaces, work location, distancing, and face coverings. We use the Danish tabulation, validated against occupation-linked infection records (Online Appendix A.5). Its predictive performance is strongest early in the pandemic; that validation concerns infection exposure, not the subsequent economic effects studied here. The first

principal component summarizes the six dimensions.[9]

Let e_o denote the exposure score of occupation o, and let s_{io}^{2019} be its share of industry i's pre-pandemic employment, normalized over occupations with matched scores. We construct industry exposure as $E_i = \sum_o s_{io}^{2019} e_o$, and E collects these scores across industries. The measure captures an industry's vulnerability to workplace disruption based on its pre-pandemic occupational composition. It does not use realized employment losses or subsequent prices. The occupational scores themselves were developed for COVID-19, so "predetermined" refers to the employment shares and network weights, not to the date at which the occupational risk assessment was constructed. The index measures relative workplace exposure, not infection probabilities.

An industry's production can also be affected by workplace disruption at its suppliers. We measure this exposure using the same input–output coefficients that enter the price accounting:

$$\mathcal{E}_i = (AE)_i = \sum_{i'}^{I} a_{ii'} E_{i'} = s_i \bar{E}_i, \qquad s_i = \sum_{i'}^{I} a_{ii'}, \qquad \bar{E}_i = \sum_{i'}^{I} \frac{a_{ii'}}{s_i} E_{i'}, \tag{3}$$

where $a_{ii'}$ is the element of the previously defined matrix A.

Supplier exposure depends on both the importance of domestic intermediate inputs in production, s_i, and the average exposure of the suppliers from which those inputs are purchased, $\bar{E}_i$. The measure includes purchases from other establishments in the same industry. Twelve supplier industries without measured exposure scores remain in the network and are assigned zero for constructing the index; this is a missing-data convention, not an assumption that they were unaffected by COVID-19.[10] The regressions account for the resulting differences in exposure coverage. The one-step operator keeps the supplier interpretation transparent; alternative network-depth conventions are discussed in Online Appendix A.3.

[9] The component loadings are estimated from the country-averaged Danish, Dutch, and U.K. scores and applied to the Danish scores. A positive affine transformation matches the mean and standard deviation of the equally weighted six-dimension average. Online Appendix A.5 documents these steps, the occupation concordances, and coverage.

[10] The unscored set consists of eleven agricultural industries and state and local government. EXO and exposure-coverage exclusions overlap. The regression sample excludes unscored observations, while their input links remain in A.

2.2 Empirical Results

Inflation accounting. Table 1 shows that a substantial part of the post-COVID increase in industry prices is not accounted for by measured labor and input costs. The table aggregates equation (2) with 2017 value-added weights on the regression sample. Over 2019–2022, cumulative industry inflation was 13.29 pp, of which 3.42 pp (25.8%) appeared in the margin residual. Measured unit labor costs contributed 5.07 pp (38.2%), reflecting 10.08 pp from wage growth offset by −5.01 pp from rising output per worker. Domestic and imported input prices accounted for the remaining 4.79 pp (36.1%), almost entirely through domestic suppliers.

Table 1: Accounting decomposition of inflation dynamics, 2019–2022.

	All industries		Excluding retail	
	pp	share (%)	pp	share (%)
Industry inflation, $\Delta \log P$	13.29	100.0	12.47	100.0
Margin residual, ΔMARGIN	3.42	25.8	2.33	18.7
Unit labor costs, ΔULC	5.07	38.2	5.28	42.4
Wage growth	10.08	75.9	9.93	79.6
Labor productivity (sign reversed)	−5.01	−37.7	−4.64	−37.2
Input prices	4.79	36.1	4.86	39.0
Supply-chain price, $A\Delta \log P$	4.47	33.6	4.51	36.2
Imported inputs, ΔIMP	0.32	2.4	0.34	2.8

Notes: Cumulative pp over 2019–2022 and shares of industry inflation. Columns use normalized 2017 value-added weights on 330 industries; the second pair excludes retail trade and gasoline stations and renormalizes the remaining weights, without removing those suppliers from other industries' input baskets. Margin, unit labor costs, and input prices sum to inflation before rounding; indented rows partition labor costs and input prices. Wage growth is weighted by b_i and A contains the fixed benchmark coefficients in equation (2).

Figure 2 shows a marked shift in the composition of inflation during the recovery. In 2020–2021, the margin residual contributed 4.41 of the 5.17 pp of industry inflation, while measured unit labor costs made a negative contribution. By 2021–2022, unit labor costs had become the dominant component, contributing 3.52 pp, while the margin contribution declined to 0.82 pp. Domestic-input price pressure remained positive in both years. The initial inflation surge thus preceded the large increase in measured labor costs.

The rise in the labor-cost contribution reflects the reversal of the earlier productivity gains, not a larger wage contribution. Between these two years, the wage contribution falls from 3.95 to 2.37 pp, whereas the

signed productivity contribution rises from −5.37 to 1.15 pp. Higher output per worker initially offsets wage growth; its subsequent decline removes that offset and raises unit labor costs. The productivity slowdown can therefore help sustain cost pressure without requiring wage growth to accelerate.

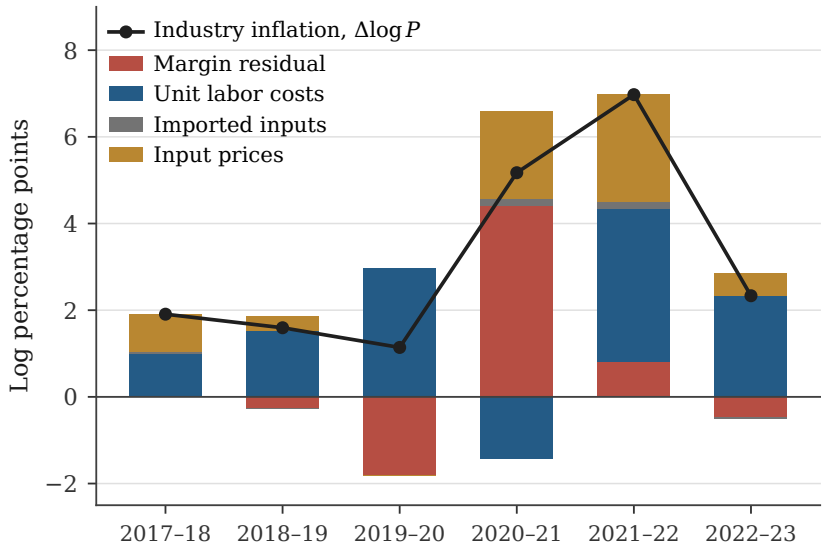

Figure 2: Industry inflation and its accounting components by year.

Notes: Annual pp, aggregated with 2017 value-added weights over the 330-industry regression sample. The line is industry inflation; the bars are the margin residual, CES-adjusted labor-cost contribution, and domestic and imported input-price contributions. Components add to inflation by equation (2). Years denote the endpoints of annual changes.

Retail trade contributes disproportionately to the aggregate margin residual, so Table 1 also excludes retail trade and gasoline stations and renormalizes the remaining weights. BEA measures retail output primarily as distribution services—the difference between merchandise sales and the cost of goods resold—rather than total merchandise sales (Bureau of Economic Analysis, 2011). This accounting convention does not mechanically raise our price-over-cost residual. Excluding retail reduces the residual contribution to 2.33 pp, or 18.7% of industry inflation, while unit labor costs account for 42.4%. A substantial cumulative margin residual therefore remains outside retail.[11]

To connect the industry accounts to the model's aggregate price measure, we also construct a PCE-weighted gross-output price index. Fixed 2017 PCE commodity weights, collected in the vector $c = [c_j]$, are mapped to industries using the BEA make-share matrix $\Theta = [\theta_{ij}]$, where θ_{ij} is industry i's share in the production of commodity j (i indexes industries and j commodities). The result is the vector of

[11]The prominence of trade and distribution in the early margin-residual increase leaves room for sector-specific forces alongside the common rebuilding mechanism. This accounting concentration is distinct from the exposure gradient: Panel C of Table 2 shows that the supplier-margin relationship remains positive after the direct contributions of trade, commodity, and utility suppliers are excluded.

industry weights $g = \Theta c$, with elements $g_i = \sum_j \theta_{ij} c_j$. Removing the direct weights of the exogenous (EXO) sectors without renormalizing leaves weights summing to 0.71. We refer to $g^\top \Delta \log P$ under these weights as non-EXO gross-output inflation (N-GO); retaining the EXO weights gives GO inflation.[12]

Supply-chain propagation. A buyer's domestic-input price contribution is the cost-weighted sum of changes in its suppliers' selling prices. Applying the accounting identity to these suppliers gives

$$(A\Delta \log P)_i = (A\Delta\text{MARGIN})_i + (A\Delta\text{ULC})_i + (A\Delta\text{IMP})_i + (A\Delta\text{MAT})_i. \tag{4}$$

This decomposition traces supplier-price pressure to four accounting sources: suppliers' margin residuals, unit labor costs, imported inputs, and purchases from further upstream producers. Importantly, a rise in a supplier's margin residual raises the buyer's measured input costs without necessarily raising the buyer's own margin. The exposure index and the outcome decomposition use the same benchmark supplier weights. Applying A therefore provides a consistent measurement of supplier exposure and price pressure, not an independent source of causal identification.[13]

Regression design. We test whether the relationship between pandemic exposure and industry outcomes changed during the inflation surge. Specifically, we compare average annual changes over 2017–2019 with those over 2019–2022. For each outcome $y_{i,w}$, we estimate

$$y_{i,w} = \alpha_i + \tau_w + \big(\beta X_i + \lambda_s s_i + \lambda_q q_i\big) D_w + \varepsilon_{i,w}, \tag{5}$$

where w indexes the two windows, D_w indicates 2019–2022, and α_i and τ_w are industry and window fixed effects. The coefficient β measures how much the annual relationship between exposure and the outcome changed relative to the pre-pandemic period. We annualize the cumulative changes by dividing by two and three years, respectively, and weight industries by 2017 value added. Multiplying β by three

[12] Online Appendix A.1.5 compares these indexes with published PCE and CPI inflation. Online Appendix equation (A.34) gives the network decomposition, which attributes domestic-input inflation to its upstream margin, labor-cost, and import-price sources. Its weights and attribution differ from Table 1.

[13] In a common-slope benchmark, $\Delta\text{MARGIN} = \alpha\mathbf{1} + \beta E + u$, where u collects industry-specific disturbances. Applying matrix A gives $A\Delta\text{MARGIN} = \alpha s + \beta AE + Au$. A diversified supplier basket can average out weakly correlated disturbances while preserving the common exposure slope. This is one possible reason for greater precision at the supplier level.

expresses the change in the exposure gradient over the three-year post-pandemic window; it does not recover the unconditional post-pandemic relationship.

At the own-industry level, $X_i = E_i$, and the dependent variable is the industry's own outcome; no network-loading controls are required ($\lambda_s = \lambda_q = 0$). At the supplier level, $X_i = \mathcal{E}_i$, and the dependent variable is the corresponding outcome aggregated across the industry's suppliers using A. We control for total domestic-input loading, s_i, and the loading on suppliers with measured exposure scores, $q_i = \sum_{i'}^{I} a_{ii'} \mathbf{1}\{E_{i'} \text{ observed}\}$. Both controls are interacted with the post-pandemic indicator. The first separates exposure from the overall importance of domestic inputs; the second accounts for differences in exposure coverage and makes the coefficient invariant to an additive renormalization of the observed scores. These controls address the incomplete-shares issue discussed by Borusyak et al. (2022) and are included for measurement reasons, independently of their effects on statistical significance.

We report results for all 330 industries and separately for the 232 middle and upstream industries, denoted $m+l$. This distinction separates consumer-facing producers from industries with a larger indirect role in the production network. We classify industries using the *finalness* index, g_i/κ_i, the ratio of an industry's PCE weight to its benchmark Domar weight, where $\kappa = L^\top g$ and $L = (I - A)^{-1}$ is the Leontief inverse. Industries with finalness of at least 70 percent are classified as consumer-facing; the remainder become $m + l$.

The event study identifies changes in exposure gradients, not the effect of the pandemic relative to an untreated economy. A causal interpretation requires that, absent COVID-19, industries with different exposure scores would have experienced stable differences in outcome growth, conditional on the included controls. Industry fixed effects remove persistent differences in growth rates, but cannot eliminate pandemic-specific demand, productivity, or broad-sector disturbances correlated with exposure. Predetermined occupational shares and network weights prevent realized outcomes from entering the exposure measure, but do not by themselves establish the identifying assumption. Online Appendix A.4.1 examines the timing of the relationship across the two pandemic phases; these comparisons are informative but cannot establish counterfactual parallel trends.

Fact 1. Exposure predicts employment losses and supplier-price pressure. Table 2 shows that greater exposure is associated with weaker employment growth at both the own-industry and supplier-network levels.[14] In the full sample, the supplier-employment coefficient is −2.58 ($t = -4.29$); own employment also declines with exposure, with a larger and more precisely estimated relationship among middle and upstream industries (denoted $m + l$ above). Because the outcome measures employment growth through 2022, these coefficients capture the combined effects of the initial contraction and the subsequent recovery. They therefore indicate persistent employment weakness relative to the pre-pandemic exposure gradient, rather than measuring the initial destruction of employment alone.

Greater supplier exposure is also associated with substantially higher supplier-price inflation. The coefficient is 9.19 in the full sample ($t = 7.02$) and 10.47 among middle and upstream industries ($t = 7.01$). Own-industry price inflation is positively related to exposure but less precisely estimated: the coefficient is 1.35 ($t = 2.40$) in the full sample and 2.85 ($t = 5.39$) in $m+l$. The evidence is therefore strongest for price pressure along exposed supplier networks, with a corresponding own-price relationship among middle and upstream producers. Because the two regressions use different outcomes and exposure measures, their coefficients are not directly comparable as pass-through elasticities.

Panel B shows that much of the exposure-related increase in supplier prices appears in the suppliers' margin residuals rather than in measured labor costs. In the full sample, the supplier-margin coefficient is 5.53 ($t = 4.05$), compared with a total supplier-price coefficient of 9.19. Thus, roughly 60 percent of the estimated supplier-price gradient is accounted for by the margin residual. Purchases from further upstream producers contribute another 2.73 pp, and imported inputs contribute 0.50; the measured labor-cost coefficient is small and statistically insignificant. At the own-industry level, margin coefficients are imprecise, while domestic-input costs contribute significantly to the price gradient among middle and upstream industries (0.96, with an import contribution of 0.12). The four components add to the price coefficient by construction, because the dependent variables satisfy the same identity and the regression design is common, although their standard errors do not. This partition identifies the accounting origins

[14] Significance stars in regression tables throughout are based on heteroskedasticity-robust t-statistics. Because industries may share suppliers, disturbances can be correlated across industries even when they belong to different sectors, and neither robust nor sector-clustered standard errors need capture all such dependence (Adão et al., 2019; Cameron and Miller, 2015). Online Appendix Table A6 reports both sets of t-statistics for every coefficient, and Online Appendix A.3.2 discusses their limitations.

of the exposure relationship, not separate causal contributions of rebuilding costs or markup shocks.

The supplier-margin relationship is not driven exclusively by commodity producers, trade, or utilities. Panel C repeats the regression after excluding selected suppliers from the network calculation. Removing the EXO blocks and retail leaves a positive coefficient of 4.82 in the full sample. Excluding wholesale trade and utilities as well reduces it to 4.06 ($t = 3.98$), with a corresponding coefficient of 3.98 ($t = 4.73$) among middle and upstream industries. The relationship therefore persists when these sectors' direct contributions are removed. The exclusions do not eliminate their indirect effects through other suppliers, nor do they imply that the remaining pressure is evenly distributed. They also do not measure the excluded sectors' contribution to aggregate inflation, which is a distinct accounting question.

Table 2: COVID-19 exposure, outcomes and the cost partition at two levels, 2019–2022.

	Own industries y_i on E_i		Supplier networks $(Ay)_i$ on $(AE)_i$	
Outcome y	Full	$m + l$	Full	$m + l$
Panel A. Employment, prices and quantities				
Employment, $\Delta \log N$	-1.22^{**}	-2.40^{***}	-2.58^{***}	-2.63^{***}
Price, $\Delta \log P$	1.35^{**}	2.85^{***}	9.19^{***}	10.47^{***}
Real output, $\Delta \log Y$	-1.71^{***}	-3.55^{***}	-3.32^{***}	-3.82^{***}
Panel B. Accounting components of the price gradient				
Margin, ΔMARGIN	-0.08	0.43	5.53^{***}	6.31^{***}
Labor costs, ΔULC	1.15^{**}	1.33	0.43	0.75
Imports, ΔIMP	0.03	0.12^{***}	0.50^{***}	0.52^{***}
Domestic inputs, ΔMAT	0.26^{**}	0.96^{***}	2.73^{***}	2.88^{***}
Panel C. Supplier-margin regression: excluded suppliers				
None			5.53^{***}	6.31^{***}
EXO and retail			4.82^{***}	4.88^{***}
EXO, trade, utilities			4.06^{***}	3.98^{***}
Industries	330	232	330	232

Notes: Coefficients from equation (5): changes in annual exposure gradients over 2019–2022 relative to 2017–2019, with industry and window effects and 2017 value-added weights. Own outcomes are regressed on E_i; supplier outcomes are aggregated with A and regressed on $(AE)_i$, with s_i and q_i interacted with the pandemic window. Panel B components sum to the price coefficient before rounding. Panel C removes supplier columns, not buyer observations: EXO plus retail and gasoline stations (18 industries), then wholesale and utilities as well (31 industries). Stars are based on heteroskedasticity-robust t-statistics: $^{*}p < 0.10$, $^{**}p < 0.05$, $^{***}p < 0.01$. The $m + l$ sample contains middle and upstream industries, defined in Section 2.2.

Fact 2. Exposed supplier networks had weaker production growth. The data show evidence of disrupted supply. Relative to the pre-pandemic period, more exposed supplier networks exhibited faster price growth and slower real-output growth (Table 2, Panel A). This combination points to a contraction of supply, because higher demand along an unchanged supply curve should raise prices and quantities together. In the full sample, the supplier price coefficient is 9.19 ($t = 7.02$) and the supplier real-output coefficient is -3.32 ($t = -7.23$), with similar values in $m + l$ (10.47 and -3.82). The higher supplier prices raised the input costs of the industries that buy from these networks. The industries' own prices and output show the same pattern, most clearly among middle and upstream producers, with a price coefficient of 2.85 ($t = 5.39$) and a real-output coefficient of -3.55 ($t = -3.08$).

Fact 3. Supplier exposure is also associated with buyers' selling-price growth. The preceding results locate price pressure in industries' supplier networks. We next relate supplier exposure to the prices these industries charge their own customers. We estimate equation (5) with the buyer's own price growth as the outcome and $\mathcal{E}_i$ as the regressor, retaining the same windows, weights, and loading controls (Online Appendix A.3.3). The coefficients are 16.98 in the full sample and 25.21 among middle and upstream industries (Table A7). Both are statistically significant with heteroskedasticity-robust and with sector-clustered standard errors. The association thus extends from input costs to buyers' selling prices.

This relationship is not confined to exposure to extractive and petroleum-refining suppliers: separating that exposure leaves a positive buyer-price gradient in both samples. Broader energy and commodity partitions retain positive and significant input-cost and supplier-margin relationships. The buyer-price relationship becomes smaller and imprecise in the full sample; among middle and upstream industries it remains positive and significant at the 1 percent level under all three definitions. The evidence therefore links supplier exposure to both incoming cost pressure and selling-price growth, with the latter relationship more robust among intermediate-input producers. These conditional associations do not identify a causal pass-through elasticity.

3 Model

We model an annual economy that begins in its pre-pandemic steady state in $t = 0$ (2019). An unanticipated contraction in $t = 1$ (2020) leaves producers with unevenly depleted workforces, and as the recovery takes hold from $t = 2$ (2021) onward, firms face the costs of expanding beyond this inherited capacity. This section formalizes the production network and the convex cost of workforce rebuilding, followed by price and wage adjustment, inflation expectations, final demand, and equilibrium. Reduced-form wedges match the observed sectoral paths; Section 4 explains their calibration and their role in the counterfactuals.

3.1 Environment and production network

Because we solve the model nonlinearly and calibrate it to sectoral paths, we represent the U.S. production network using a simplified network of four supply chains and three vertical tiers, constructed to group industries with strong input–output links while balancing gross output across chains (Section 4). The economy consists of twenty-four production nodes organized into twelve chain-by-tier composites, indexed by $i = 1, \ldots, 12$. Each composite belongs to one of four interconnected supply chains and occupies an upstream, middle, or consumer-facing position within that chain.[15] We divide each composite into two nodes, indexed by $j \in \{H, S\}$, representing industries with more severe (hit, H) and less severe (safe, S) employment contractions. This distinction preserves heterogeneity in inherited workforce capacity within similar network positions.

Outside the endogenous network is an exogenous (EXO) block containing real-estate, finance-and-government, and energy categories and imported inputs. Firms choose the quantities of EXO inputs they purchase while taking EXO prices as given. Section 4 details the empirical construction of these nodes, the EXO block, and the corresponding input–output coefficients.

Variables indexed by (i, j) refer to individual hit or safe nodes, variables indexed only by i refer to tier-

[15] Online Appendix A.2 describes the four chains. Ranked by 2019 employment, C_2 is the largest, with 40.2 million workers. It runs from agriculture and food processing to restaurants, hospitals, and social services. C_1, with 36.8 million, supplies professional and information services to retail and other consumer-facing services. C_3, with 23.4 million, covers physicians' offices and outpatient care, accommodation, and transportation, fed by chemicals and pharmaceuticals. C_4, with 17.8 million, is durable manufacturing and construction.

level aggregates, and variables without either index refer to economywide aggregates. For parameters, the omission of j indicates a common value for the hit and safe nodes within tier i.

Each node comprises a fixed measure of monopolistically competitive firms producing differentiated varieties and charging positive markups. Real gross output of node (i, j) is produced according to $Y_{ij,t} = \exp(a^e_{i,t}) Z_{ij} V^{1-\alpha_i}_{ij,t}$, where Z_{ij} absorbs cross-sectional differences in productivity and capital, α_i is the capital share embedded in the reduced-form production technology, and $a^e_{i,t}$ is a time-varying effective productivity wedge. The variable-input composite combines labor $N_{ij,t}$ and intermediate inputs $m_{ij,t}$:

$$V_{ij,t} = \left[\eta^{1/\rho}_{ij} N^{(\rho-1)/\rho}_{ij,t} + (1-\eta_{ij})^{1/\rho} m^{(\rho-1)/\rho}_{ij,t}\right]^{\rho/(\rho-1)}, \tag{6}$$

where η_{ij} is the labor weight and ρ is the elasticity of substitution between labor and intermediate inputs. For tractability, this same elasticity governs the substitution between hit and safe nodes within a tier. Within each tier, hit and safe output are aggregated according to

$$Y_{i,t} = \left[\sum_{j\in\{H,S\}} s^{1/\rho}_{ij} Y^{(\rho-1)/\rho}_{ij,t}\right]^{\rho/(\rho-1)}. \tag{7}$$

The weights s_{ij} sum to one within tier i, and $P_{i,t}$ denotes the corresponding price index. The tier composite can be purchased by final users or used as an intermediate input elsewhere in the network.

The intermediate-input bundle used by node (i, j) combines inputs from the twelve endogenous tiers and the EXO block:

$$m_{ij,t} = \left[\sum_{k=1}^{12} \omega^{1/\rho}_{i,k} m^{(\rho-1)/\rho}_{ij,k,t} + (\omega^{EXO}_i)^{1/\rho} (m^{EXO}_{ij,t})^{(\rho-1)/\rho}\right]^{\rho/(\rho-1)} \tag{8}$$

where $m_{ij,k,t}$ denotes intermediates purchased by node (i, j) from endogenous supplier tier k, while $m^{EXO}_{ij,t}$ denotes purchases from the EXO block. The corresponding unit price of this intermediate-input bundle is

$$p^m_{i,t} = \left[\sum_{k=1}^{12} \omega_{i,k} P^{1-\rho}_{k,t} + \omega^{EXO}_i \left(P^{EXO}_{i,t}\right)^{1-\rho}\right]^{1/(1-\rho)}, \tag{9}$$

where $P^{EXO}_{i,t}$ is the price index of the EXO inputs purchased by tier i, and $\sum_{k=1}^{12} \omega_{i,k} + \omega^{EXO}_i = 1$. Thus, $p^m_{i,t}$ summarizes the input-cost pressures faced by tier i. An increase in $P_{k,t}$ raises the production costs of its

customers according to the input–output weight $\omega_{i,k}$, propagating the initial cost pressure downstream. Online Appendix A.7 reports the associated conditional input demands and price indices.

3.2 Cost wall (CW)

A firm's inherited employment provides its workforce capacity, denoted by $N_{ij,t}^{\mathrm{CW}}$ for node (i, j). While firms can employ workers up to this capacity without an additional rebuilding premium, expanding beyond it requires recruiting, screening, training, and reorganizing production. We formalize these non-wage adjustment costs as a quadratic premium above the inherited-capacity threshold—the *cost wall* (CW)—that applies only when employment exceeds inherited capacity. We measure employment above capacity relative to steady-state employment as $\Delta N_{ij,t}^{+} = \max\{(N_{ij,t} - N_{ij,t}^{\mathrm{CW}})/N_{ij}^{ss},\, 0\}$. The rebuilding premium is $\mathcal{W}_{ij,t} = \gamma_i \left(\Delta N_{ij,t}^{+}\right)^2$, where γ_i scales its magnitude. The premium is zero below the threshold and increases quadratically above it.

When the cost wall binds, the employment gap decomposes into two components: $\Delta N_{ij,t}^{+} = (N_{ij,t} - N_{ij}^{ss})/N_{ij}^{ss} + (N_{ij}^{ss} - N_{ij,t}^{\mathrm{CW}})/N_{ij}^{ss}$. The first measures employment relative to steady state; the second measures the inherited capacity shortfall. Holding the other component fixed, an increase in employment and an equal-sized loss of inherited capacity have the same effect on the premium. Both are measured relative to steady-state employment. Demand expansion and capacity destruction can therefore activate the same convex cost schedule, although their other effects on the economy may differ.

A distinctive feature of the early recovery was the preservation of organizational capital through temporary layoffs: a substantial fraction of the workers separated in 2020 remained attached to their former employers and available for rapid recall. We embed this *warm pool* of recoverable matches in the 2021 capacity threshold by setting

$$N_{ij,t}^{\mathrm{CW}} = \begin{cases} N_{ij,1} + \psi \max\left\{N_{ij}^{ss} - N_{ij,1},\, 0\right\}, & t = 2, \\ N_{ij,t-1}, & \text{otherwise}, \end{cases} \tag{10}$$

where $t = 1$ denotes 2020, $t = 2$ denotes 2021, and N_{ij}^{ss} is the node's steady-state employment in 2019. The parameter $\psi \in [0, 1]$ is the share of the 2020 employment shortfall that can be restored in 2021 without

incurring the additional rebuilding premium, so the reopening-year threshold expands to accommodate these recalls; from 2022 onward, the threshold is the previous year's employment. Thus, employment restored in one year raises the capacity available in the next.

The cost wall raises the effective unit cost of labor:

$$w^e_{ij,t} = \tilde{w}_{ij} W_t \left(1 + \mathcal{W}_{ij,t}\right) \exp\left(1_{t=1} \tau^e_{ij}\right),$$

where W_t is the aggregate base wage, $\tilde{w}_{ij}$ captures cross-sectional wage differences, and τ^e_{ij} is a transitory labor wedge operating only in 2020. During recovery, nodes paying the same base wage can therefore face different effective labor costs. For a given employment path and rebuilding-cost coefficient, a larger inherited capacity loss raises the premium.

Recruiting and training expenditures are investments in workforce-specific organizational capital whose benefits extend over the duration of the employment match. We therefore calibrate γ_i using rebuilding costs amortized over the expected match duration, as described in Section 4.

The cost wall affects inflation through marginal cost. Combining the CES input-cost index with the production technology gives real marginal cost, measured relative to the node's own output price $P_{ij,t}$:

$$MC_{ij,t} = \frac{\left[\eta_{ij}\left(w^e_{ij,t}\right)^{1-\rho} + (1-\eta_{ij})\left(p^m_{i,t}\right)^{1-\rho}\right]^{1/(1-\rho)}}{P_{ij,t}(1-\alpha_i)} \frac{V_{ij,t}}{Y_{ij,t}}. \tag{11}$$

In equation (11), the bracketed term is the unit cost of the variable-input composite. The factor $V_{ij,t}/[(1-\alpha_i)Y_{ij,t}]$ converts this into the nominal cost of an additional unit of output; division by $P_{ij,t}$ expresses marginal cost relative to the node's output price. The rebuilding premium raises the labor-cost component. As suppliers pass their own cost increases into prices, it also raises customers' intermediate-input costs. Price adjustment, specified next, determines how these marginal-cost pressures affect inflation.

3.3 Prices and expectations

Prices and base wages adjust gradually. Inflation expectations place weight on the nominal anchor, past inflation, and the model-implied future path.

Sticky prices. Each production node (i, j) comprises a sector of symmetric monopolistically competitive producers facing constant-elasticity demand with a within-node elasticity of $\varepsilon_i > 1$. Firms set prices subject to a Rotemberg-style quadratic adjustment cost relative to the nominal anchor $\bar{\Pi}$, plus an asymmetric term that activates only when inflation falls below that anchor. The full derivation of the pricing equation from the firm's problem is provided in Online Appendix A.7.2.

For node (i, j), let $\Psi_i(\Pi) \equiv \Pi\left[\bar{\phi}_i(\Pi - \bar{\Pi}) + \lambda_i(\Pi - \bar{\Pi})^-\right]$ denote the asymmetric Rotemberg marginal adjustment-cost expression evaluated at inflation Π. The pricing first-order condition in per-unit-output form then reads

$$\Psi_i(\Pi_{ij,t}) = \varepsilon_i\left(MC_{ij,t} - \tfrac{\varepsilon_i - 1}{\varepsilon_i} + \mu^e_{i,t} + 1_{t=1}\bar{\mu}^e_i\right) + \beta\,\mathbb{E}_t\left[\Psi_i(\Pi_{ij,t+1})\,\tfrac{Y_{ij,t+1}}{Y_{ij,t}}\right], \tag{12}$$

where $\Pi_{ij,t} \equiv P_{ij,t}/P_{ij,t-1}$ is gross inflation and $(\cdot)^- \equiv \min\{0, \cdot\}$. The parameter $\bar{\phi}_i$ governs symmetric price-adjustment costs, while λ_i adds rigidity below the nominal anchor. The residual pricing wedge $\mu^e_{i,t}$ is common to both nodes within tier i, and $\beta = 0.96$ is the annual discount factor. A common demand elasticity across tiers implies a steady-state price-to-marginal-cost ratio of $\varepsilon_i/(\varepsilon_i - 1)$. In the calibration, adjustment-cost parameters vary across chains in consumer-facing tiers and take common values in the middle and upstream tiers (Section 4). The current-period term combines the deviation of marginal cost from its steady-state level with the pricing wedges. The final term reflects the effect of today's price choice on next period's price-adjustment cost. Both current costs and expected future adjustment therefore enter the pricing decision.

The pricing equation distinguishes the collapse from the recovery. The structural 2020 wedge $\bar{\mu}^e_i$ operates only in the collapse year, whereas $\mu^e_{i,t}$ accounts for the remaining price residual, which is concentrated in 2021–2024. In the counterfactuals, we set the recovery wedge to zero in all periods but retain the structural 2020 wedge, which offsets the downward cost pressure from the measured 2020 productivity increase.[16]

[16] Removing the structural 2020 wedge would lower the model's initial price path because the measured productivity increase exerts downward cost pressure. The distinction matters for the level of the counterfactual price path and its comparison with the model floor in Section 5.

Base wage. The base wage is sticky and follows a reduced-form wage Phillips curve:

$$\frac{W_t}{W_{t-1}} = \bar{\Pi}\left(\frac{N_t}{N^{ss}}\right)^{\phi_w}\left(\frac{LS^{ss}}{LS_{t-1}}\right)^{\iota_a}\left(\prod_{k=1}^{n}\frac{\Pi_{t-k}}{\bar{\Pi}}\right)^{\iota_w}, \tag{13}$$

where ϕ_w governs the response of base-wage growth to aggregate employment, and ι_w governs backward indexation. In logs, the indexation term is $\iota_w \sum_{k=1}^{n}(\log \Pi_{t-k} - \log \bar{\Pi})$. We set $n = 4$, so current wage growth responds to inflation over the preceding four years. This permits gradual wage adjustment to cumulative inflation rather than only to the most recent observation. Limited adjustment of continuing workers' wages is consistent with the firm-level wage-growth norms documented by Hurst et al. (2026); those findings motivate the specification without directly identifying its parameters.

The middle term in equation (13) anchors a labor-share measure based on the aggregate base wage, $LS_t \equiv W_t N_t/(P_t \mathcal{Y}_t)$. Here P_t and $\mathcal{Y}_t$ are the aggregate price index and real final-output measure defined in equations (20) and (19). Its weight, $\iota_a = 0.05$, is chosen to limit its effect over 2019–2024 while pulling the share toward LS^{ss} over the terminal transition. This reduced-form restriction stabilizes the wage share; it does not impose equality between the real wage and the physical marginal product of labor.[17] Aggregate employment is $N_t = \sum_{i=1}^{12}\sum_{j\in\{H,S\}} N_{ij,t}$, with $N^{ss} = \sum_{i=1}^{12}\sum_{j\in\{H,S\}} N_{ij}^{ss}$. Aggregate gross inflation is $\Pi_t = P_t/P_{t-1}$; annual log inflation is $100 \log \Pi_t$, and cumulative log inflation relative to 2019 is $100 \log(P_t/P_0)$.

Paid wages. The rebuilding premium raises effective labor costs without requiring an equal increase in measured wages. We therefore distinguish the effective wage used in production from the wage recorded in the data. The attribution parameter x_{ij}^e determines how much of the premium enters measured pay:

$$w_{ij,t} = \tilde{w}_{ij}\, W_t \left(1 + x_{ij}^e \mathcal{W}_{ij,t}\right), \tag{14}$$

where $x_{ij}^e \in [0, 1]$ is the wage-attribution share. It is calibrated to observed wage paths after solving for the allocation. We do not attribute the residual pricing wedge $\mu_{i,t}^e$ to measured wages. This restriction keeps the wage consequences of rebuilding separate from residual price movements, though it can limit the model's ability to reproduce later wage catch-up.

[17] After 2024, the exogenous paths are held at their terminal values. Labor productivity can therefore differ from its initial steady-state level.

Inflation expectations. During the surge, one-year-ahead inflation expectations rose much less than realized inflation (Appendix Figure A6, Panel A). To reflect this pattern rather than generate counterfactual un-anchoring, we decouple firms' inflation beliefs from their quantity forecasts: firms have perfect foresight over their own quantities but evaluate the pricing condition (12) using a common aggregate inflation forecast, $\Pi^e_{t+1|t}$. We implement this distinction through the reduced-form expectations operator

$$\mathbb{E}_t\left[\Psi_i(\Pi_{ij,t+1})\,\tfrac{Y_{ij,t+1}}{Y_{ij,t}}\right] \equiv \Psi_i(\Pi^e_{t+1|t})\,\tfrac{Y_{ij,t+1}}{Y_{ij,t}}. \tag{15}$$

Here $Y_{ij,t+1}/Y_{ij,t}$ comes from the solved transition path. The operator specifies how firms form the expectation in the pricing condition, in place of full rational expectations over the nonlinear expression. We parameterize the common inflation forecast as

$$\Pi^e_{t+1|t} = \nu_{\text{forward}}\,\Pi^{\text{model}}_{t+1} + \nu_{\text{past}}\,\Pi_t + \nu_{\text{target}}\,\bar{\Pi}, \qquad \nu_{\text{forward}} + \nu_{\text{past}} + \nu_{\text{target}} = 1, \tag{16}$$

where Π^{model}_{t+1} is next period's aggregate inflation on the solved model path. The weights determine reliance on that future inflation, current inflation, and the nominal anchor. The baseline places substantial weight on the anchor ($\bar{\Pi}$). We also consider perfect foresight of aggregate inflation ($\nu_{\text{forward}} = 1$) as a robustness check. Under the aggregation convention in equation (15), this aggregate forecast is used in each node's pricing condition. Relative to the baseline, this variant implies a larger contemporaneous response of expectations than observed in Appendix Figure A6, Panel A.

Market clearing, final demand, and MPC. For each tier $k = 1, \ldots, 12$, output equals final demand plus intermediate demand from all nodes:

$$Y_{k,t} = D_{k,t}(\mathcal{Y}_t) + \sum_{i=1}^{12} \sum_{j \in \{H,S\}} \omega_{i,k} \left(\frac{P_{k,t}}{p^m_{i,t}}\right)^{-\rho} m_{ij,t}. \tag{17}$$

In consumer-facing tiers, final demand primarily represents personal consumption expenditures; in middle and upstream tiers, it may also include investment, government consumption, exports, and inventory accumulation. We do not distinguish among these categories or model households explicitly. Instead, a

time-varying shifter determines the level of final demand, and a coefficient denoted by MPC governs its response to aggregate real output relative to the observed path:

$$D_{k,t}(\mathcal{Y}_t) = D_k^{ss} \exp\left(\xi_{k,t}^e + \text{MPC} \cdot \left(\log \mathcal{Y}_t - \log \mathcal{Y}_t^{\text{data}}\right)\right), \tag{18}$$

where $\xi_{k,t}^e$ is a time-varying final-demand shifter recovered from the accounting fit (Section 4), $\mathcal{Y}_t^{\text{data}}$ is the observed real aggregate output path, and D_k^{ss} is the tier's steady-state final demand, the residual of the 2017 input–output identity (gross output minus intermediate demand from the endogenous tiers), held fixed throughout the transition. Real aggregate output is the gross-output sum, each tier weighted by the steady-state final-demand share of its chain:

$$\mathcal{Y}_t \;=\; \sum_{k=1}^{12} \frac{D_{c(k)}^{ss}}{Y_{c(k)}^{ss}}\, Y_{k,t}, \tag{19}$$

where $c(k)$ is the chain containing tier k, and D_c^{ss} and Y_c^{ss} are the chain's 2017 final demand from the SUT—PCE plus government consumption, investment, exports, and inventory change, net of imports—and its gross output. The ratio D_c^{ss}/Y_c^{ss} supplies a fixed final-demand weight common to the tiers of a chain, so $\mathcal{Y}_t$ is the model's real final-output aggregate. In the fully fitted model, $\mathcal{Y}_t = \mathcal{Y}_t^{\text{data}}$ and final demand reduces to $D_k^{ss} \exp(\xi_{k,t}^e)$. In counterfactuals, deviations of aggregate output from its observed path activate the MPC feedback, even when the recovered demand shifters are held fixed.

Exogenous sectors (EXO). The EXO block contains the real-estate, finance-and-government, and energy categories and imported inputs, all outside the endogenous production network. Their prices are exogenous, but endogenous producers choose their purchases from the EXO block as part of the intermediate-input bundle, with tier-specific weights. Selected EXO categories also enter the aggregate price index directly through their PCE shares; imported inputs are excluded from this direct component and affect the aggregate price index only through their influence on endogenous producers' costs. The fixed-weight aggregate price index combines the twelve endogenous tier composites with the direct PCE

contribution of the EXO block:

$$P_t = \sum_{k=1}^{12} c_k^{\text{PCE}} P_{k,t} + c^{\text{PCE-EXO}} P_t^{\text{PCE-EXO}}, \qquad \sum_{k=1}^{12} c_k^{\text{PCE}} + c^{\text{PCE-EXO}} = 1. \tag{20}$$

In counterfactuals that remove EXO price shocks, both the tier-specific EXO input-price indices and the direct PCE-EXO price index are held at their steady-state values in every year, including 2020. This is a model counterfactual that also removes indirect cost transmission; it is distinct from the empirical N-GO index, which excludes EXO sectors' direct aggregation weights.

3.4 Equilibrium

Given the initial steady state, the paths of EXO prices, and the reduced-form wedges, an equilibrium is a sequence of node-level prices, employment, production, and intermediate-input choices, together with the aggregate wage and inflation rate, such that: firms minimize production costs; workforce capacity and rebuilding costs evolve according to the cost-wall equations; prices satisfy the pricing condition; the base wage and inflation expectations follow their respective laws of motion; and output markets clear throughout the production network.

4 Calibration

The model is annual, with a steady state calibrated to 2019. All targets are expressed relative to chain-level trends.[18] We solve the nonlinear transition through 2050, treating the initial COVID contraction as unanticipated. Exogenous paths are recovered for 2020–2024 and held at their terminal values thereafter. The transition solver accommodates both the baseline adaptive-anchored inflation expectations and the perfect-foresight alternative; solving the quantity paths by foresight does not impose rational inflation expectations in the baseline.

Following the business-cycle-accounting methodology of Chari et al. (2007), we recover wedges that reconcile the model's equilibrium conditions with observed sectoral output, employment, and prices. The

[18] Real output and employment are detrended using 2017–2024 trends, while gross-output deflators and wages are detrended using the pre-pandemic 2017–2019 period. Online Appendix A.6 describes the construction.

resulting fitted transition reproduces tier-level gross-output prices to within 0.02 percentage points and tracks tier-level gross output and employment closely, with deviations of up to 3 percentage points in 2020 (Online Appendix Figure A2). This fitted transition establishes the structural accounting framework. We assess the rebuilding mechanism through counterfactuals that retain the recovered demand and productivity paths while removing selected cost and pricing components. In particular, the rebuilding contribution compares paths with and without the cost wall, with EXO price shocks and recovery-period residual pricing wedges set to zero in both and the structural 2020 pricing wedge retained in both. Section 5 describes the complete sequential decomposition.

The wage and price blocks allow limited short-run adjustment. We set the elasticity of annual base-wage growth to aggregate employment at $\phi_w = 0.15$. This choice is motivated by evidence of a relatively flat post-2000 Phillips curve (Furlanetto and Lepetit, 2024; Hazell et al., 2022; Del Negro et al., 2020), although those estimated price-inflation slopes are not direct estimates of the wage-rule parameter. Backward wage indexation is $\iota_w = 0.20$ and applies to four years of lagged inflation deviations rather than a single lag. The price block has no backward indexation ($\delta_{\text{index}} = 0$). Online Appendix A.4.2 examines the resulting cost–price relationships.

Table 3 summarizes the parameter values. Panel A reports technology and adjustment parameters; Panel B summarizes the accounting wedges and wage-attribution rule. The remainder of the section describes the details.

Network structure. The four chains and three tiers preserve upstream-to-downstream relationships in a tractable network. We construct the chains by twice applying a balanced spectral bisection to the BEA detail-level input–output graph, choosing partitions that limit trade across the cut. Each chain sources approximately 45–60% of its intermediates internally (C_1 58%, C_2 45%, C_3 48%, C_4 60%). These shares indicate concentration within chains without making them closed systems.[19]

Within each chain, we sort industries by *finalness*, $\text{finalness}_i \equiv g_i/\kappa_i$, where g_i is the direct PCE weight and κ_i is the Domar weight defined in Section 2. Industries with finalness of at least 70 percent form the consumer-facing tier h. We split the remaining industries at the gross-output-weighted median of

[19]The within-chain intermediate share for chain C is $\sum_{i\in C}\sum_{j\in C}\omega_{ij}\,\text{VA}_i \big/ \sum_{i\in C}\text{VA}_i$, where ω_{ij} is industry j's share of industry i's intermediate input bill (rows of Ω sum to one).

Table 3: Calibration summary

Parameter	Description	Value	Source
Panel A: Technology and adjustment parameters			
ρ	CES substitution elasticity	0.39	KLEMS
γ_i	Rebuilding-cost coefficient	per tier	Text
c^{wall}	Average rebuilding premium, 2021–22	0.13	Text
$q_0,\ q_1$	Monthly quit rates (normal, peak)	0.0225, 0.030	JOLTS
ψ	Warm-pool share	0.20	CPS/QWI
$\bar{\phi}_{c,h}$	Rotemberg price-adjustment cost, h tier	0.6–4.7	PSW
$\bar{\phi}_{ml}$	Rotemberg price-adjustment cost, m, l tiers	2.86	PSW
$\lambda_{c,h},\ \lambda_{ml}$	Downward-rigidity coefficient	1.9–14.1, 8.6	Text
ϕ_w	Base-wage response to employment	0.15	Text
ι_w	Wage indexation, per lag	0.20	Text
n	Wage indexation horizon (years)	4	Text
ι_a	Labor-share long-run anchor weight	0.05	Text
δ_{index}	Price indexation	0	Text
ε	Within-node demand elasticity	5	Text
β	Discount factor	0.96	Annual
α_i	Tier capital share	per tier	BEA 2017 SUT
η_{ij}	CES labor weight	per node	BEA 2017 SUT
$\tilde{w}_{ij}$	Steady-state wage premium	per node	BEA 2017 SUT
$\omega_{i,k}$	Domestic I–O coefficients	12×12	BEA 2017 SUT
ω_i^{EXO}	EXO-input share, per tier	per tier	BEA 2017 SUT
D_c^{ss}/Y_c^{ss}	Chain final-demand share, net of imports	per chain	BEA 2017 SUT
Panel B: Calibrated objects			
$a_{i,t}^e$ (12×5)	Productivity wedge	Matches tier-level N path	
$\xi_{i,t}^e$ (12×5)	Final-demand wedge	Matches tier-level Y path	
$\bar{\tau}_i^e$ (12)	Tier-mean labor wedge, 2020	Normalized into $a_{i,2020}^e$	
$\Delta\tau_c^e$ (4)	Hit/safe labor-wedge spread, 2020	Chain stdev(min$\{0, \Delta \log N\}$), QCEW	
$\bar{\mu}_i^e$ (12)	Structural 2020 pricing wedge	Matches tier-level P_{GO} in 2020	
x_{ij}^e	Wage-attribution share	Tier wage paths, 2021–24; shared by hit/safe	
$\mu_{i,t}^e$ (12×5)	Residual pricing wedge	Closes tier-level P_{GO} gap, 2020–24	

Notes: Here i indexes the twelve chain-by-tier composites and $j \in \{H, S\}$ the hit and safe nodes. The target $c^{\text{wall}} = 0.13$ is the additional labor-cost premium relative to the base wage, averaged over binding observations in 2021–2022; equation (21) determines γ_i. The baseline applies $\rho = 0.39$ to labor–input, across-input, and hit–safe substitution; $\varepsilon = 5$ governs demand within nodes. Panel B gives roles in the joint accounting fit; wage attribution is calibrated afterward. Detrending follows Appendix A.6. PSW denotes Pasten et al. (2020).

finalness into a middle tier m and an upstream tier l. We then split each chain-by-tier group into hit and safe nodes using the distribution of 2020 employment changes, weighted by 2019 employment. Online Appendix A.2.1 describes the median-based rule and its finer-industry refinement where a single BEA industry dominates a tier.

Figure A1 in Online Appendix A.2 shows the resulting intermediate-input shares across the 24 nodes: the blocks along its diagonal display the within-chain concentration of purchases, and the cells outside them the cross-chain links through which cost pressures can spread. Figure 3 shows the constructed chains and the input flows between them. Each ribbon is a purchase by the buying sector on the right from the selling sector on the left, and its width shows the importance of that flow to the buyer. Panel A draws purchases from lower tiers and Panel B purchases from higher tiers, on a common scale. Each bar is the cell's total input purchases, and its black segment is the part drawn as ribbons in that panel. Purchases from upstream tiers are more than twice as large as purchases from downstream tiers, so cost pressure at upstream producers travels mainly toward consumer-facing producers, within and across chains.

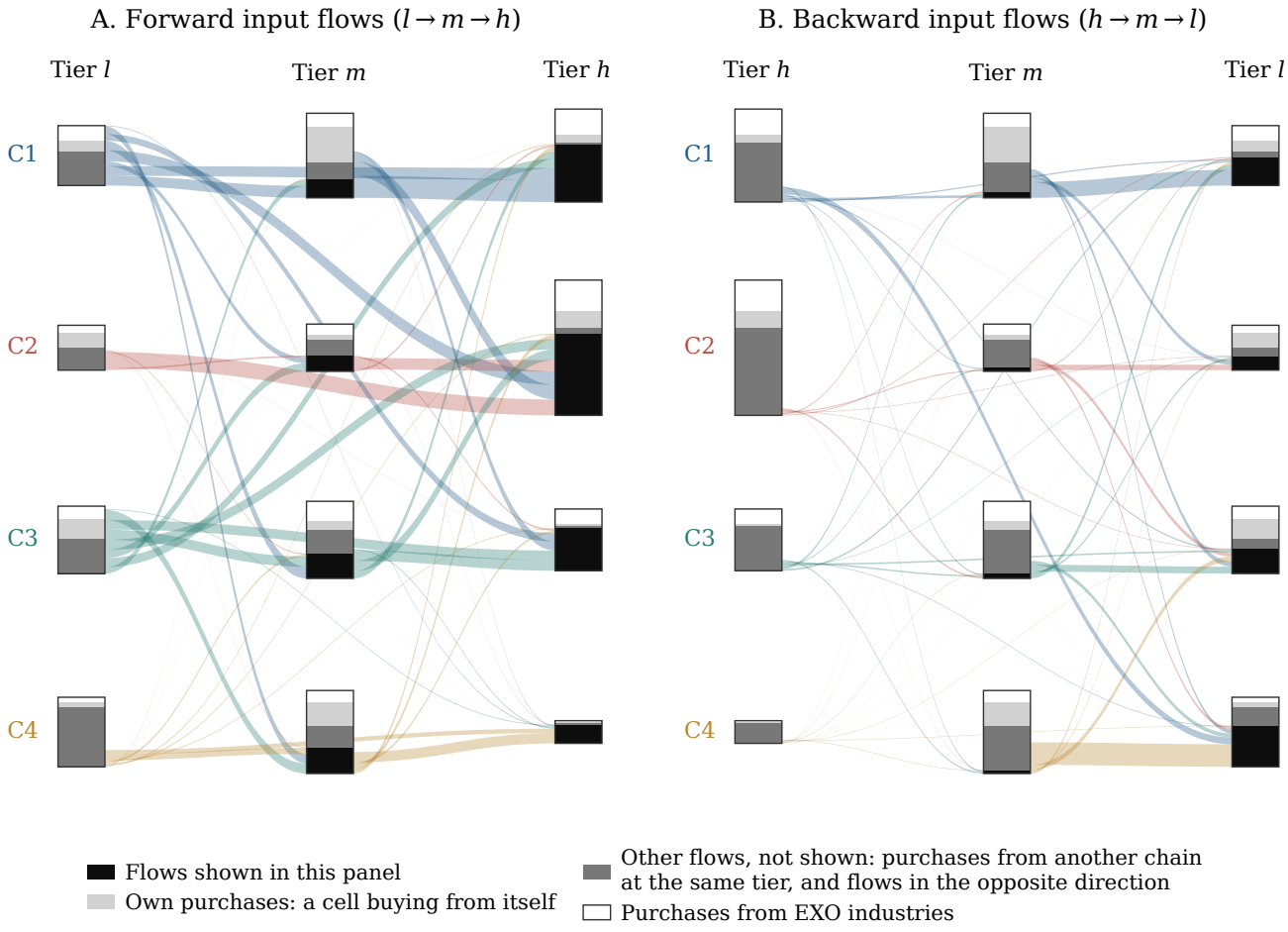

Figure 3: Model production network structure.

Notes: Each bar is one chain-by-tier cell, combining its hit and safe nodes, drawn at its total purchases of domestic intermediate inputs. Ribbons are directional flows: purchases by the buying sector on the right from the selling sector on the left, from lower to higher tiers in Panel A and from higher to lower tiers in Panel B. Black is the part of those purchases shown as ribbons in this panel. Dark gray is the cell's other purchases within the twelve cells that this panel does not draw: from another chain at the same tier, or in the opposite direction. Light gray is what the cell buys from itself. White is what it buys from the sixteen EXO industries. Network construction is described in Online Appendix A.2.

The chains differ in industry composition. C_1 combines professional and information services; C_2 combines personal services and food production; C_3 links health and hospitality to chemical inputs; and C_4 combines manufacturing and construction. Online Appendix A.2.2 provides the detailed composition.

Production. We set the common substitution elasticity to $\rho = 0.39$, following the estimate in Section 2. At first order, the accounting decomposition requires only the labor–input elasticity; the other substitution elasticities do not enter that identity. Using the same value for all three margins in the nonlinear model is an additional calibration restriction. The sensitivity exercises vary substitution across inputs and producers.

Recalls from unemployment. Because an unusually large share of pandemic layoffs, and even of business closures, was temporary in 2020, the calibration must separate transient disruptions from persistent capacity destruction. To measure the employment shortfall that enters the cost wall, we apply the growth rate between January–February 2020 and January–February 2021 to the 2019 annual-average employment level. This measure excludes the short-lived March–April 2020 layoffs that were largely reversed by year-end. Measuring it between the 2019 and 2020 annual averages instead would raise it by only about 3 percent, because employment in early 2021 was still nearly as depressed as the 2020 average. Recoverable matches among the remaining shortfall are handled through the warm-pool share ψ.

We set ψ by combining a stock measure of temporary layoffs with a flow measure of recalls. For the stock measure, in January 2021 there were 10.1 million unemployed, versus 5.8 million in January 2020, and 2.7 million workers on temporary layoff, versus 0.65 million in January 2020. Excess unemployment was therefore $4.3 = 10.1 - 5.8$ million, of which excess temporary layoffs ($2.1 = 2.7 - 0.65$ million) were about half.[20]

For the flow measure, the Quarterly Workforce Indicators record hires of workers rehired by an employer they had left within the prior four quarters. Pooled over the 341 endogenous industries and taken in excess of each industry's own 2017–2019 same-quarter baseline, excess recalls over 2020:Q2–2021:Q1 were 2.1 million against 4.4 million excess separations in 2020:Q1–Q2, a recall ratio of 46 percent; the ratio

[20] This calculation uses seasonally adjusted CPS data reported in U.S. Bureau of Labor Statistics (2021). Additional evidence on recalls from unemployment-insurance records for California is in California Policy Lab (2021).

is 36 percent in the hit tiers, where capacity destruction is concentrated, and 66 percent in safe industries. We use these ratios as proxies for the share of temporary separations that preserve a recoverable employment relationship.

Multiplying them by the one-half temporary-layoff share gives ψ between 0.18 and 0.23, and we set $\psi = 20\%$. This is a calibration approximation that combines two data sources. Under the capacity rule each node's positive shortfall scales with $1 - \psi$, so the endpoints 0.18 and 0.23 change the shortfall by +2.5% and −3.75% relative to the baseline, without changing the ranking of the 24 nodes.[21]

Capacity rebuilding cost (CW). The quantitative scale of the mechanism hinges on the rebuilding-cost target, c^{wall}. We discipline it using microeconomic estimates of hiring expenditures, their response to hiring intensity and labor-market tightness, and the expected duration of employment matches. Online Appendix A.10.1 reports sensitivity to this target and related calibration choices. Expressed as a fraction of the base wage W, the target is constructed from hiring costs evaluated at the 2022 peak of U.S. labor-market tightness and turnover. We impose the same target in every tier: this peak-input estimate equals each tier's average premium over its binding observations in 2021–2022. We then choose each tier's coefficient γ_i to satisfy

$$\gamma_i = \frac{c^{\text{wall}}}{\overline{(\Delta N^+)^2}_i}, \qquad \overline{(\Delta N^+)^2}_i = \frac{\sum_{t\in\mathcal{T}} \left(\Delta N^+_{i,t}\right)^2 \mathbf{1}\{\Delta N^+_{i,t} > 0\}}{\sum_{t\in\mathcal{T}} \mathbf{1}\{\Delta N^+_{i,t} > 0\}}, \tag{21}$$

where i denotes the tier and $\mathcal{T} = \{2021, 2022\}$ collects the peak rebuilding years. This restriction equates the tier-level rebuilding premium, averaged over the binding observations in these two years, to c^{wall}; it does not require the premium to equal that target in each year or at every firm. Here $\Delta N^+_{i,t}$ is the positive part of tier i's detrended employment growth. The same γ_i applies to the hit and safe nodes within a tier. They therefore face the same cost schedule, but each node's premium depends on its own expansion.

To discipline c^{wall}, we draw on the labor literature estimating the convexity of hiring costs in extraordi-

[21] Recalls are same-employer hires with a four-quarter lookback, so the ratio is a lower bound on retained workforce-embodied capital and does not capture recalls of 2020 separations that occurred later in 2021; the underlying LEHD data exclude Alaska and Michigan; we report pooled ratios because per-industry ratios are noisy. The classification into hit and safe industries uses no recall data, so the gap between their recall rates is independent evidence that it separates temporary from permanent separations.

narily tight markets.[22] We anchor our estimates to Linckh et al. (2025), Muehlemann and Strupler Leiser (2018), and Muehlemann and Pfeifer (2016). Specifically, Linckh et al. (2025) estimate that a one-standard-deviation increase in local labor market tightness (measured by the vacancy-to-unemployment ratio, V/U) raises post-match hiring costs—primarily adaptation and disruption time—by 10 to 12%. Using this estimated response in our calibration, we observe that the U.S. V/U ratio rose from roughly 1.2 in late 2019 to 2.0 at its 2022 peak, an increase of approximately three standard deviations relative to its historical distribution (Domash and Summers, 2022).[23]

Linckh et al. (2025) estimate that filling a skilled-worker vacancy costs approximately 22 weeks of wages in normal times (2015–2019), with roughly 80% of that cost arising after the match, in informal training and disruption of incumbent workers. We take this as the normal-times average cost per hire, $Q_0 = 22/52 \approx 0.423$ for a normalized unit wage. (The shorter baseline in Muehlemann and Strupler Leiser (2018) gives a lower c^{wall}, which we include among the sensitivity exercises.) To obtain the tight-market cost, we extrapolate the 10 to 12% response of post-match costs per standard deviation of tightness to the total cost per hire and apply a three-standard-deviation tightening: $1 + 3 \times 0.12 = 1.36$, which raises the cost per hire to $Q_1 = 30/52 \approx 0.577$, an additional eight weeks of wages.

Asset-price evidence provides an independent check on the scale: Merz and Yashiv (2007) estimate the marginal cost of a hire at 1.48 times output per worker, which at their sample wage share of 0.66 is about 2.2 quarters, or roughly 29 weeks, of wages. That is a marginal-cost estimate, whereas Q_1 is an average cost that we convert to marginal cost below; the two are comparable in scale.[24] Regional evidence from Gitti (2026), which shows new-hire wages responding to tightness only above a labor-shortage threshold, is consistent with this convexity across markets. It speaks to wages rather than to the nonwage cost.

[22] Both c^{wall} and $\gamma_i(\Delta N^+)^2$ measure an additional labor cost relative to the base wage, rather than an increase in the cost of all inputs. We therefore match them directly. The industry's labor-cost share enters when the effective wage is translated into production marginal cost through equation (11); it is not an additional adjustment to the target.

[23] Cross-sector tightness patterns motivate the common target. JOLTS openings over CPS unemployment by prior supersector are +2.5 to +4.9 SD above their 2001–2019 baseline in ten of eleven supersectors (financial activities: +0.8 SD). The average, about +3.5 SD, is slightly above the 3 SD used here. In a regression on the 2020 employment collapse, the slope is close to zero ($\beta = -0.012$ SD per pp, $R^2 < 0.01$, $N = 11$, WLS by 2019 employment). Leisure and hospitality, which lost 23 pp, tightened no more in V/U than transportation, which lost less than 1 pp. Forsythe et al. (2022) find similar patterns using more granular job-postings data.

[24] Their estimate is evaluated at a mean gross hiring rate of 8.9% per quarter. It is imprecise—a standard error of 0.57 spans roughly 18 to 40 weeks—but it is identified from U.S. corporate market values rather than from firm-level cost accounting, so it is informative as an independent check on the level.

A hire creates workforce-specific capital: the firm pays an upfront cost Q and uses the resulting productive relationship until separation. Following the quasi-fixed-factor interpretation of labor (Merz and Yashiv, 2007), we convert this expenditure into the annualized user cost $(r + \delta(q))Q$. Higher turnover shortens the expected duration of the relationship and raises its annualized cost. Here $r = 0.06$ is the firm's real discount rate for this investment, and $\delta(q) = 12[-\log(1-q)]$ converts the monthly quit rate q into an annualized separation hazard. We use the 2017–2019 JOLTS average ($q_0 = 0.0225$) and the recovery peak ($q_1 = 0.030$), implying hazards of 0.273 and 0.366, respectively.[25]

A second source of rising costs is firm-level hiring intensity. Let H denote the hiring rate. With a hiring-cost schedule $C(H) = H^\eta$ and $\eta = 1.3$ (Muehlemann and Pfeifer, 2016), marginal cost is $C'(H) = \eta C(H)/H$. Thus, η converts average into marginal hiring cost at a given hiring rate. We use the rise in quits as a proxy for increased hiring intensity: the implied change along the marginal-cost schedule is $(q_1/q_0)^{\eta-1} \approx 1.09$, given $q_1/q_0 = 1.33$. This intensity adjustment is separate from the market-tightness adjustment to Q.[26]

We further scale down the resulting c^{wall} estimate by the share of the wage bill representing "skilled" workers in the relevant sense. We estimate that roughly four-fifths of the wage bill aligns with the Linckh et al. (2025) definition of workers requiring meaningful training. Assuming that hiring workers outside this definition entails no convexity, we set $\kappa_{\text{skill}} = 0.8$.

Combining these elements yields the final calibration target:

$$c^{\text{wall}} = \kappa_{\text{skill}}\, \eta \left[(q_1/q_0)^{\eta-1} \big(r + \delta(q_1)\big) Q_1 \;-\; \big(r + \delta(q_0)\big) Q_0 \right], \tag{22}$$

The bracket compares annualized hiring costs under tight-market and normal conditions. At $Q_0 = 22/52$, $Q_1 = 30/52$, $q_0 = 0.0225$, $q_1 = 0.030$, and $r = 0.06$, the normal-times user cost is $(r + \delta(q_0))Q_0 \approx 0.141$.

[25] Labor-market tightness and turnover may themselves respond to inflation (Afrouzi et al., 2026); we condition on their observed values when calibrating rebuilding costs, without separately modeling this feedback.

[26] The firm-level intensity estimate in Muehlemann and Pfeifer (2016) and the market-tightness response in Linckh et al. (2025) discipline separate margins. Swiss evidence in Blatter et al. (2012) also shows convex hiring costs: marginal costs rise about 45% between the first and tenth hire. Using aggregate U.S. corporate-sector data and Q-theory, Merz and Yashiv (2007) estimate hiring-rate curvature of 3.40 (SE 0.15). Their aggregate variation can combine firm intensity and market tightness, so this is not directly the same parameter as our η. For a 33% rise in hiring, their estimate implies a marginal-cost ratio of approximately 2.0, compared with $1.09 \times 1.36 \approx 1.5$ from our two cost adjustments. Accounting additionally for the shorter expected match duration raises our annualized user-cost ratio to about 1.9. This last adjustment reflects turnover, not hiring-cost curvature. Differences in samples and identification limit a direct comparison.

Including the higher hiring intensity, the corresponding tight-market value is $(q_1/q_0)^{\eta-1}(r+\delta(q_1))Q_1 \approx 0.268$. The factor $\eta = 1.3$ converts the cost difference to marginal hiring cost, and $\kappa_{\text{skill}} = 0.8$ adjusts for the wage-bill share of workers requiring substantial training. Thus, $c^{\text{wall}} = 0.8\times1.3\times(0.268-0.141) \approx 0.13$. This is the additional premium relative to normal hiring costs, not the full cost of a hire.

Price stickiness. We calibrate price-adjustment costs using the monthly price-change frequencies of Pasten et al. (2020) (PSW). We first convert each industry's monthly non-reset probability, $1-f_m^i$, into the probability of no reset over a year, $\lambda_a^i = (1-f_m^i)^{12}$. We then average these annual probabilities within each chain-by-tier cell and map the result into $\bar{\phi}_i$ by matching the local Calvo and Rotemberg pricing slopes.[27] PSW frequencies match 218 of the 357 BEA industries directly. For unmatched industries, we use progressively broader NAICS/BEA matches and analogous industries for twenty uncovered service categories. We use 2019 QCEW wage bills as the aggregation weights. The baseline retains four chain-specific consumer-facing values and uses a common value, $\bar{\phi}_{ml} = 2.86$, for the middle and upstream tiers; Online Appendix A.8 details the matching, the aggregation, and the resulting values.

Downward price rigidity. Prices adjust more readily above than below the nominal anchor. This asymmetry limits deflation during the initial contraction. Guided by evidence on asymmetric price adjustment (Eichenbaum et al., 2011; Cavallo et al., 2024), we consider a 3–5× range and set $\lambda_i = 3\bar{\phi}_i$ in the baseline. In the specified adjustment-cost function, this makes curvature below the anchor four times curvature above it. We impose the same ratio across tiers: $(\lambda_{C1,h}, \lambda_{C2,h}, \lambda_{C3,h}, \lambda_{C4,h}) = (1.88, 9.95, 14.07, 6.26)$ and $\lambda_{ml} = 8.58$. The sensitivity exercises include a lower value.

Inflation expectations. We discipline the expectations operator with the Cleveland Fed model-implied series, using the Michigan household survey as a comparison. The adding-up-constrained projection in Online Appendix A.9 loads primarily on the target and past inflation and permits a negative coefficient on realized future inflation. We therefore impose $(\nu_{\text{forward}}, \nu_{\text{past}}, \nu_{\text{target}}) = (0,\ 0.25,\ 0.75)$

[27] The conversion is $\bar{\phi}_i \approx (\varepsilon-1)\lambda_a^i/[(1-\lambda_a^i)(1-\beta\lambda_a^i)]$, with $\beta = 0.96$ and $\varepsilon = 5$. It is a calibration convention based on a local equivalence, not an exact equivalence of the nonlinear transition paths.

as a parsimonious nonnegative calibration, not as estimated structural information weights. The perfect-foresight variant provides a sensitivity check.

MPC. We set the final-demand feedback coefficient in equation (18) to MPC = 0.4. As a benchmark, the heterogeneous-agent, incomplete-markets model of Dupor et al. (2023) implies an average annual MPC of 0.37 and is disciplined by cross-regional estimates of consumer-spending responses to ARRA government spending. In our log-demand specification, MPC is the elasticity of final demand with respect to aggregate real output, holding the recovered shifter and observed reference path fixed; the consumption estimate guides its scale rather than directly estimating that coefficient.

Accounting wedges. Five sets of wedges bridge the model and the sectoral data. First, the final-demand shifter $\xi^e_{i,t}$ and the productivity wedge $a^e_{i,t}$ jointly match gross output and employment; conditional on output, the productivity wedge determines the path of employment N needed to match the path of measured Y/N. Second, the transitory 2020 labor wedge τ^e_{ij} targets the uneven employment collapse between hit and safe nodes. After its tier-mean component is normalized into $a^e_{i,2020}$, the remaining hit–safe contrasts, $\Delta\tau^e_i \equiv \tau^e_{i,S} - \tau^e_{i,H}$, are scaled by four chain-level amplitudes to match the excess dispersion of employment declines. The calibration moment isolates capacity destruction by replacing positive employment growth by zero before taking its standard deviation; it is distinct from the mean-centered dispersion measure used in the descriptive comparison.

Predetermined exposure and realized employment losses serve different purposes in the two parts of the paper. The event study uses exposure to trace pandemic-related disruption without constructing its regressor from realized employment or prices. The model instead requires the distribution of workforce capacity inherited at reopening, which we discipline with observed employment losses and the recall adjustment. Conditional on that inherited state, the rebuilding premium depends on subsequent expansion, not on whether the initial losses arose from workplace disruption or weak demand. Recovery demand is captured separately by the wedges $\xi^e_{i,t}$. We therefore directly target the dispersion of employment losses rather than the dispersion of exposure in the model calibration.

The pricing wedges match tier-level prices. The structural 2020 wedge $\bar{\mu}^e_i$ matches collapse-year prices,

while $\mu^e_{i,t}$ closes the remaining price residual, which is concentrated in 2021–2024. The rebuilding counterfactuals retain the former and remove the latter in all periods. These are distinct roles within a joint accounting fit, not separate one-equation estimates.

The wage-attribution share x^e_{ij} maps the rebuilding premium into measured wages through equation (14). It does not enter the remaining equilibrium conditions and is calibrated after solving the allocation. Hit and safe nodes within a tier share the same value.[28]

Other parameters. Two remaining parameters govern the terminal wage-share adjustment and steady-state pricing. The small coefficient ι_a anchors the labor share while limiting its influence during 2019–2024. The demand elasticity $\varepsilon = 5$ implies a price-to-marginal-cost ratio of 1.25, or a 20% price–marginal-cost gap as a share of revenue. For comparison, the input–output-based surplus-to-gross-output ratio averages approximately 24% across endogenous industries.[29] This accounting surplus is not a direct estimate of the price–marginal-cost gap, since it also covers returns to fixed inputs and other unmeasured costs.

5 Results

We now assess whether the workforce-rebuilding mechanism can account for the empirical pattern: substantial early price pressure beyond measured costs, concentrated in disrupted supply networks. With the rebuilding-cost scale disciplined externally, we first quantify its aggregate inflation contribution conditional on the demand and productivity paths inferred from the recovery. We then examine how the recovery path shapes the inflation–employment relationship and relative prices, before isolating the contribution of uneven inherited capacity.

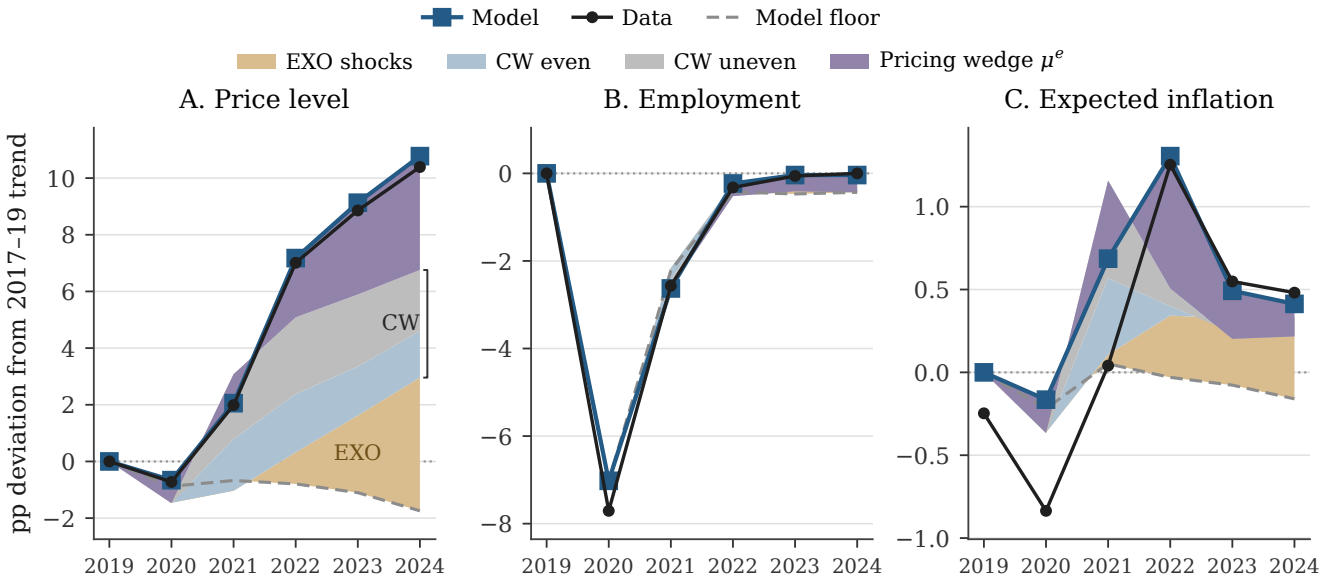

Figure 4: Saturated model decomposition of detrended data aggregates.

Notes: Price level, employment, and one-year-ahead expected inflation relative to the benchmarks in Appendix A.6. "Model" (blue squares) is the fitted model, with all wedges and the EXO price shocks. Black circles are the data, with the Cleveland Fed expectations series in Panel C. The dashed model floor sets the recovery pricing wedges ($\mu^e = 0$), the EXO price shocks, and the rebuilding costs ($\gamma_i = 0$) to zero and retains the structural 2020 wedges. Each band is the difference between two successive paths, removed top-down. The recovery pricing wedges μ^e (purple) are "Model" minus "Model $\mu^e = 0$". The EXO shocks (amber) are "Model $\mu^e = 0$" minus "Model $\mu^e = 0$, no EXO". The rebuilding contribution is "Model $\mu^e = 0$, no EXO" minus the model floor, split into rebuilding with capacity even within pairs (light blue, CW even) and within-pair unevenness (gray, CW uneven), as defined in Section 5.2. The bands plus the floor add up to the fitted path. Contributions depend on the removal order.

5.1 Inflation accounting

Figure 4 reports a top-down decomposition of the PCE-weighted gross-output price level, employment, and expected inflation, alongside their observed paths. The price panel shows cumulative above-trend inflation. Starting from the fitted transition, we remove the recovery pricing wedges, the exogenous price shocks, and finally the workforce rebuilding costs, re-solving the model at each step without re-calibrating it.[30] The last path is the model floor: the recovery generated by the recovered demand and

[28] For each tier, we search over $[0, 1]$ for the largest value of x_{ij}^e that does not make model-implied wages exceed the observed tier wage path during 2021–2024 (ECI/QCEW). This restriction implements the closest fit without overshooting; it is not an independent estimate of a bargaining parameter.

[29] Alternative calculations yield ratios between 20% and 30%. We use $(GO_i - CE_i - MAT_i)/GO_i$ in the 2017 detail use table at producer prices, where GO_i is industry gross output, CE_i is compensation of employees, and MAT_i is intermediate-input expenditure. Taxes on production remain in the residual. Ratios are winsorized at the 3rd and 97th percentiles and aggregated across the 341 endogenous BEA industries using value-added weights, yielding 23.7% (24.2% without winsorization).

[30] The decomposition is top-down. Starting from the fitted model, each step removes one more component in every period, including 2020, and re-solves the model holding all other calibrated parameters fixed. The first step sets the twelve recovery pricing wedges to zero ($\mu^e = 0$). While these wedges are concentrated in 2021–2024, removing their 2020 remainders directly lowers 2020 inflation by 0.81 percentage points. The second step removes the fifteen exogenous price shocks: the real-estate, finance-and-government, and energy blocks, and twelve tier-level import prices. Removing them in 2020 extracts the 2020

productivity shifters alone, with the structural 2020 pricing wedge retained. The rebuilding contribution is the difference between the wall-on and wall-off paths after removing the first two components. Both paths hold the recovered demand and productivity shifters and the structural 2020 pricing wedge fixed. This difference isolates the inflationary contribution of the rebuilding friction.

The cost wall mechanism accounts for much of the inflation surge through its 2022 peak. Specifically, rebuilding costs contribute 4.8 pp to cumulative above-trend inflation, roughly two-thirds of the observed 7.2-pp increase, or 79 percent of the surge net of the EXO contribution. This inflationary pressure is front-loaded: the cost wall adds 4.1 pp through 2021 alone, exceeding the observed 2.1-pp increase because other components offset part of the pressure. The EXO contribution is small and negative through 2021 and about 1 pp by 2022. Residual recovery-period pricing becomes more important later, contributing roughly 4.0 pp by 2024. Expected inflation peaks in 2022 in both the model and the data, although it rises earlier in the model, in 2021.

The model floor lies below the pre-pandemic price trend because of the wage Phillips curve (equation (13)). Employment remains below steady state for several years, so the labor-market slack term puts persistent downward pressure on base-wage growth. With rebuilding costs, EXO price shocks, and recovery pricing wedges removed, this slack produces deflation relative to trend. Backward indexation then transmits lower prices to future wage growth, even beyond 2025, when employment recovers. The early increase in measured output per worker, partly driven by the productivity wedges, deepens the shortfall by lowering unit costs. This drag dissipates slowly: the price shortfall is greatest in 2024, remains about 0.2 pp through the end of the decade, and becomes negligible only in the mid-2030s.

The observed labor productivity path is consistent with the workforce-rebuilding narrative. Selective losses of lower-productivity jobs raised measured output per worker in 2021 (Crust et al., 2020; Fernald and Li, 2022; Stewart, 2022). As employment recovered, the reversal of this composition change, together with training and organizational disruptions, slowed productivity growth the following year. Decreasing returns in the model are insufficient to generate this cycle, so the calibration absorbs it into the exogenous

energy-price collapse, isolating domestic sources of inflation. The third step sets the rebuilding-cost parameters to zero ($\gamma = 0$). Every path keeps the structural 2020 pricing wedge $\bar{\mu}_i^e$, the 2020 labor wedge τ_{ij}^e, and the demand and productivity wedges $\xi_{i,t}^e$ and $a_{i,t}^e$ in all years. In this decomposition, the 2020 employment collapse remains essentially unchanged across these paths. Online Appendix A.10.3 presents an alternative specification solved under perfect foresight.

productivity wedges.

The cost decomposition shows how this sequence shifts inflation over time. The 2021 productivity burst holds inflation down by 3.4 pp, against a long-run contribution near 1 pp a year, deferring 2.4 pp of price pressure. In 2022, productivity takes only 0.1 pp out of inflation: the reversal returns about 0.9 pp of the deferred pressure, and productivity's contribution swings by 3.3 pp between the two years. This coincides with material costs' largest contribution, 7.9 pp. The sequence therefore lengthens the episode by shifting pressure into the year when network costs were at their peak.[31]

Figure 5 shows why the inflation–employment relationship depends on the recovery path. Current employment alone does not determine the cost of expansion: that cost also depends on the workforce inherited from the preceding period and on how rapidly producers must add to it. Employment restored today enlarges the capacity available tomorrow, so gradual restoration spreads adjustment over smaller increments. Rapid rebuilding can therefore generate substantial inflation while aggregate employment remains below its previous level. Panel A shows the steepening of the impact response to expansionary demand shocks, while Panel B follows the episode through inflation–employment space. Rebuilding pressure is strongest early in reopening. The subsequent reversal of the productivity offset helps sustain inflation as measured unit labor costs rise. The recovery trajectory consequently need not follow the impact-response curve obtained from a shock to steady state.[32]

The model also generates within-chain price dispersion in 2019–2021, a statistic the calibration does not target. It exceeds the data in C_1 and falls short in C_3 and C_4 (Panel C; Online Appendix A.10.4 adds the 2021–2023 window).

5.2 Role of shock unevenness

In a networked production economy, the distribution of inherited workforce capacity following the 2020 contraction dictates the inflationary impact of rebuilding just as much as the aggregate scale of the decline. Within any given chain-by-tier group, the hit producer suffered a more severe 2020 employment contraction than its safe counterpart. To reach the same employment level relative to its steady state,

[31] Online Appendix A.10.3 reports the comparison under perfect-foresight inflation expectations, which changes the timing and persistence of the response.

[32] Regional evidence in Cerrato and Gitti (2025) and Gitti (2026) documents state-dependent inflation–activity relationships.

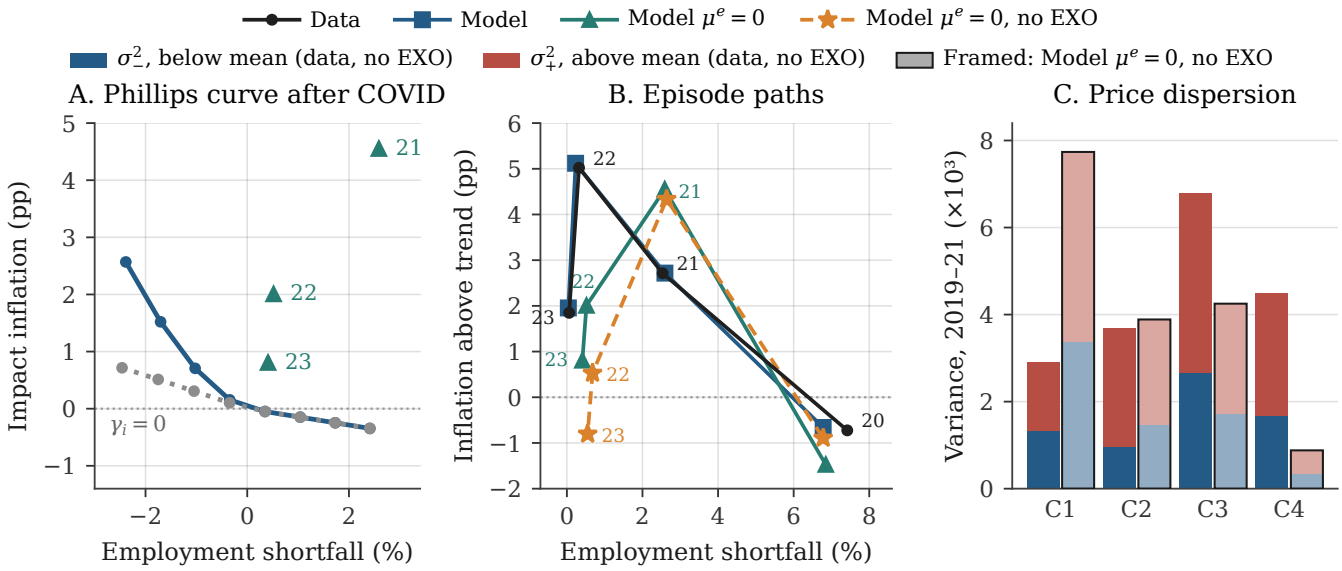

Figure 5: Aggregate and relative-price implications of workforce rebuilding.

Notes: Adaptive-anchored expectations, MPC = 0.40. Model paths: "Model" retains all fitted wedges and the EXO price shocks. "Model $\mu^e = 0$" sets the recovery pricing wedges to zero and keeps the EXO price shocks and the rebuilding costs. "Model $\mu^e = 0$, no EXO" also sets the EXO price shocks to zero. All model paths retain the structural 2020 pricing wedge. Panel A traces the model's impact Phillips curve from steady state. Each point is the first-period response of inflation and of the employment shortfall to a separate one-period aggregate shock to the final-demand shifter ξ^e of equation (18), of size ±0.1, ±0.3, ±0.5, or ±0.7 percent, so points differ by shock size, not by date. The solid blue curve retains the rebuilding costs and the dotted gray curve sets them to zero ($\gamma_i = 0$). Triangles mark the 2021–2023 outcomes of "Model $\mu^e = 0$" along the recovery. Panel B plots annual inflation against the employment shortfall over 2020–2023 for the data and the three model paths. Panel C reports the within-chain variance of cumulative 2019–2021 log price growth, multiplied by 10^3 and split around the weighted mean, for the data, which exclude the EXO industries (solid bars, left), and for "Model $\mu^e = 0$, no EXO" (framed bars, right). Sources and weights: Online Appendix A.11.

the hit producer must expand much further beyond its inherited capacity. Because adjustment costs are convex, this steeper expansion path incurs a disproportionately large premium. Buyers ultimately pay this premium because the outputs of hit and safe producers are imperfect substitutes, preventing them from costlessly redirecting purchases to unaffected suppliers.

To quantify the aggregate importance of this unevenness in our saturated model, we redistribute each pair's inherited capacity in proportion to its producers' steady-state employment.[33] This counterfactual ensures the employment decline of hit and safe producers is no longer uneven, while the aggregate capacity decline matches the baseline. For example, in the consumer-facing tier of chain C_1, the hit and safe producers initially inherit capacities equal to 87 and 113 percent of their respective steady-state employment. The counterfactual reassignment thus equalizes both to 99.3 percent, meaning that in this

[33] Let $C_{ij} = N^{CW}_{ij,2}$ be the recall-adjusted 2020 inherited workforce size and $C_i = C_{iH} + C_{iS}$. The even path assigns $C^{even}_{ij} = N^{ss}_{ij} C_i / (N^{ss}_{iH} + N^{ss}_{iS})$, so $\sum_j C^{even}_{ij} = C_i$.

specific tier, very little aggregated capacity is lost relative to 2019. Broad differences across the supply chains remain, such as the 86 percent capacity in the middle tier of C_3 versus the 103 percent capacity upstream. There is, therefore, still unevenness in this system because our exercise *only* eliminates within-tier unevenness.

The reassignment changes only the capacity threshold at the start of 2021. We keep the 2020 allocation, cost coefficients, and recovered demand and productivity shifters fixed, remove recovery pricing wedges and EXO shocks in both paths, and re-solve the recovery. From 2022 onward, each path's inherited capacity is its own previous-year employment under equation (10). The paths without rebuilding costs coincide.

Perhaps one of the more striking results of the paper is that redistributing capacity eliminates half of inflationary pressure implied by CW. Specifically, equalizing inherited capacity within pairs reduces the contribution of workforce rebuilding through 2022 from 4.76 to 2.05 percentage points—a 57 percent reduction. In Figure 4, the gray band captures the contribution of unevenness graphically. Online Appendix A.10.2 reports the numerical comparison and sensitivity to the substitution structure.

5.2.1 Comparison with the Great Recession

The aggregate employment collapse of the Great Recession was similar in size to that of 2020: employment changed by −6.5% between 2007 and 2009 and by −6.8% in 2020. Yet only the COVID recovery was accompanied by an inflation surge. In our framework, three features of the Great Recession kept rebuilding pressure low.

First, its recovery was slow. Four years into the recovery, employment stood at −0.4% relative to its pre-collapse level, against 4.8% after 2020. Within two years, employment gains in the industries that had contracted amounted to about 32 percent of their losses, against 92 percent after the pandemic (Figure 1, Panel A). Producers therefore rebuilt their workforces in small annual steps, and because rebuilding costs are convex in the pace of expansion, small steps generate little additional cost.

Second, its expansion was no more uneven than in normal times, although its losses were comparably dispersed. Over the collapse windows, the cross-industry variance of employment changes was similar in the two recessions (Online Appendix A.11). Over the two recovery years, the variance of employ-

ment growth was close to its 2017–2019 level after the Great Recession, whereas after the pandemic it was about two and a half times that level, mostly because of industries expanding faster than average (Figure 1, Panel B). Section 5.2 shows that uneven inherited capacity accounts for more than half of the COVID rebuilding-implied contribution. A gradual recovery spreads the rebuilding of the most depleted producers over time. As a result, even comparably uneven losses generate little rebuilding-implied inflation pressure.

Third, the labor market stayed slack. The calibration disciplines the rebuilding-cost coefficients γ_i with the hiring-cost premium of equation (22), which depends on how far quit rates exceed their normal level. Quit rates in 2010–2013 remained below that level, so the same calibration applied to the Great Recession would assign little or no premium and correspondingly small coefficients. Applying the coefficients calibrated to the tight labor market of 2021–2022 to that recovery would therefore overstate its rebuilding costs.

Together, these features imply that workforce rebuilding was not a material source of inflation after 2009. Consistent with this, the cross-industry dispersion of price growth outside commodity-price-linked industries did not rise during the recovery from the Great Recession, whereas in 2020–2021 and 2021–2022 it averaged about eight times its 2017–2019 level (Figure 1, Panels C and D, and Online Appendix Figure A7). The model also generates substantial within-chain price dispersion in 2019–2021 (Figure 5, Panel C). The comparison also shows why aggregate employment can be a misleading gauge of inflationary pressure: what matters is how rapidly producers expanded beyond their inherited workforces, how unevenly that expansion was distributed across producers, and how costly hiring was while they did so.

6 Conclusion

Measured labor and intermediate-input costs leave much of the initial post-COVID inflation surge unexplained. Consistent with a disruption to workforce capital, predetermined occupational COVID-19 exposure predicts both the depth of employment losses and the location of subsequent price pressure along supply chains. We interpret these dynamics through the convex, largely nonwage costs of restoring depleted workforces, which raise marginal production costs and propagate through the production

network. Recruiting and training costs rise more than proportionally with the pace of hiring, so marginal costs depend on how fast producers expand beyond the workforces they retained. When disciplined by microeconomic hiring-cost estimates and conditional on the observed demand and recovered productivity paths, this mechanism accounts for approximately two-thirds of cumulative above-trend inflation through the 2022 peak. Through 2021 its contribution exceeds the observed above-trend increase because other components offset part of the pressure. This contribution depends on the uneven distribution of capacity destruction and on the pace of the subsequent rebound. The same mechanism explains why inflation surged in the rapid recovery from COVID-19 but stayed subdued in the gradual recovery from the Great Recession. Together, these features shape the convexity of the aggregate Phillips curve, allowing inflation to surge during a high-hiring recovery even while aggregate employment remains below its pre-recession level.

This framework offers a structural lens for evaluating cross-country differences in job-retention policies. During the pandemic, European short-time-work schemes preserved existing employment relationships (Giupponi et al., 2022), whereas U.S. support relied heavily on income replacement for displaced workers.[34] By protecting organizational capital, the European approach may have limited workforce-rebuilding costs during reopening. The later onset of European inflation in 2021 aligns with this interpretation (Blanchard and Bernanke, 2024), although differences in demand stimulus and energy shocks prevent a direct causal comparison. Evaluating the macroeconomic and inflationary consequences of policies that preserve employment matches remains a direction for future research.

References

Acemoglu, Daron, Vasco M. Carvalho, Asuman Ozdaglar, and Alireza Tahbaz-Salehi, "The Network Origins of Aggregate Fluctuations," *Econometrica*, 2012, *80* (5), 1977–2016.

Adão, Rodrigo, Michal Kolesár, and Eduardo Morales, "Shift-Share Designs: Theory and Inference," *Quarterly Journal of Economics*, 2019, *134* (4), 1949–2010.

Aepli, Manuel, Samuel Muehlemann, Harald Pfeifer, Jürg Schweri, Felix Wenzelmann, and Stefan C. Wolter, "The Impact of Hiring Costs for Skilled Workers on Apprenticeship Training: A Comparative Study," Discussion Paper 16919, IZA Institute of Labor Economics April 2024.

[34]The United States also supported job retention through the Paycheck Protection Program; see Autor et al. (2022).

Afrouzi, Hassan, Andrés Blanco, Andrés Drenik, and Erik Hurst, "A Theory of How Workers Keep up with Inflation," *The Quarterly Journal of Economics*, May 2026, *141* (2), 945–1004.

Arias, Jonas E., Juan F. Rubio-Ramírez, and Minchul Shin, "Are Fiscal Transfers Inflationary?," Working Paper 26-23, Federal Reserve Bank of Philadelphia 2026.

Atalay, Enghin, "How Important Are Sectoral Shocks?," *American Economic Journal: Macroeconomics*, 2017, *9* (4), 254–280.

Atkeson, Andrew and Patrick J. Kehoe, "Modeling and Measuring Organization Capital," *Journal of Political Economy*, 2005, *113* (5), 1026–1053.

Autor, David, David Cho, Leland D. Crane, Mita Goldar, Byron Lutz, Joshua K. Montes, William B. Peterman, David D. Ratner, Daniel Villar Vallenas, and Ahu Yildirmaz, "The $800 Billion Paycheck Protection Program: Where Did the Money Go and Why Did it Go There?," NBER Working Paper 29669, National Bureau of Economic Research January 2022.

Ball, Laurence, Daniel Leigh, and Prachi Mishra, "Understanding U.S. Inflation During the COVID Era," *Brookings Papers on Economic Activity*, 2022, *Fall 2022*, 1–54.

Baqaee, David and Emmanuel Farhi, "The Macroeconomic Impact of Microeconomic Shocks: Beyond Hulten's Theorem," *Econometrica*, 2019, *87* (4), 1155–1203.

_ and _, "Supply and Demand in Disaggregated Keynesian Economies with an Application to the COVID-19 Crisis," *American Economic Review*, 2022, *112* (5), 1397–1436.

Barrot, Jean-Noël and Julien Sauvagnat, "Input Specificity and the Propagation of Idiosyncratic Shocks in Production Networks," *The Quarterly Journal of Economics*, 2016, *131* (3), 1543–1592.

Beaudry, Paul, Chenyu Hou, and Franck Portier, "On the Fragility of the Nonlinear Phillips Curve View of Recent Inflation," NBER Working Paper 33522, National Bureau of Economic Research 2025.

Benigno, Pierpaolo and Gauti B. Eggertsson, "It's Baaack: The Surge in Inflation in the 2020s and the Return of the Non-Linear Phillips Curve," Working Paper 31197, National Bureau of Economic Research 2023. October 29, 2025 revision.

Bernanke, Ben S. and Olivier J. Blanchard, "What Caused the US Pandemic-Era Inflation?," *American Economic Journal: Macroeconomics*, 2025, *17* (3), 1–35.

Blanchard, Olivier J. and Ben S. Bernanke, "An Analysis of Pandemic-Era Inflation in 11 Economies," Working Paper 32532, National Bureau of Economic Research May 2024.

Blanco, Andrés, Corina Boar, Callum J. Jones, and Virgiliu Midrigan, "Non-Linear Inflation Dynamics in Menu Cost Economies," NBER Working Paper 32094, National Bureau of Economic Research 2024.

Blatter, Marc, Samuel Muehlemann, and Samuel Schenker, "The costs of hiring skilled workers," *European Economic Review*, January 2012, *56* (1), 20–35.

Boehm, Christoph E., Aaron Flaaen, and Nitya Pandalai-Nayar, "Input Linkages and the Transmission of Shocks: Firm-Level Evidence from the 2011 Tōhoku Earthquake," *Review of Economics and Statistics*, 2019, *101* (1), 60–75.

_ **and Nitya Pandalai-Nayar**, "Convex Supply Curves," *American Economic Review*, 2022, *112* (12), 3941–3969.

Bohr, Clement E., "Capacity Buffers: Explaining the Retreat and Return of the Phillips Curve," 2024. ECB Forum on Central Banking, Sintra.

Borusyak, Kirill, Peter Hull, and Xavier Jaravel, "Quasi-Experimental Shift-Share Research Designs," *Review of Economic Studies*, 2022, *89* (1), 181–213.

Bureau of Economic Analysis, "A Primer on BEA's Industry Accounts," Technical Report, U.S. Department of Commerce May 2011.

California Policy Lab, "Analysis of Unemployment Insurance Claims in California," Technical Report, California Policy Lab, UCLA and UC Berkeley December 2021.

Cameron, A. Colin and Douglas L. Miller, "A Practitioner's Guide to Cluster-Robust Inference," *Journal of Human Resources*, 2015, *50* (2), 317–372.

Carvalho, Vasco M., Makoto Nirei, Yukiko U. Saito, and Alireza Tahbaz-Salehi, "Supply Chain Disruptions: Evidence from the Great East Japan Earthquake," *Quarterly Journal of Economics*, 2021, *136* (2), 1255–1321.

Cavallo, Alberto, Francesco Lippi, and Ken Miyahara, "Large Shocks Travel Fast," *American Economic Review: Insights*, 2024, *6* (4), 558–574.

Cerrato, Andrea and Giulia Gitti, "The Return of the Phillips Curve: Evidence from US Cities," June 2025. Working paper, Federal Reserve Bank of Boston and Collegio Carlo Alberto.

Chari, V. V., Patrick J. Kehoe, and Ellen R. McGrattan, "Business Cycle Accounting," *Econometrica*, 2007, *75* (3), 781–836.

Coibion, Olivier and Yuriy Gorodnichenko, "What Can Survey Forecasts Tell Us about Information Rigidities?," *Journal of Political Economy*, 2012, *120* (1), 116–159.

Comin, Diego A., Robert C. Johnson, and Callum J. Jones, "Supply Chain Constraints and Inflation," Working Paper 31179, National Bureau of Economic Research 2023. October 2025 version also issued as IMES Discussion Paper 2025-E-15, Bank of Japan.

Crust, Erin E., Mary C. Daly, and Bart Hobijn, "The Illusion of Wage Growth," *FRBSF Economic Letter*, 2020, *2020* (26), 01–05.

Del Negro, Marco, Michele Lenza, Giorgio E. Primiceri, and Andrea Tambalotti, "What's Up with the Phillips Curve?," *Brookings Papers on Economic Activity*, 2020, *2020* (1), 301–373.

di Giovanni, Julian, Şebnem Kalemli-Özcan, Alvaro Silva, and Muhammed A. Yıldırım, "Global Supply Chain Pressures, International Trade, and Inflation," Working Paper 30240, National Bureau of Economic Research 2022.

Domash, Alex and Lawrence H. Summers, "How Tight Are U.S. Labor Markets?," Working Paper 29739, NBER 2022.

Dupor, Bill, Marios Karabarbounis, Marianna Kudlyak, and M. Saif Mehkari, "Regional Consumption Responses and the Aggregate Fiscal Multiplier," *The Review of Economic Studies*, November 2023, *90* (6), 2982–3021.

Eichenbaum, Martin, Nir Jaimovich, and Sergio Rebelo, "Reference Prices, Costs, and Nominal Rigidities," *American Economic Review*, 2011, *101* (1), 234–262.

Fernald, John G. and Huiyu Li, "The Impact of COVID on Productivity and Potential Output," Working Paper 2022-19, Federal Reserve Bank of San Francisco 2022.

Ferrante, Francesco, Sebastian Graves, and Matteo Iacoviello, "The Inflationary Effects of Sectoral Reallocation," *Journal of Monetary Economics*, 2023, *140*, 64–81.

Fornaro, Luca, "Fiscal Stimulus with Supply Constraints," *IMF Economic Review*, 2025, *73* (3), 708–732.

Forsythe, Eliza, Lisa B. Kahn, Fabian Lange, and David Wiczer, "Where have all the workers gone? Recalls, retirements, and reallocation in the COVID recovery," *Labour Economics*, 2022, *78*, 102251.

Furlanetto, Francesco and Antoine Lepetit, "The Slope of the Phillips Curve," Finance and Economics Discussion Series 2024-043, Board of Governors of the Federal Reserve System 2024. Forthcoming as a chapter in the *Handbook of Inflation*, eds. G. Ascari and R. Trezzi.

Gagliardone, Luca, Mark Gertler, Simone Lenzu, and Joris Tielens, "Anatomy of the Phillips Curve: Micro Evidence and Macro Implications," *American Economic Review*, November 2025, *115* (11), 3941–3974.

Giannone, Domenico and Giorgio E. Primiceri, "The Drivers of Post-Pandemic Inflation," Working Paper 32859, National Bureau of Economic Research 2024.

Gitti, Giulia, "Nonlinearities in the Regional Phillips Curve with Labor Market Tightness," July 2026. Working paper, Collegio Carlo Alberto and University of Turin.

Giupponi, Giulia, Camille Landais, and Alice Lapeyre, "Should We Insure Workers or Jobs During Recessions?," *Journal of Economic Perspectives*, 2022, *36* (2), 29–54.

Guerrieri, Veronica, Guido Lorenzoni, Ludwig Straub, and Iván Werning, "Macroeconomic Implications of COVID-19: Can Negative Supply Shocks Cause Demand Shortages?," *American Economic Review*, 2022, *112* (5), 1437–1474.

Harding, Martín, Jesper Lindé, and Mathias Trabandt, "Understanding Post-COVID Inflation Dynamics," *Journal of Monetary Economics*, 2023, *140*, S101–S118.

Haubrich, Joseph, George Pennacchi, and Peter Ritchken, "Inflation Expectations, Real Rates, and Risk Premia: Evidence from Inflation Swaps," *Review of Financial Studies*, 2012, *25* (5), 1588–1629.

Hazell, Jonathon, Juan Herreño, Emi Nakamura, and Jón Steinsson, "The Slope of the Phillips Curve: Evidence from U.S. States," *Quarterly Journal of Economics*, 2022, *137* (3), 1299–1344.

Heise, Sebastian, Jeremy Pearce, and Jacob P. Weber, "Wage Growth and Labor Market Tightness," January 2026. Version dated January 23, 2026.

Hurst, Erik, Christina Patterson, Nela Richardson, and Ye Liv Wang, "Sticky Wage Norms and the Real Wage Cost of Unexpected Inflation," August 2026. Working paper, University of Chicago and ADP Research.

Linckh, Carolin, Samuel Muehlemann, and Harald Pfeifer, "Beggars Cannot Be Choosers: Labor Market Tightness and Hiring Standards, Wages, and Hiring Costs," Working Paper 247, Swiss Leading House "Economics of Education" 2025.

Merz, Monika and Eran Yashiv, "Labor and the Market Value of the Firm," *American Economic Review*, 2007, *97* (4), 1419–1431.

Miyauchi, Yuhei, "Matching and Agglomeration: Theory and Evidence from Japanese Firm-to-Firm Trade," *Econometrica*, 2024, *92* (6), 1869–1905.

Moscarini, Giuseppe and Fabien Postel-Vinay, "The Job Ladder: Inflation vs. Reallocation," Working Paper 31466, National Bureau of Economic Research 2023.

Muehlemann, Samuel and Harald Pfeifer, "The Structure of Hiring Costs in Germany: Evidence from Firm-Level Data," *Industrial Relations: A Journal of Economy and Society*, 2016, *55* (2), 193–218.

_ **and Mirjam Strupler Leiser**, "Hiring Costs and Labor Market Tightness," *Labour Economics*, 2018, *52*, 122–131.

Oi, Walter Y., "Labor as a Quasi-Fixed Factor," *Journal of Political Economy*, 1962, *70* (6), 538–555.

Oude Hengel, Karen M., Alex Burdorf, Anjoeka Pronk, Vivi Schlünssen, Zara A. Stokholm, Henrik A. Kolstad, Karin van Veldhoven, Ioannis Basinas, Martie van Tongeren, and Susan Peters, "Exposure to a SARS-CoV-2 infection at work: development of an international job exposure matrix (COVID-19-JEM)," *Scandinavian Journal of Work, Environment & Health*, 2022, *48* (1), 61–70.

Pasten, Ernesto, Raphael Schoenle, and Michael Weber, "The Propagation of Monetary Policy Shocks in a Heterogeneous Production Economy," *Journal of Monetary Economics*, 2020, *116*, 1–22.

Prescott, Edward C. and Michael Visscher, "Organization Capital," *Journal of Political Economy*, 1980, *88* (3), 446–461.

Rubbo, Elisa, "Networks, Phillips Curves, and Monetary Policy," *Econometrica*, 2023, *91* (4), 1417–1455.

_ , "What Drives Inflation? Lessons from Disaggregated Price Data," Working Paper 32194, National Bureau of Economic Research 2024.

Schmitt-Grohé, Stephanie and Martín Uribe, "Heterogeneous Downward Nominal Wage Rigidity: Foundations of a Nonlinear Phillips Curve," Working Paper 30774, National Bureau of Economic Research 2022.

Stewart, Jay, "Why Was Labor Productivity Growth So High During the COVID-19 Pandemic? The Role of Labor Composition," *International Productivity Monitor*, Spring 2022, *42*, 87–103.

U.S. Bureau of Labor Statistics, "Temporary Layoffs Remain High Following Unprecedented Surge in Early 2020," *The Economics Daily* February 10, 2021.

van der Feltz, Sophie, Vivi Schlünssen, Ioannis Basinas, Luise M. Begtrup, Alex Burdorf, Jens P. E. Bonde, Esben M. Flachs, Susan Peters, Anjoeka Pronk, Zara A. Stokholm, Martie van Tongeren, Karin van Veldhoven, Karen M. Oude Hengel, and Henrik A. Kolstad, "Associations between an international COVID-19 job exposure matrix and SARS-CoV-2 infection among 2 million workers in Denmark," *Scandinavian Journal of Work, Environment & Health*, 2023, *49* (6), 375–385.

Online Appendix

Not for Publication

Organizational Capital Destruction and Post-COVID Inflation

Lukasz A. Drozd Marina M. Tavares

A.1 Inflation Accounting Framework Derivations 50
A.2 Production Network Aggregation for the Model 59
A.3 Empirical Results: Robustness 68
A.4 Empirical Results: Extensions 71
A.5 Construction of Industry COVID-19 Exposure 73
A.6 Detrending Data for Model Calibration 74
A.7 Price Indices, Input Demands, and Price Setting 76
A.8 Calibration of Model Price Stickiness Parameters 78
A.9 Inflation Expectations Anchoring Estimates 79
A.10 Quantitative Results: Robustness and Sensitivity 81
A.11 Data Sources 85

A.1 Inflation Accounting Framework Derivations

This appendix derives the inflation decomposition framework used in Section 2 of the paper. Throughout, i and i' index industries ($i, i' \in \{1, \dots, I\}$), j indexes commodities ($j \in \{1, \dots, J\}$), and $t = 1, 2, \dots$ indexes time. Time subscripts are suppressed. For any variable X, we denote its log change between consecutive periods by $\Delta \log X \equiv \log X_t - \log X_{t-1}$. All expansions are first-order approximations around the 2017 benchmark and parameters of the decomposition are held fixed at the 2017 values. The empirical margin component is defined residually, so it also absorbs higher-order approximation terms. The symbolic steps are reproduced and verified in the Mathematica notebook `Mathematica/A1_calculations.nb` of the replication package.

A.1.1 Setup

Consider an economy comprising I industries and J commodities. Each domestic commodity j is a CES aggregate of the outputs of the industries that produce it:

$$\widetilde{Y}_j = \left[\sum_{i=1}^{I} \theta_{ij}^{1/\rho_Y} \, Y_i^{(\rho_Y - 1)/\rho_Y} \right]^{\rho_Y/(\rho_Y - 1)}, \qquad \sum_{i=1}^{I} \theta_{ij} = 1, \tag{A.1}$$

where $\widetilde{Y}_j$ denotes the domestic supply of commodity j (a tilde distinguishes commodity-level quantities and prices from their industry-level counterparts), $\theta_{ij} \geq 0$ is industry i's time-invariant production weight in commodity j, and $\rho_Y > 0$ is the time-invariant elasticity of substitution across producers of the same commodity.

To produce output (Y_i), industry i combines predetermined capital (K_i), labor (N_i), and a composite intermediate-input bundle (M_i). The intermediate-input bundle consists of the industry's purchases of domestic varieties, $\tilde{m}_{ij}^{\mathrm{DOM}}$, and imported varieties, $\tilde{m}_{ij}^{\mathrm{IMP}}$, of each commodity j—where, throughout, the tilde notation $\tilde{\cdot}$ means that a given quantity or price pertains to a commodity and not to industry raw output. The production technology is a nested CES structure. The outer nest is Cobb–Douglas in capital and a variable-input composite, V_i; the middle nest

aggregates labor and intermediate inputs:

$$Y_i = Z_i \, V_i^{\,1-\alpha_i}, \qquad Z_i \equiv z_i K_i^{\alpha_i}, \tag{A.2}$$

$$V_i = \left[\eta_i^{1/\rho} N_i^{(\rho-1)/\rho} + (1-\eta_i)^{1/\rho} M_i^{(\rho-1)/\rho} \right]^{\rho/(\rho-1)}, \tag{A.3}$$

$$M_i = \left[\sum_{j=1}^{J} (\zeta_{ij}\omega_{ij})^{1/\rho_m} \left(\tilde{m}_{ij}^{\mathrm{DOM}}\right)^{(\rho_m-1)/\rho_m} + \sum_{j=1}^{J} \left((1-\zeta_{ij})\omega_{ij}\right)^{1/\rho_m} \left(\tilde{m}_{ij}^{\mathrm{IMP}}\right)^{(\rho_m-1)/\rho_m} \right]^{\rho_m/(\rho_m-1)}. \tag{A.4}$$

In equation (A.2), $\alpha_i \in (0,1)$ is the time-invariant capital share in industry i, z_i is potentially time-varying total factor productivity, and $Z_i = z_i K_i^{\alpha_i}$ combines productivity with predetermined capital. In equation (A.3), $\eta_i \in (0,1)$ is the time-invariant labor weight and $\rho > 0$ is the time-invariant elasticity of substitution between labor and intermediate inputs. Equation (A.4) defines the intermediate bundle, where $\omega_{ij} \geq 0$ is the weight of commodity j (with $\sum_j \omega_{ij} = 1$), $\zeta_{ij} \in [0,1]$ is the domestically sourced share of that commodity, and $\rho_m > 0$ is the elasticity of substitution both across commodities and between their domestic and imported varieties. These share parameters are time invariant.

Firms are price takers in input markets. Let P_i denote the price industry i receives per unit of output, W_i its wage per worker, and P_i^M the price of its cost-minimizing intermediate-input bundle, which by equation (A.4) can be summarized by the price index:

$$P_i^M = \left[\sum_{j=1}^{J} \zeta_{ij}\omega_{ij} \left(\widetilde{P}_j^{\mathrm{DOM}}\right)^{1-\rho_m} + \sum_{j=1}^{J} (1-\zeta_{ij})\omega_{ij} \left(\widetilde{P}_j^{\mathrm{IMP}}\right)^{1-\rho_m} \right]^{1/(1-\rho_m)}, \tag{A.5}$$

where $\widetilde{P}_j^{\mathrm{DOM}}$ and $\widetilde{P}_j^{\mathrm{IMP}}$ are the prices of domestic and imported commodities that enter the bundle in equation (A.4). The variable production cost of industry i then solves:

$$C_i(Y_i) \equiv \min_{N_i,\, M_i} \{ W_i N_i + P_i^M M_i \} \quad \text{subject to} \quad Z_i V_i^{\,1-\alpha_i} \geq Y_i. \tag{A.6}$$

Output prices need not equal average cost or marginal cost, which is $C_i'(Y_i) \equiv dC_i(Y_i)/dY_i$. We define the industry margin as the output price relative to average variable cost, equivalently revenue relative to total variable cost, mirroring equation (1) in the text:

$$\mu_i \equiv \frac{P_i}{C_i(Y_i)/Y_i} = \frac{P_i Y_i}{C_i(Y_i)} = \frac{1}{1-\alpha_i} \frac{P_i}{C_i'(Y_i)}. \tag{A.7}$$

Under the Cobb–Douglas specification assumed above, the margin is proportional to the markup, and the inner CES nest over labor and intermediate inputs does not change this fact.

A.1.2 Derivation

First-order conditions. The solution to the cost-minimization problem (A.6) equates the marginal rate of substitution between labor and intermediate inputs to their relative price:

$$\frac{\partial V_i/\partial N_i}{\partial V_i/\partial M_i} = \left(\frac{\eta_i}{1-\eta_i}\right)^{1/\rho} \left(\frac{M_i}{N_i}\right)^{1/\rho} = \frac{W_i}{P_i^M}. \tag{A.8}$$

Rearranging equation (A.8) yields the relative demand for intermediate inputs,

$$\frac{M_i}{N_i} = \frac{1-\eta_i}{\eta_i} \left(\frac{W_i}{P_i^M}\right)^{\rho}, \tag{A.9}$$

which shows that the input-to-labor ratio rises with the relative cost of labor, with elasticity ρ. Given the constant returns to scale of the variable-input composite V_i, the minimized variable cost is linear in V_i and

$$C_i = P_i^V \, V_i, \qquad P_i^V = \left[\eta_i W_i^{1-\rho} + (1-\eta_i)\left(P_i^M\right)^{1-\rho}\right]^{1/(1-\rho)}, \qquad V_i = \left(\frac{Y_i}{Z_i}\right)^{1/(1-\alpha_i)}, \tag{A.10}$$

where P_i^V is the dual CES price index of the composite and the final equality inverts the production function (A.2). Defining s_i^N as labor's share in variable production cost, equations (A.9)–(A.10) imply

$$s_i^N \equiv \frac{W_i N_i}{C_i} = \frac{\eta_i W_i^{1-\rho}}{\eta_i W_i^{1-\rho} + (1-\eta_i)\left(P_i^M\right)^{1-\rho}}. \tag{A.11}$$

For later use (matrix notation), it is convenient to collect industry i's imported inputs into one sub-bundle. Let $s_i^{\text{IMP}} \equiv \sum_j (1-\zeta_{ij})\omega_{ij}$ denote the imported share of industry i's input bundle, and define the price of its imported-input bundle as the CES dual of the imported varieties,

$$\begin{aligned} P_i^{\text{IMP}} &= \left[\sum_{j=1}^{J} \frac{(1-\zeta_{ij})\omega_{ij}}{s_i^{\text{IMP}}} \left(\widetilde{P}_j^{\text{IMP}}\right)^{1-\rho_m}\right]^{1/(1-\rho_m)}, \\ \text{so that} \qquad P_i^M &= \left[\sum_{j=1}^{J} \zeta_{ij}\omega_{ij} \left(\widetilde{P}_j^{\text{DOM}}\right)^{1-\rho_m} + s_i^{\text{IMP}} \left(P_i^{\text{IMP}}\right)^{1-\rho_m}\right]^{1/(1-\rho_m)}. \end{aligned} \tag{A.12}$$

The second equality rewrites equation (A.5) with the imported varieties nested in their own bundle. Cost minimization across producers likewise yields the domestic commodity price $\widetilde{P}_j^{\text{DOM}}$ as the CES dual of equation (A.1),

$$\widetilde{P}_j^{\text{DOM}} = \left[\sum_{i=1}^{I} \theta_{ij} P_i^{1-\rho_Y}\right]^{1/(1-\rho_Y)}. \tag{A.13}$$

The associated first-order conditions give the expenditure shares; that is, industry i's expenditure share on domestic commodity j is $\zeta_{ij}\omega_{ij}(\widetilde{P}_j^{\text{DOM}}/P_i^M)^{1-\rho_m}$, its share on imported commodity j is $(1-\zeta_{ij})\omega_{ij}(\widetilde{P}_j^{\text{IMP}}/P_i^M)^{1-\rho_m}$, and industry i's share of the domestic production value of commodity j is $\theta_{ij}(P_i/\widetilde{P}_j^{\text{DOM}})^{1-\rho_Y}$.

We evaluate the expansion around the 2017 benchmark, at which the base-year quantities and prices satisfy the system. By defining the units of N_i, M_i, $\tilde{m}_{ij}^{\text{DOM}}$, $\tilde{m}_{ij}^{\text{IMP}}$, Y_i, and $\widetilde{Y}_j$ in 2017 dollars, we normalize all steady-state prices to one:

$$W_i = P_i^M = \widetilde{P}_j^{\text{DOM}} = \widetilde{P}_j^{\text{IMP}} = P_i = 1 \qquad \text{in 2017.} \tag{A.14}$$

This is the log-linearization point. While expenditure shares are invariant to this choice of units, the CES weights are not, and the normalization pins them down to match the observed 2017 shares. It is thus important that 2017 is a relatively "stable" year in terms of relative prices, which it is.

Evaluating equation (A.11) and the three share expressions at unit prices gives

$$\eta_i = s_i^N, \qquad \zeta_{ij}\omega_{ij} = \frac{\tilde{m}_{ij}^{\text{DOM}}}{M_i}, \qquad (1-\zeta_{ij})\omega_{ij} = \frac{\tilde{m}_{ij}^{\text{IMP}}}{M_i}, \qquad \theta_{ij} = \frac{S_{ij}}{\sum_{i'} S_{i'j}}, \tag{A.15}$$

where S_{ij} denotes the value of commodity j produced by industry i. The labor weight equals the 2017 labor share in variable production cost, the bundle weights equal the 2017 domestic and imported expenditure shares, and the commodity weights equal each industry's 2017 share in the value of the commodity's domestic output. We use BEA supply–use input–output tables to pin down these parameters (see Section A.1.3 for details).

Because the relative demand function (A.9) is log-linear, first-differencing it gives

$$\Delta \log M_i = \Delta \log N_i - \rho \left(\Delta \log P_i^M - \Delta \log W_i \right). \tag{A.16}$$

Log-linearizing the cost function (A.10), where $C_i = P_i^V V_i$ and $V_i = (Y_i/Z_i)^{1/(1-\alpha_i)}$, around the steady state (A.15) gives

$$\Delta \log C_i = s_i^N \, \Delta \log W_i + (1 - s_i^N) \, \Delta \log P_i^M + \frac{\Delta \log Y_i - \Delta \log Z_i}{1 - \alpha_i}. \tag{A.17}$$

Log-linearizing the production structure in equations (A.2)–(A.3) gives[35]

$$\Delta \log Y_i = \Delta \log Z_i + (1 - \alpha_i) \left[s_i^N \, \Delta \log N_i + (1 - s_i^N) \, \Delta \log M_i \right]. \tag{A.18}$$

Equation (A.18) says that output growth is productivity growth plus the variable-input share times the cost-share-weighted growth of inputs. Rearranging it to isolate the productivity term and substituting the first-order condition (A.16) eliminates the unobservable Z_i:

$$\begin{aligned} \frac{\Delta \log Y_i - \Delta \log Z_i}{1 - \alpha_i} &= s_i^N \, \Delta \log N_i + (1 - s_i^N) \, \Delta \log M_i \\ &= \Delta \log N_i - (1 - s_i^N) \rho \left(\Delta \log P_i^M - \Delta \log W_i \right), \end{aligned} \tag{A.19}$$

Holding relative prices fixed, output growth in excess of productivity growth is accommodated by employment expansion.

Log-linearizing the intermediate-input bundle price (A.5) yields

$$\Delta \log P_i^M = \sum_{j=1}^{J} \zeta_{ij} \omega_{ij} \, \Delta \log \widetilde{P}_j^{\mathrm{DOM}} + \sum_{j=1}^{J} (1 - \zeta_{ij}) \omega_{ij} \, \Delta \log \widetilde{P}_j^{\mathrm{IMP}}. \tag{A.20}$$

Because the elasticity of a CES price index with respect to any component equals that component's expenditure share, input-price inflation is the share-weighted average of domestic and imported commodity inflation; the elasticity ρ_m drops out at first order. Log-linearizing the imported-input bundle price (A.12) gives

$$\begin{aligned} \Delta \log P_i^{\mathrm{IMP}} &= \sum_{j=1}^{J} \frac{(1 - \zeta_{ij}) \omega_{ij}}{s_i^{\mathrm{IMP}}} \, \Delta \log \widetilde{P}_j^{\mathrm{IMP}}, \\ \text{so that} \qquad \Delta \log P_i^M &= \sum_{j=1}^{J} \zeta_{ij} \omega_{ij} \, \Delta \log \widetilde{P}_j^{\mathrm{DOM}} + s_i^{\mathrm{IMP}} \, \Delta \log P_i^{\mathrm{IMP}}. \end{aligned} \tag{A.21}$$

Input-price inflation is the share-weighted average of domestic commodity inflation and of the inflation of the industry's own imported-input bundle. Following the same logic for the domestic commodity price (A.13) gives

$$\Delta \log \widetilde{P}_j^{\mathrm{DOM}} = \sum_{i=1}^{I} \theta_{ij} \, \Delta \log P_i. \tag{A.22}$$

Commodity inflation is the output-share-weighted average of the inflation rates of the producing industries, and ρ_Y likewise drops out at first order. Both elasticities continue to govern quantity substitution and second-order terms.

[35] Log-differentiating equation (A.3) gives $\Delta \log V_i = \omega_i^N \, \Delta \log N_i + (1 - \omega_i^N) \, \Delta \log M_i$, where $\omega_i^N \equiv \eta_i^{1/\rho} N_i^{(\rho-1)/\rho} / V_i^{(\rho-1)/\rho} = (N_i/V_i) \, \partial V_i / \partial N_i$ is the elasticity of the composite with respect to labor. Cost minimization sets $W_i = P_i^V \, \partial V_i / \partial N_i$, which gives $\omega_i^N = W_i N_i / (P_i^V V_i) = s_i^N$.

First-differencing the margin equation (A.7), industry inflation equals margin growth plus unit-cost growth:

$$\Delta \log P_i = \Delta \log \mu_i + \Delta \log\left(\frac{C_i}{Y_i}\right). \tag{A.23}$$

Eliminating $\Delta \log Z_i$ and $\Delta \log M_i$ by substituting equation (A.19) into the cost equation (A.17) gives the last term

$$\begin{aligned}\Delta \log\left(\frac{C_i}{Y_i}\right) &= s_i^N \Delta \log W_i + (1 - s_i^N)\Delta \log P_i^M - \Delta \log\left(\frac{Y_i}{N_i}\right) \\ &\quad - (1 - s_i^N)\rho\left(\Delta \log P_i^M - \Delta \log W_i\right) \\ &= \left[s_i^N + (1 - s_i^N)\rho\right]\Delta \log W_i + (1 - s_i^N)(1 - \rho)\Delta \log P_i^M - \Delta \log\left(\frac{Y_i}{N_i}\right).\end{aligned} \tag{A.24}$$

To simplify notation, we define the wage and input-price coefficients

$$b_i \equiv \rho + (1 - \rho)\, s_i^N, \qquad d_i \equiv (1 - s_i^N)(1 - \rho), \qquad b_i + d_i = 1. \tag{A.25}$$

which gives

$$\Delta \log\left(\frac{C_i}{Y_i}\right) = b_i \Delta \log W_i + d_i \Delta \log P_i^M - \Delta \log\left(\frac{Y_i}{N_i}\right). \tag{A.26}$$

The above expression says that unit-cost growth is a weighted sum of wage growth and input-price growth, with weights that add to one, less labor productivity growth. In the Cobb–Douglas case ($\rho = 1$), $b_i = 1$ and $d_i = 0$, so unit-cost growth depends on wage growth net of labor productivity alone. For $\rho < 1$, intermediate-input prices pass directly into unit costs ($d_i > 0$), the more so the smaller is ρ.

Substituting the unit-cost equation (A.26) into the margin identity (A.23), and substituting for the bundle price using equations (A.22) and (A.21), yields the decomposition for a single industry:

$$\begin{aligned}\underbrace{\Delta \log P_i}_{\text{industry inflation}} &= \underbrace{\Delta \log \mu_i}_{\text{margin}} + \underbrace{b_i \Delta \log W_i}_{\text{wage}} \underbrace{- \Delta \log(Y_i/N_i)}_{\text{labor productivity}} \\ &\quad + \underbrace{d_i \sum_{j=1}^{J} \zeta_{ij}\omega_{ij} \sum_{i'=1}^{I} \theta_{i'j}\Delta \log P_{i'}}_{\text{domestic inputs}} + \underbrace{d_i\, s_i^{\text{IMP}} \Delta \log P_i^{\text{IMP}}}_{\text{imported inputs}}.\end{aligned} \tag{A.27}$$

Industry inflation thus decomposes into margin growth, wage growth scaled by b_i, labor-productivity growth entering negatively, the inflation of the domestic industries that supply it, weighted by d_i times each supplier's 2017 share in its input purchases, and the inflation of its imported-input bundle, weighted by d_i times its 2017 imported share.

We next rewrite the above equation in matrix form. Let Ω and ζ be the $J \times I$ matrices with elements $\Omega_{ji} = \omega_{ij}$ and $\zeta_{ji} = \zeta_{ij}$, so that column i of Ω stores industry i's bundle weights and column i of ζ its domestic shares, and let Θ be the $I \times J$ matrix with elements $\Theta_{ij} = \theta_{ij}$, where column j stores the producer weights of commodity j. Stacking equations (A.22) and (A.21) across all industries and commodities gives

$$\begin{aligned}\Delta \log P^M &= (\zeta \odot \Omega)^\top \Theta^\top \Delta \log P + \operatorname{diag}(s^{\text{IMP}})\Delta \log P^{\text{IMP}}, \\ \Delta \log P^{\text{IMP}} &= \operatorname{diag}(s^{\text{IMP}})^{-1}\left[(\mathbf{1} - \zeta) \odot \Omega\right]^\top \Delta \log \widetilde{P}^{\text{IMP}},\end{aligned} \tag{A.28}$$

where $\odot$ is the Hadamard (elementwise) product, $\mathbf{1}$ is a $J \times I$ matrix of ones, $\Delta \log P^M$, $\Delta \log P$, and $\Delta \log P^{\text{IMP}}$ are the $I \times 1$ vectors of input-bundle, output, and imported-input-bundle inflation, $\Delta \log \widetilde{P}^{\text{IMP}}$ is the $J \times 1$ vector of commodity import-price inflation, and $\operatorname{diag}(s^{\text{IMP}})$ is the diagonal matrix of imported shares. In equation (A.28), $\Theta^\top$ maps industry inflation into domestic commodity inflation, while $(\zeta \odot \Omega)^\top$ maps commodity inflation back into

industry-level input-bundle inflation; imported inputs enter through each industry's own imported bundle and are not routed through Θ. We define the domestic and imported input matrices

$$A \equiv \operatorname{diag}(d)\,(\zeta \odot \Omega)^{\top}\Theta^{\top}, \qquad A^{\mathrm{IMP}} \equiv \operatorname{diag}(d)\operatorname{diag}(s^{\mathrm{IMP}}), \tag{A.29}$$

where $\operatorname{diag}(d)$ is the diagonal matrix of the coefficients d_i; both matrices are $I \times I$, and A^{IMP} is diagonal with entries $d_i s_i^{\mathrm{IMP}}$. The element $A_{ii'}$ is d_i times the 2017 share of industry i's input purchases that consisted of domestic commodities produced by industry i':

$$A_{ii'} = d_i \sum_{j=1}^{J} \zeta_{ij}\omega_{ij}\theta_{i'j}. \tag{A.30}$$

Stacking the industry decomposition (A.27) across industries and applying these network matrices yields equation (2) of the main text:

$$\Delta \log P = \underbrace{\Delta \log \mu}_{\Delta\mathrm{MARGIN}} + \underbrace{\underbrace{\operatorname{diag}(b)\,\Delta \log W}_{\Delta\mathrm{WAGE}} \underbrace{-\Delta \log(Y/N)}_{\Delta\mathrm{PROD}}}_{\Delta\mathrm{ULC}} + \underbrace{A\,\Delta \log P}_{\Delta\mathrm{MAT}} + \underbrace{A^{\mathrm{IMP}}\Delta \log P^{\mathrm{IMP}}}_{\Delta\mathrm{IMP}}, \tag{A.31}$$

where $\Delta \log \mu$, $\Delta \log W$, $\Delta \log(Y/N)$, and $\Delta \log P^{\mathrm{IMP}}$ are the $I \times 1$ vectors of margin, wage, labor-productivity, and imported-input-bundle growth and $\operatorname{diag}(b)$ is the diagonal matrix of the coefficients b_i. In the empirical application, $\Delta \log \mu$ is the residual that makes the decomposition hold exactly for every industry and year.

We can use the above equation to form an aggregate inflation index. Let g be an $I \times 1$ vector of industry weights that sum to one, and define aggregate inflation under these weights as $\Pi \equiv g^{\top}\Delta \log P$. For the PCE weights, $g = \Theta c$ with c the $J \times 1$ vector of 2017 PCE weights over commodities; for value-added weights, g is the share of the value added of industry i in GDP. Premultiplying the identity (A.31) by $g^{\top}$ gives the *direct decomposition* of inflation used in Table 1 in the text,

$$\Pi = \underbrace{g^{\top}\Delta\mathrm{MARGIN}}_{\Pi_{\mathrm{MARGIN}}} + \underbrace{g^{\top}\operatorname{diag}(b)\,\Delta \log W}_{\Pi_{\mathrm{WAGE}}} + \underbrace{g^{\top}\left[-\Delta \log(Y/N)\right]}_{\Pi_{\mathrm{PROD}}} + \underbrace{g^{\top}\Delta\mathrm{MAT}}_{\Pi_{\mathrm{MAT}}} + \underbrace{g^{\top}\Delta\mathrm{IMP}}_{\Pi_{\mathrm{IMP}}}, \tag{A.32}$$

where $\Pi_{\mathrm{ULC}} = \Pi_{\mathrm{WAGE}} + \Pi_{\mathrm{PROD}}$, given our convention that the productivity term measures the impact of productivity on prices, and hence positive productivity growth implies $\Pi_{\mathrm{PROD}} < 0$.

Because input-cost inflation depends on suppliers' price changes, the identity is a linear system in $\Delta \log P$,

$$\Delta \log P = \Delta\mathrm{MARGIN} + \Delta\mathrm{ULC} + \Delta\mathrm{IMP} + A\Delta \log P,$$

which gives

$$\Delta \log P = L\,(\Delta\mathrm{MARGIN} + \Delta\mathrm{ULC} + \Delta\mathrm{IMP}) \qquad \text{where} \qquad L \equiv (I - A)^{-1} = I + A + A^2 + \cdots, \tag{A.33}$$

where L is the Leontief inverse. With the PCE weight vector $g = \Theta c$, $\kappa \equiv L^{\top}g$ gives the benchmark Domar weights used to define each industry's finalness, g_i/κ_i.[36]

[36] Premultiplying the Leontief formulation (A.33) by $g^{\top}$ instead yields the *resolved decomposition*:

$$\Pi = g^{\top}L\,\Delta\mathrm{MARGIN} + g^{\top}L\,\Delta\mathrm{ULC} + g^{\top}L\,\Delta\mathrm{IMP}. \tag{A.34}$$

This decomposition consistently reallocates domestic input-cost inflation to the upstream margin, labor-cost, and import-price sources from which it originates. We do not use it in text but the results are similar.

A.1.3 Parameterization

All coefficients are evaluated once, at the 2017 benchmark, and held fixed across every year of the decomposition and in the exposure regressions. To link the pre- and post-2022 NAICS vintages, the 2017 detail supply–use tables are harmonized into a square system of $I = J$ industries and commodities; supplementary rows and columns (scrap, secondhand goods, noncomparable imports, the rest-of-the-world adjustment, customs duties, and private households) and industries without price data are dropped. Online Appendix A.11 lists the underlying series. The mapping from the tables to the coefficients is as follows.

- **Bundle weights ω.** The bundle weights are the column shares of the intermediate-use block,

$$\omega_{ij} = \frac{U_{ji}}{\sum_{k=1}^{J} U_{ki}}, \qquad \sum_{j=1}^{J} \omega_{ij} = 1,$$

  where U $(J \times I)$ is the BEA Use table at producer prices, with each element U_{ji} corresponding to industry i's 2017 purchases of commodity j for intermediate use. Producer-price valuation means that retail/wholesale/transportation margins are recorded as purchases of the margin industries' output and separated from other intermediate goods flows.

- **Domestic sourcing shares ζ.** ζ_{ij} is the domestic share of industry i's 2017 purchases of commodity j: one minus the ratio of the import-matrix entry to the use-table entry, $\zeta_{ij} = 1 - U^{\text{IMP}}_{ji}/U_{ji}$, where U^{IMP} is the BEA 2017 import matrix $(J \times I)$, which records industry i's imports of commodity j; cells with no use are treated as fully domestic.

- **Commodity weights θ.** The commodity weights are the column shares of the make table,

$$\theta_{ij} = \frac{S_{ij}}{\sum_{i'=1}^{I} S_{i'j}}, \qquad \sum_{i=1}^{I} \theta_{ij} = 1,$$

  where S $(I \times J)$ is the BEA make (supply) table, with entry S_{ij} corresponding to industry i's 2017 production of commodity j.

- **Labor share s_i^N.** We define it as compensation of employees CE_i divided by variable cost at producer prices,

$$s_i^N = \frac{CE_i}{\sum_{j=1}^{J} U_{ji} + CE_i + T_i},$$

  where T_i is taxes on production and imports net of subsidies (BEA series V00200). The denominator is the non-surplus production cost, so s_i^N is a share of cost rather than of value added. Taxes on production and imports enter the 2017 cost base and are held constant, so their changes are absorbed by the margin residual. Pandemic subsidies affect the reported annual cost accounts and leave the fixed 2017 benchmark unchanged. Effectively, we assume that profits are payments for intangible capital.

- **Elasticity ρ.** Estimated from KLEMS (see details in Section A.1.4). The coefficients b_i and d_i then follow from equation (A.25).

- **Network matrices.** A is assembled from d, ζ, Ω, and Θ by equation (A.29), A^{IMP} from d and the imported shares $s_i^{\text{IMP}} = \sum_j (1 - \zeta_{ij})\omega_{ij}$, and $L = (I - A)^{-1}$.

- **Final-demand weights.** c is the 2017 personal-consumption-expenditure column of the Use table over commodities, normalized to sum to one, and $g = \Theta c$. In the regressions and in Table 1 we use the value-added share of industry i as g; the data–model comparison uses PCE weights.

- **Annual log changes.** $\Delta \log P_i$ and $\Delta \log Y_i$ come from the BEA gross-output price and quantity indexes by industry; $\Delta \log N_i$ and $\Delta \log W_i$ from QCEW employment and average payroll per worker mapped to the BEA industries; and $\Delta \log \widetilde{P}_j^{\text{IMP}}$ from the BLS import price indexes (International Price Program), which price imported items at the product level under the Harmonized Tariff Schedule and publish them in NAICS-based series in which imported goods are classified by the output industry of the product. We map these series to the BEA commodity codes and aggregate them with Census import values as weights, so the import price is a product-level price throughout, and $\Delta \log P_i^{\text{IMP}}$ follows by equation (A.21).

The decomposition is applied at annual frequency: the period in $\Delta \log X$ is a calendar year, because the gross-output accounts and the supply–use benchmark are annual. It enters the paper in four places. First, the industry accounting: for every industry and year we compute ΔWAGE, ΔPROD, ΔMAT, and ΔIMP from the observed series with the fixed 2017 coefficients, and ΔMARGIN as the residual of equation (2); cumulative contributions over a window are sums of the annual contributions. Table 1 in the main text aggregates these components over the regression sample with value-added weights. Second, the exposure measures: the same matrix A defines supplier exposure $\mathcal{E} = AE$ in equation (3), and the supplier components $A\,\Delta\text{MARGIN}_t$, $A\,\Delta\text{ULC}_t$, $A\,\Delta\text{IMP}_t$, and $A^2\Delta \log P_t$ are the outcomes of the supplier regressions in Table 2. Third, the classification: $\kappa = L^\top g$ and finalness g_i/κ_i separate consumer-facing industries from the middle and upstream industries $m + l$ and define the tiers of the model. Fourth, the comparison with the model: the model targets GO inflation under PCE weights, Π^{PCE}, and decomposes it into the contributions of the EXO and the non-EXO industries; N-GO is the non-EXO contribution.

A.1.4 Annex I: KLEMS-based estimate of ρ

The only substitution elasticity in the first-order decomposition is ρ. We estimate it from the first-order condition (A.9). Multiplying both sides by P_i^M / W_i and taking logs gives

$$\log\left(\frac{P_i^M M_i}{W_i N_i}\right) = \log\left(\frac{1-\eta_i}{\eta_i}\right) + (1-\rho)\log\left(\frac{P_i^M}{W_i}\right), \tag{A.35}$$

which says that the ratio of intermediate-input spending to the wage bill depends on the relative price of inputs with elasticity $1-\rho$: for $\rho < 1$, a rise in the relative price of inputs raises the spending ratio.

Data. The BEA–BLS Industry-Level Production Account (KLEMS), 1997–2023 release, at its 63 summary industries. For each industry and year we take nominal labor compensation and the index of hours worked; nominal materials inputs and the materials quantity index; and nominal purchased-services inputs and the services quantity index. Energy inputs are excluded from the bundle.

Construction. For industry i in year t, the wage w_{it} is labor compensation per hour: labor compensation divided by the hours index. The deflator of each input component $k \in \{\text{materials}, \text{services}\}$ is its nominal value divided by its quantity index, and the bundle price is their share-weighted geometric mean,

$$\log P_{it}^M = \sum_k \varsigma_{kit} \log\big(\text{deflator}_{kit}\big), \qquad \varsigma_{kit} = \frac{\text{nominal}_{kit}}{\sum_{k'} \text{nominal}_{k'it}},$$

with the shares taken at their current values. The regression variables are

$$y_{it} = \log\left(\frac{\text{materials}_{it} + \text{services}_{it}}{\text{labor compensation}_{it}}\right), \qquad x_{it} = \log\left(\frac{P_{it}^M}{w_{it}}\right),$$

the empirical counterparts of the left-hand side and of $\log(P_i^M / W_i)$ in equation (A.35).

Sample. 1998–2023; 62 industries after dropping Funds, trusts, and other financial vehicles; 1,612 industry-years, a balanced panel of 26 years.

Regression. Ordinary least squares with industry and year fixed effects,

$$y_{it} = FE_i + FE_t + \beta\, x_{it} + u_{it}, \qquad \beta = 1 - \rho, \tag{A.36}$$

where the industry effect FE_i absorbs $\log[(1-\eta_i)/\eta_i]$, the year effect FE_t absorbs movements common to all industries, and u_{it} is the error. Standard errors are clustered by industry (62 clusters) and computed with the within estimator; the equivalent dummy-variable regression gives the same $\widehat{\beta}$ and a standard error of 0.169. The estimate is $\widehat{\beta} = 0.606$ with standard error 0.168, so $\widehat{\rho} = 1 - \widehat{\beta} = 0.39$ with 95% confidence interval $[0.06, 0.72]$. In first differences with year effects, $\widehat{\rho} = 0.09$ (confidence interval $[-0.17, 0.34]$) on the full sample and 0.28 ($[0.05, 0.50]$) after trimming the 0.5 percent largest absolute changes in x and y; two-year differences give 0.11 and 0.29. The fixed-effects estimate is higher than estimates obtained at finer levels of disaggregation (e.g., Atalay, 2017; Boehm et al., 2019), and the network propagation in equation (A.33) strengthens as ρ falls, so the baseline is conservative in this respect. The script `estimate_rho_klems.py` in the replication package builds the panel from the vendored KLEMS workbook and reproduces these estimates.

A.1.5 Annex II: Comparison of GO inflation to published indices

Every aggregate price measure in the paper is a weighted sum of the industries' gross-output price changes, $\Pi = g^{\top}\Delta \log P$, with the weights g fixed at their 2017 values and the industry deflators taken from the BEA gross-output accounts. Two weight vectors are used, and each is applied to two sets of industries, which gives four measures.

The first weight vector is value added. Industry i's weight is its share of 2017 value added, $g_i^{VA} = VA_i / \sum_{i'} VA_{i'}$, so that each industry counts in proportion to the income it generates. These are the weights of the industry accounting in Table 1. The second weight vector is personal consumption. Industry i's weight is the share of 2017 personal consumption expenditure spent directly on its output, $g^{PCE} = \Theta c$, where c is the 2017 PCE column of the use table over commodities, normalized to sum to one, and Θ is the make matrix of Section A.1.3; each industry counts in proportion to its direct contribution to consumer prices. These are the weights of the comparison between the data and the model: the model targets GO inflation under PCE weights and decomposes it into the contributions of the EXO and the non-EXO industries.

Under either weight vector, gross-output inflation (GO) uses all I industries, with weights summing to one. Non-EXO gross-output inflation (N-GO) removes the exogenous (EXO) industries, whose prices the model takes as given: the extractive and refining industries, real estate, finance and insurance, and government.[37] In the main text and in the comparison with the model, N-GO is the sum over the remaining industries with their weights left as they are, so that it is the contribution of the non-EXO industries to GO inflation and GO minus N-GO is the contribution of the EXO industries; the removed industries carry about 29 percent of the PCE weights, so the remaining PCE weights sum to 0.71. For the comparison with published price indices, the tables below instead rescale the remaining weights to sum to one, which turns this contribution into the inflation rate of the non-EXO basket; the two differ only by the weight sum. The four measures reported are therefore GO and the non-EXO basket index under value-added weights, Π^{VA} and $\Pi^{VA}_{\text{N-GO}}$, and the same two under PCE weights, Π^{PCE} and $\Pi^{PCE}_{\text{N-GO}}$.

[37] The EXO set comprises 16 BEA industries. Extractive and refining: oil and gas extraction; drilling oil and gas wells; copper, nickel, lead, and zinc mining; iron, gold, silver, and other metal ore mining; and petroleum refineries. Real estate: housing and real estate. Finance and insurance: monetary authorities and depository credit intermediation; nondepository credit intermediation; securities and commodity contracts intermediation and brokerage; other financial investment activities; direct life insurance carriers; insurance carriers except direct life; insurance agencies, brokerages, and related activities; and funds, trusts, and other financial vehicles. Government: federal government and state and local government. The same set is excluded from the regression sample in Section 2.

Tables A1 and A2 report, respectively, the value-added-weighted and the PCE-weighted measures, cumulated from 2019, next to the published indices: BEA PCE and core PCE (FRED series PCEPI and PCEPILFE) and BLS CPI (CPIAUCSL). The comparison has two purposes. It shows how the paper's gross-output-based measures track the published consumer price indices, which differ from them in coverage (consumer goods and services rather than all gross output), in valuation (purchaser rather than producer prices), and in weighting (current rather than fixed 2017 weights). And it shows how much the choice of weights matters for the aggregate, since the same industry deflators enter both tables. N-GO and core PCE remove different parts of the basket: core PCE excludes food and energy and retains housing, whereas N-GO removes the EXO industries listed above, so the two are distinct measures and are not expected to coincide.

Table A1: Cumulative inflation from 2019 under value-added weights: the paper's measures and published indices.

	Headline measures			N-GO and core PCE	
Year	GO Inflation	BEA PCE	CPI	N-GO Inflation	BEA Core PCE
2020	+1.00	+1.11	+1.25	+1.12	+1.35
2021	+6.41	+5.14	+5.82	+6.42	+4.84
2022	+13.45	+11.48	+13.51	+13.52	+10.04
2023	+15.82	+15.21	+17.55	+15.80	+14.13
2024	+18.26	+17.79	+20.46	+17.73	+17.03

Notes: Cumulative log percentage changes from 2019. GO aggregates the 357 industries' gross-output deflators with fixed 2017 value-added weights $g_i^{VA} = VA_i / \sum_{i'} VA_{i'}$. N-GO removes the EXO industries (extractive and refining, real estate, finance and insurance, and government) and renormalizes the remaining weights to sum to one. Published benchmarks are BEA PCE and core PCE (FRED PCEPI, PCEPILFE) and BLS CPI (CPIAUCSL); core PCE excludes food and energy and retains housing.

Table A2: Cumulative inflation from 2019 under PCE weights: the paper's measures and published indices.

	Headline measures			N-GO and core PCE	
Year	GO Inflation	BEA PCE	CPI	N-GO Inflation	BEA Core PCE
2020	+1.58	+1.11	+1.25	+1.85	+1.35
2021	+6.96	+5.14	+5.82	+7.08	+4.84
2022	+13.74	+11.48	+13.51	+13.86	+10.04
2023	+16.63	+15.21	+17.55	+16.62	+14.13
2024	+19.06	+17.79	+20.46	+18.53	+17.03

Notes: Cumulative log percentage changes from 2019. GO aggregates the 357 industries' gross-output deflators with fixed 2017 PCE weights $g^{PCE} = \Theta c$. N-GO removes the EXO industries, which carry about 29 percent of the PCE weights, and renormalizes the remaining weights to sum to one. Published benchmarks are BEA PCE and core PCE (FRED PCEPI, PCEPILFE) and BLS CPI (CPIAUCSL); core PCE excludes food and energy and retains housing.

A.2 Production Network Aggregation for the Model

This appendix describes how the 341 endogenous industries are aggregated into the model's 24 production nodes. We first group industries into four supply chains using their input–output links. Within each chain, we form three tiers according to their proximity to final consumption. Each chain-by-tier group is then divided into hit and safe nodes according to the severity of its industries' employment losses in 2020. These labels are relative: safe industries need not have escaped contraction, and hit industries need not all have contracted.

A.2.1 Aggregation procedure

We begin with the 341 × 341 structural intermediate-input operator of Online Appendix A.1, restricted to the endogenous industries (excluding the 16 EXO industries):

$$A \;=\; \operatorname{diag}(d)\,(\zeta \odot \Omega)^{\top}\,\Theta^{\top}.$$

The element $A_{ii'}$ is the benchmark coefficient mapping supplier i''s price growth into industry i's input-cost contribution. We use a symmetric weighted adjacency matrix,

$$W \;=\; \tfrac{1}{2}\big(A + A^{\top}\big), \qquad W_{ii} = 0.$$

We set the diagonal to zero because purchases within an industry do not link distinct industries. The weight $W_{ii'}$ averages the two directional input-cost links between industries i and i'.

Let D be the diagonal matrix of weighted degrees, where $D_{ii} = \sum_{i'} W_{ii'}$ measures the total link strength of industry i. We form the normalized graph Laplacian

$$\mathcal{L} \;=\; I - D^{-1/2}\,W\,D^{-1/2}.$$

We compute the Fiedler vector f, the eigenvector associated with the second-smallest eigenvalue of $\mathcal{L}$. Its ordering tends to place strongly connected industries together. We use that ordering to construct a gross-output-balanced partition; the split is determined by cumulative output, not by the zero of the eigenvector.

After sorting the industries by their Fiedler values f_i in ascending order, we traverse the list and accumulate their 2017 gross output. The network is bisected at the industry where cumulative gross output reaches one half of the group's total. We apply the spectral bisection recursively until four chains are obtained. Each subsequent bisection uses only the sub-block of A corresponding to the industries being split, ignoring external links. Sorted by descending 2017 gross output, the four chains $(C_1, \ldots, C_4)$ contain 46, 76, 101, and 118 industries, respectively.

Within each chain, we rank industries by *finalness*, g_i/κ_i, the ratio of the direct PCE weight to the total weight κ_i defined by the accounting network. The consumer-facing tier (h) contains industries with finalness of at least 0.70. We divide the remaining industries at the gross-output-weighted median of finalness: the lower group forms the upstream tier (l), and the upper group the middle tier (m). This produces twelve chain-by-tier groups.

Each of the twelve cells is then split into a *hit* node, comprising the industries with the largest employment declines from 2019 to 2020 in the QCEW annual averages, and a *safe* node, comprising the remainder. Traversing the industries in order of employment decline, we assign them to the hit node until their cumulative 2019 employment reaches one half of the cell's total. In seven of the twelve cells, this split is made between whole BEA industries. In five cells ($C_{1,h}$, $C_{2,m}$, $C_{3,l}$, $C_{4,h}$, and $C_{4,l}$), a single dominant BEA industry prevents a balanced bisection. For these cells, we rank and split the six-digit NAICS components. The parent BEA industry's gross output, wage bill, and its input–output rows and columns are then prorated between the hit and safe nodes according to the 2019 employment shares of its components.

A.2.2 Chain composition and industry shares

Table A3 lists the industries assigned to each chain and tier. The descriptions below summarize their economic composition; all shares refer to value added unless otherwise stated. The tiers indicate relative proximity to consumption, not exclusive trading relationships: upstream producers can sell to final users, and consumer-facing producers can supply other firms.

- **Retail and telecommunications (C_1):** This chain accounts for approximately 35 percent of value added, the largest share among the four chains. The consumer-facing tier is dominated by retail trade (nearly

75 percent of the tier) alongside wired and wireless telecommunications. The middle and upstream tiers supply professional services rarely purchased directly by households: publishing, broadcasting, legal, and employment services comprise the bulk of the middle tier, followed by computer systems design, software publishing, and data processing. Upstream, corporate management accounts for over a quarter of the tier, followed by architecture and engineering, custom programming, management consulting, and advertising. These services connect the chain's consumer-facing industries to business-service suppliers.

- **Personal services and food (C_2):** Comprising 25 percent of value added, this chain is heavily skewed toward final consumption. Nearly two-thirds of its value added resides in the consumer-facing tier, led by hospitals, full- and limited-service restaurants, universities, nursing and community care, and dental practices. The middle tier consists primarily of logistics, grocery, and nondurable wholesale (together constituting 80 percent of the tier), supplemented by civic organizations and spectator sports. The upstream tier is anchored by scientific research and development (nearly two-thirds of the tier), followed by rail transportation and agricultural production.
- **Health and hospitality (C_3):** This chain accounts for roughly 20 percent of value added, distributed relatively evenly across its tiers. Consumer-facing sectors include physician offices, accommodation, air transportation, outpatient care, and pharmaceutical preparations. The middle tier comprises electric power and petroleum wholesale (nearly 40 percent of the tier), alongside accounting, dining establishments, drug wholesale, waste management, and transit. The upstream tier is the most fragmented in the system, with no single industry exceeding 15 percent of the tier's value added; it includes building services, support transportation, machinery rental, warehousing, couriers, mining support, and printing. Its middle tier includes energy suppliers as well as service producers.
- **Manufacturing and construction (C_4):** The smallest chain (under 20 percent of value added) and the only one dominated by upstream production: nearly half of its value added sits upstream, with only 12.5 percent in the consumer-facing tier. Automotive repair and motor vehicle manufacturing face the consumer (roughly two-thirds of the tier), followed by communications equipment, appliances, and computer equipment. The middle tier consists of durable-goods, appliance, and machinery wholesale, alongside aircraft, motor-vehicle parts, semiconductors, and plastics. The upstream tier is overwhelmingly dominated by construction (over 80 percent of the tier), trailed by a fragmented distribution of metal, machinery, and parts manufacturers. Its substantial production of investment goods helps explain its relatively small direct PCE weight; indirect links to consumer-facing industries remain.

The hit/safe split also differs across chains. In C_3, large employment losses occurred at both consumer-facing and upstream producers, including accommodation, air transportation, transit, laundry, airport operations, and oil-and-gas support activities. Physician and outpatient care were comparatively stable, while warehousing and courier services expanded.

In C_2, losses were concentrated nearer final consumption. Restaurants, amusement and recreation, and nursing care contracted sharply, while hospitals, schools, and home health care were less affected. Employment was more resilient in the upstream agricultural and research industries. There, the hit label identifies the lower half of the employment-growth distribution, including some industries that expanded.

In C_1, differences within retail are important: department stores, automotive dealers, and clothing retailers contracted, while supermarkets, warehouse clubs, and online retail expanded. The finer-industry split described above retains this variation within the aggregate retail category.

In C_4, employment losses were smaller and more similar across tiers. Upstream losses exceeded those in the consumer-facing tier, reflecting declines in commercial and industrial construction and oil-field machinery. Residential building, remodeling, and light truck manufacturing were less affected. Across the network, a safe node can therefore represent either a smaller contraction or an expansion.

Table A3: BEA industries in each chain and tier of the model production network.

Cell (industries)	BEA detail industries and codes, by 2017 value added
C_1 consumer-facing (h) (6)	Retail trade (RTRADE)†; Wired telecommunications carriers (517110)*; Wireless and other telecom (WLTEL)†; Other educational services (611B00)†; Performing arts companies (711100)*; Computer terminals and other computer peripheral equipment manufacturing (334118)*
C_1 middle (m) (24)	Publishing, broadcasting and information services (INFOS)*; Legal services (541100); Employment services (561300); Computer systems design services (541512); Software publishers (511200); Data processing, hosting, and related services (518200); Professional and commercial equipment and supplies (423400)*; Motion picture and video industries (512100)*; Investigation and security services (561600)*; Business support services (561400)*; Pipeline transportation (486000)*; Personal and household goods repair and maintenance (811400)*; Office administrative services (561100)*; Search, detection, and navigation instruments manufacturing (334511); Electronic and precision equipment repair and maintenance (811200); Other support services (561900)*; Independent artists, writers, and performers (711500)*; Travel arrangement and reservation services (561500)*; Promoters of performing arts and sports and agents for public figures (711A00)*; Surgical appliance and supplies manufacturing (339113); Ship building and repairing (336611); Guided missile and space vehicle manufacturing (336414); Other concrete product manufacturing (327390)*; Propulsion units and parts for space vehicles and guided missiles (33641A)
C_1 upstream (l) (16)	Management of companies and enterprises (550000)*; Architectural, engineering, and related services (541300); Custom computer programming services (541511); Management consulting services (541610); Lessors of nonfinancial intangible assets (533000)*; Advertising, public relations, and related services (541800)*; All other miscellaneous professional, scientific, and technical services (5419A0); Commercial and industrial machinery and equipment repair and maintenance (811300)*; Environmental and other technical consulting services (5416A0)*; Aircraft engine and engine parts manufacturing (336412)*; Facilities support services (561200)*; Ready-mix concrete manufacturing (327320)*; Cement manufacturing (327310); Dental laboratories (339116)*; Miscellaneous nonmetallic mineral products (327999)*; Dental equipment and supplies manufacturing (339114)*
C_2 consumer-facing (h) (44)	Hospitals (622000); Full-service restaurants (722110)*; Limited-service restaurants (722211)*; Junior colleges, colleges, universities, and professional schools (611A00); Nursing and community care facilities (623A00)*; Offices of dentists (621200); Individual and family services (624100); Offices of other health practitioners (621300); Religious organizations (813100)*; Home health care services (621600); Gasoline stations (447000); Tobacco manufacturing (312200); Other amusement and recreation industries (713900)*; Grantmaking, giving, and social advocacy organizations (813A00); Residential mental health, substance abuse, and other residential care facilities (623B00); Elementary and secondary schools (611100); Child day care services (624400)*; Veterinary services (541940); Community food, housing, and other relief services, including vocational rehabilitation services (624A00)*; Animal (except poultry) slaughtering, rendering, and processing (31161A); Bread and bakery product manufacturing (311810)*; Toilet preparation manufacturing (325620); Fruit and tree nut farming (111300); Poultry processing (311615); Breweries (312120)*; Snack food manufacturing (311910); Soft drink and ice manufacturing (312110); Death care services (812200); Amusement parks and arcades (713100)*; Greenhouse, nursery, and floriculture production (111400); Sugar and confectionery product manufacturing (311300); Frozen food manufacturing (311410); Wineries (312130)*; Vegetable and melon farming (111200); Fruit and vegetable canning, pickling, and drying (311420); Fluid milk and butter manufacturing (31151A);

continued on the next page

Table A3, continued

Cell (industries)	BEA detail industries and codes, by 2017 value added
	Cookie, cracker, pasta, and tortilla manufacturing (3118A0); Dry, condensed, and evaporated dairy product manufacturing (311514); Fishing, hunting and trapping (114000); All other food manufacturing (311990); Seasoning and dressing manufacturing (311940); Dog and cat food manufacturing (311111); Coffee and tea manufacturing (311920)*; Breakfast cereal manufacturing (311230)
C_2 middle (m) (10)	Other nondurable goods merchant wholesalers (424A00)†; Truck transportation (484000)†; Grocery and related product wholesalers (424400)†; Civic, social, professional, and similar organizations (813B00)†; Spectator sports (711200)*; Soap and cleaning compound manufacturing (325610); Water, sewage and other systems (221300)†; Distilleries (312140); Cheese manufacturing (311513); Seafood product preparation and packaging (311700)*
C_2 upstream (l) (22)	Scientific research and development services (541700); Rail transportation (482000)*; Beef cattle ranching and farming, including feedlots and dual-purpose ranching and farming (1121A0)*; Animal production, except cattle and poultry and eggs (112A00)*; Support activities for agriculture and forestry (115000)*; Oilseed farming (1111A0)*; Grain farming (1111B0)*; Dairy cattle and milk production (112120)*; Other crop farming (111900); Fertilizer manufacturing (325310)*; Metal can, box, and other metal container (light gauge) manufacturing (332430)*; Poultry and egg production (112300)*; Flavoring syrup and concentrate manufacturing (311930)*; Pesticide and other agricultural chemical manufacturing (325320); Other animal food manufacturing (311119)*; Flour milling and malt manufacturing (311210)*; Plastics bottle manufacturing (326160); Soybean and other oilseed processing (311224); Packaging machinery manufacturing (333993); Wet corn milling (311221)*; Ice cream and frozen dessert manufacturing (311520); Fats and oils refining and blending (311225)*
C_3 consumer-facing (h) (30)	Offices of physicians (621100); Accommodation (721000)*; Air transportation (481000)*; Outpatient care centers (621400); Pharmaceutical preparation manufacturing (325412); Gambling industries (except casino hotels) (713200)*; Other personal services (812900)*; Natural gas distribution (221200); Personal care services (812100)*; Medical and diagnostic laboratories (621500); General and consumer goods rental (532A00)*; Other ambulatory health care services (621900); Water transportation (483000)*; Museums, historical sites, zoos, and parks (712000)*; Photographic services (541920)*; Apparel manufacturing (315000)*; Tire manufacturing (326210)*; Sporting and athletic goods manufacturing (339920); Upholstered household furniture manufacturing (337121)*; Sanitary paper product manufacturing (322291); Carpet and rug mills (314110)*; Other furniture related product manufacturing (337900); Ophthalmic goods manufacturing (339115)*; Cut stone and stone product manufacturing (327991); Leather and allied product manufacturing (316000)*; Nonupholstered wood household furniture manufacturing (337122)*; Doll, toy, and game manufacturing (339930); Motor home manufacturing (336213); Curtain and linen mills (314120)*; Office supplies (except paper) manufacturing (339940)*
C_3 middle (m) (26)	Electric power generation, transmission, and distribution (221100); Petroleum and petroleum products (424700); Accounting, tax preparation, bookkeeping, and payroll services (541200); All other food and drinking places (722A00)*; Drugs and druggists' sundries (424200); Waste management and remediation services (562000); Transit and ground passenger transportation (485000)*; Automotive equipment rental and leasing (532100)*; Specialized design services (541400); Dry-cleaning and laundry services (812300)*; Biological product (except diagnostic) manufacturing (325414); All other chemical product and preparation manufacturing (3259A0);

continued on the next page

Table A3, continued

Cell (industries)	BEA detail industries and codes, by 2017 value added
	Sound recording industries (512200); Paper mills (322120); Glass and glass product manufacturing (327200); Plastics packaging materials and unlaminated film and sheet manufacturing (326110); Paper bag and coated and treated paper manufacturing (322220); Other petroleum and coal products manufacturing (324190); Adhesive manufacturing (325520); Fabric mills (313200); Other textile product mills (314900); Clay product and refractory manufacturing (327100); Abrasive product manufacturing (327910); Rubber and plastics hoses and belting manufacturing (326220); All other converted paper product manufacturing (322299); Stationery product manufacturing (322230)
C_3 upstream (l) (45)	Services to buildings and dwellings (561700)†; Scenic and sightseeing transportation and support activities (48A000)†; Commercial and industrial machinery and equipment rental and leasing (532400)*; Warehousing and storage (493000)†; Couriers and messengers (492000); Other support activities for mining (21311A)†; Printing (323110)*; Other basic organic chemical manufacturing (325190)†; Wholesale electronic markets and agents and brokers (425000)*; Other computer related services, including facilities management (54151A); Surgical and medical instrument manufacturing (339112); Petrochemical manufacturing (325110)*; Plastics material and resin manufacturing (325211); Paperboard container manufacturing (322210)†; Other basic inorganic chemical manufacturing (325180)*; Forestry and logging (113000)†; Paperboard mills (322130); Coal mining (212100)*; Sawmills and wood preservation (321100)†; Millwork (321910); Veneer, plywood, and engineered wood product manufacturing (321200)†; Other nonmetallic mineral mining and quarrying (2123A0)†; Stone mining and quarrying (212310)†; In-vitro diagnostic substance manufacturing (325413); Wood kitchen cabinet and countertop manufacturing (337110); Plastics pipe, pipe fitting, and unlaminated profile shape manufacturing (326120)†; Synthetic rubber and artificial and synthetic fibers and filaments manufacturing (3252A0)*; Medicinal and botanical manufacturing (325411); Lime and gypsum product manufacturing (327400)*; Asphalt shingle and coating materials manufacturing (324122); Industrial gas manufacturing (325120)*; Urethane and other foam product (except polystyrene) manufacturing (326150)*; Mineral wool manufacturing (327993)*; Concrete pipe, brick, and block manufacturing (327330)†; Asphalt paving mixture and block manufacturing (324121)*; Polystyrene foam product manufacturing (326140)*; Synthetic dye and pigment manufacturing (325130); Textile and fabric finishing and fabric coating mills (313300)*; Pulp mills (322110)*; Support activities for printing (323120)*; Laminated plastics plate, sheet (except packaging), and shape manufacturing (326130)*; Carbon and graphite product manufacturing (335991)*; Fiber, yarn, and thread mills (313100)*; Manufacturing and reproducing magnetic and optical media (334610)*; Printing ink manufacturing (325910)*
C_4 consumer-facing (h) (22)	Automotive repair and maintenance (including car washes) (811100)†; Auto and truck manufacturing (AUTOMAN); Broadcast and wireless communications equipment (334220); All other miscellaneous manufacturing (339990)†; Major household appliance manufacturing (335220); Electronic computer manufacturing (334111)*; Watch, clock, and other measuring and controlling device manufacturing (33451A)*; Ammunition, arms, ordnance, and accessories manufacturing (33299A); Travel trailer and camper manufacturing (336214); Cutlery and handtool manufacturing (332200)*; Battery manufacturing (GRNTURB)†; Motorcycle, bicycle, and parts manufacturing (336991); Jewelry and silverware manufacturing (339910)*; Computer storage device manufacturing (334112)*; Lawn and garden equipment manufacturing (333112); Boat building (336612); All other transportation equipment manufacturing (336999); Military armored vehicle, tank, and tank component manufacturing (336992); Audio and video equipment manufacturing (334300)*; Small electrical appliance manufacturing (335210); Power-driven handtool manufacturing (333991); Other household nonupholstered furniture (33712N)†

continued on the next page

Table A3, continued

Cell (industries)	BEA detail industries and codes, by 2017 value added
C_4 middle (m) (66)	Other durable goods merchant wholesalers (423A00); Household appliances and electrical and electronic goods (423600); Machinery, equipment, and supplies (423800)*; Aircraft manufacturing (336411)*; Motor vehicle and motor vehicle parts and supplies (423100)*; Semiconductor and related device manufacturing (334413); Other plastics product manufacturing (326190); Iron and steel mills and ferroalloy manufacturing (331110)*; Electromedical and electrotherapeutic apparatus manufacturing (334510); Machine shops (332710)*; Other electronic component manufacturing (33441A); Ornamental and architectural metal products manufacturing (332320); Other motor vehicle parts manufacturing (336390); Plate work and fabricated structural product manufacturing (332310)*; Air conditioning, refrigeration, and warm air heating equipment manufacturing (333415); Printed circuit assembly (electronic assembly) manufacturing (334418)*; Turned product and screw, nut, and bolt manufacturing (332720)*; Motor vehicle transmission and power train parts manufacturing (336350); Other industrial machinery manufacturing (33329A); Analytical laboratory instrument manufacturing (334516); Commercial, service and optical equipment (OTHRMACH)*; Paint and coating manufacturing (325510); Farm machinery and equipment manufacturing (333111); Other general purpose machinery manufacturing (33399A)*; Motor vehicle gasoline engine and engine parts manufacturing (336310)*; All other wood product manufacturing (3219A0); Wiring device manufacturing (335930)*; Electricity and signal testing instruments manufacturing (334515); Office furniture and custom architectural woodwork and millwork manufacturing (33721A)*; Steel product manufacturing from purchased steel (331200)*; Irradiation apparatus manufacturing (334517)*; Motor vehicle electrical and electronic equipment manufacturing (336320)*; Light fixtures and bulbs (LIGHTFX)*; Other rubber product manufacturing (326290)*; Other engine equipment manufacturing (333618)*; Other fabricated metal manufacturing (332999)*; Sign manufacturing (339950)*; Heavy duty truck manufacturing (336120); Motor vehicle steering, suspension component (except spring), and brake systems manufacturing (3363A0)*; Switchgear and switchboard apparatus manufacturing (335313); Special tool, die, jig, and fixture manufacturing (333514)*; Metal crown, closure, and other metal stamping (except automotive) (332119)*; All other miscellaneous electrical equipment and component manufacturing (335999); Nonferrous metal (except copper and aluminum) rolling, drawing, extruding and alloying (331490)*; Copper rolling, drawing, extruding and alloying (331420)*; Communication and energy wire and cable manufacturing (335920); Motor vehicle body manufacturing (336211)*; Spring and wire product manufacturing (332600)*; Motor and generator manufacturing (335312)*; Cutting and machine tool accessory, rolling mill, and other metalworking machinery manufacturing (33351B)*; Machine tool manufacturing (333517)*; Telephone apparatus manufacturing (334210)*; Other communications equipment manufacturing (334290); Fabricated pipe and pipe fitting manufacturing (332996)*; Hardware manufacturing (332500)*; Showcase, partition, shelving, and locker manufacturing (337215)*; Power, distribution, and specialty transformer manufacturing (335311)*; Truck trailer manufacturing (336212)*; Automatic environmental control manufacturing (334512)*; Mechanical power transmission equipment manufacturing (333613)*; Ground or treated mineral and earth manufacturing (327992)*; Institutional furniture manufacturing (337127)*; Heating equipment (except warm air furnaces) manufacturing (333414); Plumbing fixture fitting and trim manufacturing (332913); Speed changer, industrial high-speed drive, and gear manufacturing (333612)*; Industrial process furnace and oven manufacturing (333994)*

continued on the next page

Table A3, continued

Cell (industries)	BEA detail industries and codes, by 2017 value added
C_4 upstream (l) (30)	Construction (CNSTRCT)†; Other aircraft parts and auxiliary equipment manufacturing (336413)*; Coating, engraving, heat treating and allied activities (332800)*; Construction machinery manufacturing (333120)*; Valve and fittings other than plumbing (33291A)*; Material handling equipment manufacturing (333920)†; Motor vehicle metal stamping (336370)*; Industrial process variable instruments manufacturing (334513)*; Motor vehicle seating and interior trim manufacturing (336360)*; Ferrous metal foundries (331510)*; Measuring, dispensing, and other pumping equipment manufacturing (333914)*; Aluminum product manufacturing from purchased aluminum (33131B)*; Mining and oil and gas field machinery manufacturing (333130)*; Turbine and turbine generator set units manufacturing (333611)*; Nonferrous metal foundries (331520)*; Semiconductor machinery manufacturing (333242); Relay and industrial control manufacturing (335314)*; All other forging, stamping, and sintering (33211A)*; Fluid power process machinery (33399B)*; Metal tank (heavy gauge) manufacturing (332420)*; Railroad rolling stock manufacturing (336500)*; Nonferrous metal (except aluminum) smelting and refining (331410)*; Air and gas compressor manufacturing (333912)*; Ball and roller bearing manufacturing (332991)*; Industrial mold manufacturing (333511)*; Power boiler and heat exchanger manufacturing (332410)*; Totalizing fluid meter and counting device manufacturing (334514)*; Industrial and commercial fan and blower and air purification equipment manufacturing (333413); Custom roll forming (332114); Aluminum manufacturing and smelting (ALUMAN)*

Notes: The table lists the 341 endogenous industries in the 357-industry system; the EXO exclusions are described in Online Appendix A.1.5. Entries use BEA 2017 detail codes or the corresponding aggregate codes. Industries within each cell are ordered by 2017 value added, largest first. An asterisk denotes assignment to the hit node; a dagger denotes a BEA industry split between hit and safe nodes using six-digit NAICS employment. Unmarked industries belong to the safe node.

Figure A1 reports the resulting input shares at the 24-node level. Rows identify buyers and columns suppliers. Blocks along the diagonal contain within-chain purchases; the other blocks contain purchases across chains. On average across nodes, 57 percent of the displayed input purchases originate within the buyer's chain. This describes the concentration achieved by the aggregation, rather than an independent test of it. Adjacent hit and safe rows show differences in sourcing within a tier.

A.2.3 Excluded industries

Table A4 lists the 16 EXO industries, whose prices the model takes as given, and the 39 commodity-price-linked industries that the price-dispersion statistics exclude in addition.

Table A4: Industries excluded from the model (EXO) and from the price-dispersion statistics (commodity-price-linked).

Group (industries)	BEA detail industries and codes
EXO: extractive and refining (5)	Copper, nickel, lead, and zinc mining (212230); Drilling oil and gas wells (213111); Iron, gold, silver, and other metal ore mining (2122A0); Oil and gas extraction (211000); Petroleum refineries (324110)
EXO: housing and real estate (1)	Housing and real estate (agg.) (HOUSING)
EXO: finance and insurance (8)	Direct life insurance carriers (524113); Funds, trusts, and other financial vehicles (525000); Insurance agencies, brokerages, and related activities (524200); Insurance carriers, except direct life (5241XX); Monetary authorities and depository credit intermediation (52A000); Nondepository credit intermediation and related activities (522A00); Other financial investment activities (523900); Securities and commodity contracts intermediation and brokerage (523A00)
EXO: government (2)	Federal government (agg.) (FEDGOV); State and local government (agg.) (SLGOV)

Table A4, continued

Group (industries)	BEA detail industries and codes
Commodity-price-linked: crop production (6)	Fruit and tree nut farming (111300); Grain farming (1111B0); Greenhouse, nursery, and floriculture production (111400); Oilseed farming (1111A0); Other crop farming (111900); Vegetable and melon farming (111200)
Commodity-price-linked: animal production (4)	Animal production, except cattle and poultry and eggs (112A00); Beef cattle ranching and farming, including feedlots and dual-purpose ranching and farming (1121A0); Dairy cattle and milk production (112120); Poultry and egg production (112300)
Commodity-price-linked: meat products (2)	Animal (except poultry) slaughtering, rendering, and processing (31161A); Poultry processing (311615)
Commodity-price-linked: dairy products (4)	Cheese manufacturing (311513); Dry, condensed, and evaporated dairy product manufacturing (311514); Fluid milk and butter manufacturing (31151A); Ice cream and frozen dessert manufacturing (311520)
Commodity-price-linked: grain and oilseed milling (5)	Breakfast cereal manufacturing (311230); Fats and oils refining and blending (311225); Flour milling and malt manufacturing (311210); Soybean and other oilseed processing (311224); Wet corn milling (311221)
Commodity-price-linked: fertilizer and agricultural chemicals (2)	Fertilizer manufacturing (325310); Pesticide and other agricultural chemical manufacturing (325320)
Commodity-price-linked: basic chemicals (incl. petrochemicals) (5)	Industrial gas manufacturing (325120); Other basic inorganic chemical manufacturing (325180); Other basic organic chemical manufacturing (325190); Petrochemical manufacturing (325110); Synthetic dye and pigment manufacturing (325130)
Commodity-price-linked: resins and synthetics (2)	Plastics material and resin manufacturing (325211); Synthetic rubber and artificial and synthetic fibers and filaments manufacturing (3252A0)
Commodity-price-linked: primary metals (9)	Aluminum manufacturing and smelting (agg.) (ALUMAN); Aluminum product manufacturing from purchased aluminum (33131B); Copper rolling, drawing, extruding and alloying (331420); Ferrous metal foundries (331510); Iron and steel mills and ferroalloy manufacturing (331110); Nonferrous metal (except aluminum) smelting and refining (331410); Nonferrous metal (except copper and aluminum) rolling, drawing, extruding and alloying (331490); Nonferrous metal foundries (331520); Steel product manufacturing from purchased steel (331200)

Notes: The 16 EXO industries are the 357-industry system's industries outside the model's 341 endogenous industries, and the model takes their prices as given. The 39 commodity-price-linked industries are endogenous industries whose prices track world commodity markets. The price-dispersion statistics of Figure 1 (Panels C–D) and of the filled bars in Online Appendix Figure A7 exclude both groups, leaving 302 industries. Entries use BEA 2017 detail codes or the corresponding aggregate codes, listed alphabetically within each group.

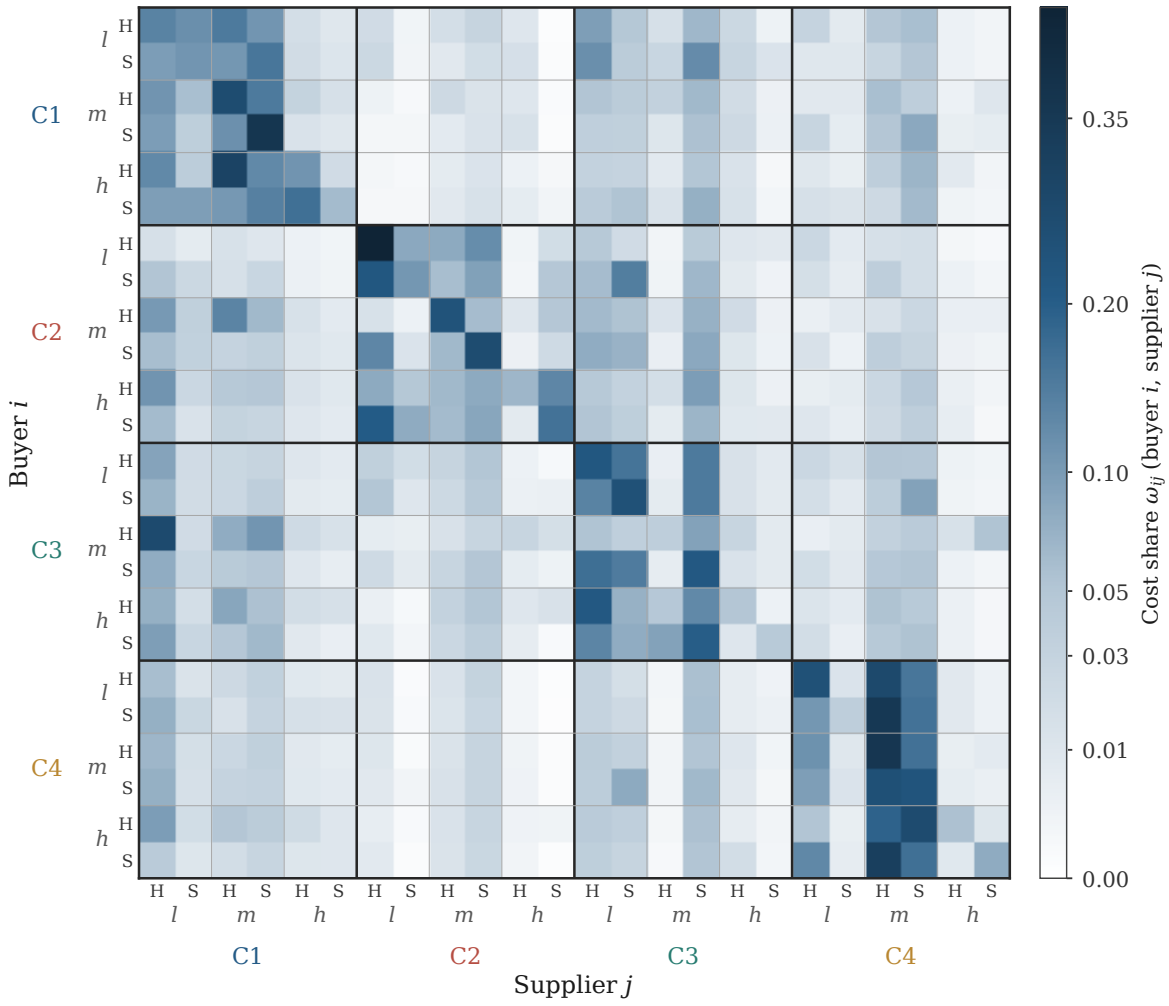

Figure A1: Intermediate-input shares across the 24 production nodes.

Notes: 2017 BEA input shares aggregated to the 24 model nodes. Rows are buyers and columns suppliers, ordered by chain, tier (l, m, h), and hit/safe status (H, S). Entries sum to one across each displayed row. Darker cells indicate larger shares; the color scale uses a square-root transformation. Diagonal blocks contain within-chain purchases.

A.3 Empirical Results: Robustness

This appendix examines three aspects of the evidence in Facts 1–3: pre-pandemic movements in exposure gradients and sensitivity to energy exposure; inference when industries share suppliers; and the relationship between supplier exposure and buyers' prices across supplier groups. Unless stated otherwise, regressions retain the two-window design of equation (5), industry and window effects, 2017 value-added weights, and the samples in Table 2. Significance stars use heteroskedasticity-robust standard errors.

Own exposure is E_i, supplier exposure is $\mathcal{E}_i = (AE)_i$, and s_i and q_i are the total-input and exposure-coverage loadings defined in the main text. We retain the direct-supplier operator A, including purchases within an industry. Direct suppliers' prices already reflect their own upstream costs; a multiround index, $A(I - \delta A)^{-1}E$, would instead assign exposure across successive supplier links. Panel C of Table 2 examines exclusions of specified supplier groups without changing this direct-supplier interpretation.

A.3.1 Pre-pandemic trends and energy prices

Table A5 compares the pandemic estimates with a placebo that applies equation (5) to 2018–2019 relative to 2017–2018. It also adds each industry's 2017 direct energy cost share, interacted with the window indicator. Panels A and B report the full sample and the middle and upstream sample, respectively.

The placebo gradients for supplier prices, supplier margins, and buyers' own prices are negative, whereas their pandemic counterparts are positive. The pandemic relationships therefore do not continue those pre-period movements. Supplier employment has a negative gradient of comparable size in both comparisons, so its placebo does not distinguish pandemic disruption from a pre-existing relationship. The energy control reduces the supplier-price and margin coefficients and weakens the placebo price relationships; the pandemic supplier-price coefficient remains positive and significant in both samples. These results show sensitivity to energy composition without eliminating the supplier-price association. The short pre-period cannot rule out reversal of a temporary disturbance, and a smaller placebo coefficient does not establish counterfactual parallel trends.

Table A5: Supplier-level regressions of Table 2 with a within-pre-period placebo and the direct energy cost share.

	2019–2022 relative to 2017–2019		Placebo: 2018–19 relative to 2017–18	
Energy cost share $\times D_w$	no	yes	no	yes
Panel A. Full sample (330 industries)				
Supplier price (buyer's input cost)	$+9.19^{***}$	$+5.22^{***}$	-7.61^{***}	-1.34
Suppliers' margin residual	$+5.53^{***}$	$+3.28^{**}$	-4.97^{***}	-2.43^{*}
Supplier employment	-2.58^{***}	-2.15^{***}	-2.28^{***}	-1.55^{**}
Buyer's own price	$+16.98^{***}$	$+7.56$	-16.23^{***}	$+0.48$
Panel B. Middle and upstream industries, $m + l$ (232)				
Supplier price (buyer's input cost)	$+10.47^{***}$	$+5.98^{***}$	-9.34^{***}	-2.44^{*}
Suppliers' margin residual	$+6.31^{***}$	$+4.08^{***}$	-6.00^{***}	-3.97^{***}
Supplier employment	-2.63^{***}	-2.36^{***}	-2.67^{***}	-1.43^{**}
Buyer's own price	$+25.21^{***}$	$+15.95^{***}$	-22.00^{***}	-1.37

Notes: Supplier-exposure coefficients from equation (5), with loading controls s_i and q_i, 2017 value-added weights, and annualized outcomes. The pandemic comparison is 2019–2022 relative to 2017–2019; the placebo is 2018–2019 relative to 2017–2018. Columns marked "yes" add the direct energy cost share interacted with D_w. Stars are based on heteroskedasticity-robust t-statistics, which for the placebo are also robust to correlation across an industry's windows: $^{*}p < 0.10$, $^{**}p < 0.05$, $^{***}p < 0.01$.

A.3.2 Inference with shared suppliers

Industries that share suppliers may have correlated regression disturbances even when they belong to different broad sectors. Table A6 therefore reports heteroskedasticity-robust and BEA-summary-sector-clustered t-statistics for every coefficient in Table 2. Sector clustering generally reduces the absolute statistics. Two of the 38 reported comparisons cross a conventional significance threshold: with sector-clustered standard errors, the full-sample own-industry domestic-input coefficient is not significant at 10 percent, and the full-sample own-industry labor-cost coefficient is significant at 10 rather than 5 percent. The other 36 retain their significance classification.

Neither estimator necessarily captures dependence between buyers in different sectors that share suppliers. Supplementary supplier-score variance calculations, reported in the replication files, give statistics of a similar order but require assumptions about dependence among the scores.

Table A6: t-statistics for the coefficients in Table 2.

	Own industries, y_i on E_i				Supplier networks, $(Ay)_i$ on $(AE)_i$			
	Full		$m+l$		Full		$m+l$	
Outcome y	Robust	Sector	Robust	Sector	Robust	Sector	Robust	Sector
Panel A. Employment, prices and quantities								
Employment, $\Delta \log N$	−2.42	−2.37	−3.80	−3.83	−4.29	−4.34	−5.43	−5.96
Price, $\Delta \log P$	2.40	2.03	5.39	4.55	7.02	5.83	7.01	5.92
Real output, $\Delta \log Y$	−3.27	−3.05	−4.36	−4.06	−7.23	−5.49	−8.64	−6.82
Panel B. Accounting components of the price gradient								
Margin, ΔMARGIN	−0.11	−0.09	0.42	0.37	4.05	3.92	4.17	3.93
Labor costs, ΔULC	1.98	1.81	1.39	1.33	0.53	0.46	1.09	1.00
Imports, ΔIMP	1.54	1.22	5.94	3.71	8.75	6.62	7.44	5.50
Domestic inputs, ΔMAT	2.08	1.58	5.66	4.39	8.57	6.66	7.39	5.47
Panel C. Supplier-margin regression: excluded suppliers								
None					4.05	3.92	4.17	3.93
EXO and retail					3.79	3.62	3.85	3.59
EXO, trade, utilities					3.98	3.51	4.73	4.12
Industries	330		232		330		232	

Notes: t-statistics for the coefficients of the main-text two-level table, with heteroskedasticity-robust standard errors ("Robust", the basis of the significance stars in the main text) and with standard errors clustered by BEA summary sector ("Sector"). Samples, outcomes, and specifications are those of the main-text table; Panel C rows are the supplier-margin regression with cumulative supplier exclusions.

A.3.3 Buyers' prices, supplier origin, and energy exposure

Table A7 examines whether the buyer-price relationship in Fact 3 is confined to exposure to energy and commodity suppliers. Panel A adds the direct energy cost share to the pooled supplier-exposure regression. Panel B separates exposure to a selected supplier group S from exposure to its complement R, $(AE)_i = (A^S E)_i + (A^R E)_i$. The matrices A^S and A^R retain the corresponding supplier columns of A. The three nested groups comprise extractive and petroleum-refining suppliers; these industries plus utilities and basic chemicals; and, additionally, agriculture, food, beverages, and primary metals. Both exposure components enter jointly, with s_i, q_i, the selected group's input loading, and its exposure-coverage loading when the latter is linearly independent. Panel B reports the coefficient on exposure to suppliers outside S.

The input-cost relationship remains positive and significant in both samples under every partition. Supplier-margin coefficients also remain positive. For buyers' own prices, the energy control and wider partitions reduce the full-sample coefficient and its precision. Among middle and upstream industries, the relationship remains positive and significant at 1 percent under all three partitions. Thus, the evidence beyond direct commodity exposure is more consistent for input costs than for buyers' prices across the full sample. These partitions do not remove commodity-price effects transmitted through other suppliers.

Table A7: Supplier exposure by supplier origin: buyers' input costs, suppliers' margins and buyers' own prices.

	Full sample		Middle and upstream	
	Baseline	Energy share	Baseline	Energy share
Panel A. Exposure to all suppliers				
Input-cost contribution	9.19***	5.22***	10.47***	5.98***
Supplier margin component	5.53***	3.28**	6.31***	4.08***
Buyer's own price	16.98***	7.56	25.21***	15.95***
Panel B. Exposure to suppliers outside the listed group				
	Full sample		Middle and upstream	
Outside extractive and refining suppliers				
Input-cost contribution	6.46***		7.53***	
Supplier margin component	3.82***		5.02***	
Buyer's own price	15.37***		19.87***	
Outside energy suppliers				
Input-cost contribution	5.44***		6.29***	
Supplier margin component	3.47***		4.31***	
Buyer's own price	7.77		15.89***	
Outside energy and other commodity suppliers				
Input-cost contribution	5.61***		6.27***	
Supplier margin component	3.64**		3.79***	
Buyer's own price	7.83		16.04***	

Notes: Coefficients in the two-window design of equation (5), in annual pp outcome units per unit of exposure. Regressions use 2017 value-added weights and loading controls s_i and q_i; samples contain 330 and 232 industries. Panel A uses exposure to all suppliers; energy-share columns add the direct energy cost share. Panel B reports the coefficient on exposure to suppliers outside each listed group from a joint regression on both exposure components, with the pooled loading controls, a group-specific input-loading control, and a group-specific score-coverage control where it is not collinear with the former; definitions are in Appendix A.3.3. Stars follow the heteroskedasticity-robust t-statistic: $^{*}p < 0.10$, $^{**}p < 0.05$, $^{***}p < 0.01$.

A.4 Empirical Results: Extensions

This appendix examines the timing of the exposure relationship, price–labor-cost comovement, and wage pressure among recent hires.

A.4.1 Timing across the pandemic windows

Table A8 separates the pandemic into two two-year windows, 2019–2021 and 2021–2023, using 2017–2019 as the reference. Each pandemic window has its own exposure interaction and, for supplier outcomes, its own loading-control interactions. The remaining specification is unchanged, and coefficients are annualized.

During 2019–2021, exposed supplier networks exhibit lower employment and output growth and higher price and margin-residual growth. During 2021–2023, the supplier-margin coefficients are negative and significant at 10 percent, the supplier-price coefficient is significant at 10 percent only among middle and upstream industries, supplier-employment growth is positive, and the supplier labor-cost contribution is positive and significant. The strongest price and margin relationships thus occur during contraction and early reopening; later, the association shifts toward employment recovery and measured labor costs. These comparisons describe the estimated timing rather than test equality of coefficients across windows.

Table A8: Three-window design: own level and supplier level by window.

	Own level: y_i on E_i		Supplier level: $(Ay)_i$ on $(AE)_i$	
Outcome y	Full	$m+l$	Full	$m+l$
Panel A. 2019–2021				
Employment, $\Delta \log N$	-1.76^{**}	-3.37^{***}	-3.55^{***}	-3.34^{***}
Price, $\Delta \log P$	1.05	1.35^{***}	7.45^{***}	8.69^{***}
Real gross output, $\Delta \log Y$	-2.80^{***}	-4.49^{***}	-4.41^{***}	-4.89^{***}
Margin residual, ΔMARGIN	-0.13	0.69	6.57^{***}	7.16^{***}
Unit labor costs, ΔULC	0.98	-0.15	-1.62^{**}	-1.24^{**}
Imported inputs, ΔIMP	0.02	0.09^{***}	0.28^{***}	0.32^{***}
Supply-chain price, ΔMAT	0.19^{**}	0.72^{***}	2.22^{***}	2.45^{***}
Panel B. 2021–2023				
Employment, $\Delta \log N$	1.17^{*}	0.42	1.70^{***}	1.43^{**}
Price, $\Delta \log P$	0.85^{**}	2.05^{***}	1.33	1.57^{*}
Real gross output, $\Delta \log Y$	1.75^{**}	-0.03	0.64	0.16
Margin residual, ΔMARGIN	0.25	-0.34	-2.19^{*}	-2.12^{*}
Unit labor costs, ΔULC	0.46	2.03	3.22^{**}	3.48^{***}
Imported inputs, ΔIMP	0.02^{**}	0.04^{***}	-0.04	-0.06^{***}
Supply-chain price, ΔMAT	0.12^{*}	0.32^{***}	0.34^{***}	0.27^{***}
Industries	330	232	330	232

Notes: The design of Table 2 estimated on three two-year windows, 2017–2019 (reference), 2019–2021 and 2021–2023, with a separate exposure gradient for each pandemic window; coefficients are annualized, so twice the coefficient is the two-year change relative to the reference-window gradient. Levels, controls, weights and star thresholds as in Table 2; standard errors are robust to heteroskedasticity and to correlation across an industry's windows.

A.4.2 Labor-cost and price comovement

To compare price–cost comovement across phases of the episode, we regress cumulative industry price growth on the unit-labor-cost contribution ΔULC in equation (2). We estimate separate regressions for 2017–2019, 2019–2021, and 2021–2023, including BEA summary-sector effects and using 2017 value-added weights and heteroskedasticity-robust standard errors. The regressor is the measured contribution, not its logarithm.

Table A9 reports the slopes for the full sample and for $m+l$, together with cross-industry dispersion and correlation. The slopes rise between the pre-pandemic and early-pandemic windows and remain elevated in 2021–2023. An analogous comparison across the model's 24 nodes gives a larger slope in 2019–2021 than in 2021–2023 under both expectations regimes. These regressions summarize conditional comovement, not causal pass-through: prices and measured labor costs respond jointly to the recovery, and the model assigns part of its rebuilding premium to measured wages through the calibrated attribution rule.

A.4.3 Worker flows and the earnings of recent hires

Average payroll may understate wage pressure concentrated among new hires. Using the Quarterly Workforce Indicators, we compare the average monthly earnings of recent hires that became full-quarter jobs, $\text{EarnHirAS}_{i,t}$, with those of all full-quarter jobs, $\text{EarnS}_{i,t}$:

$$hp_{i,t} = \log\left(\frac{\text{EarnHirAS}_{i,t}}{\text{EarnS}_{i,t}}\right).$$

Table A9: Industry price growth and measured labor-cost growth.

Subsample	2017–2019	2019–2021	2021–2023
Full sample	$+0.153^{***}$	$+0.264^{***}$	$+0.251^{***}$
$m + l$	$+0.156^{***}$	$+0.309^{***}$	$+0.283^{***}$
Full-sample dispersion and correlation:			
sd(ΔULC), pp	11.31	9.99	14.69
sd($\Delta \log P$), pp	4.69	8.12	7.53
corr($\Delta \log P$, ΔULC)	+0.29	+0.23	+0.42
N industries	330 (full); 232 ($m + l$)		

Notes: Separate cross-sectional regressions of cumulative industry price growth, $\Delta \log P_{i,w}$, on the labor-cost contribution $\Delta \text{ULC}_{i,w}$ in equation (2). Each includes BEA summary-sector fixed effects and uses 2017 value-added weights. Stars use heteroskedasticity-robust standard errors: $^{*}p < 0.10$, $^{**}p < 0.05$, $^{***}p < 0.01$. Regressions span roughly 57 BEA-66 sectors. $m + l$ denotes the middle and upstream sample defined by finalness, not a direct sales-share cutoff. These slopes summarize conditional price–cost comovement; they are not estimates of structural pass-through.

The denominator includes recent hires as well as continuing jobs. We map four-digit NAICS series to the paper's industries using 2019 employment weights and average the quarterly observations within each year. The comparison measures relative earnings across job groups, not the wage change of an otherwise identical worker.

The employment-weighted premium rises above its 2017–2019 mean in 2021, peaks in 2022, and recedes by 2024. It does not exceed an extrapolation of its pre-pandemic trend. A fixed-flow conversion multiplies the change in the premium by the stable-hire rate and the labor share. The resulting wage-cost contribution accounts for about 7 percent of the 2019–2021 margin-residual contribution and 18 percent of the 2021–2023 labor-cost contribution. These magnitudes rule out the measured recent-hire earnings premium as the principal explanation for either contribution under this accounting comparison. Recruiting, training, and production disruption entail additional costs outside the earnings measure.

A.5 Construction of Industry COVID-19 Exposure

A.5.1 Construction

The COVID-19 Job-Exposure Matrix (JEM) of Oude Hengel et al. (2022) scores ISCO-08 occupations in Denmark, the Netherlands, and the United Kingdom. We retain six dimensions: number and nature of contacts, contaminated workspaces, work location, social distance, and face covering. We omit income insecurity and migrant status, which concern precarious work rather than physical exposure. The industry index combines these scores with pre-pandemic occupational employment shares; no realized employment or price changes enter its construction.

Occupational exposure. Within each country sheet of the accompanying `Supplementary file COVID-19 JEM.xlsx`, we average duplicate ISCO-08 codes. To estimate the loadings, we average each dimension across the three countries, obtaining a 436×6 occupation-by-dimension matrix, standardize each column, and compute the first principal component of its 6×6 correlation matrix Σ. The sign is chosen so higher scores indicate greater exposure; the estimated loadings are positive. PC1 explains 73.5% of the six dimensions' variance in this matrix. Loadings are approximately 0.44 for five dimensions and 0.29 for face covering, whose correlations with the other dimensions are lower. We apply these loadings to the standardized Danish-panel scores; we use the Danish tabulation throughout because it has been validated against population-wide infection records (van der Feltz et al., 2023).

We apply a positive affine transformation to rescale the index so that its mean and standard deviation match those of the equally weighted six-dimension average:

$$e_o = \alpha + \beta v^\top \widetilde{\text{score}}_o, \qquad v \in \arg\max_{\|v\|=1} v^\top \Sigma v, \qquad \beta > 0.$$

Here $\widetilde{\text{score}}_o$ contains the six standardized scores for occupation o, and v is the first-component loading vector. The positive affine transformation preserves rankings but does not impose equal component weights or restrict the index to the original $[0, 3]$ item scale. In the estimation matrix, the first-component score and the simple average have a correlation of 0.995; their similarity does not imply identical exposure coefficients in the subsequent regressions.

ISCO-08 to SOC-2018 mapping. We link the BLS ISCO-08-to-SOC-2010 and SOC-2010-to-SOC-2018 concordances. For each SOC-2018 occupation, exposure is the unweighted mean of scores for all ISCO occupations mapped to it. The resulting mapping covers 865 SOC-2018 codes.

Industry aggregation. The Occupational Employment and Wage Statistics (OEWS) matrix contains 345 BEA industries and 789 occupations. Exposure scores match 745 occupations, covering 86.9% of industry employment on average. We normalize employment shares over matched occupations within each industry:

$$s_{io}^{2019} = \frac{\text{OEWS}_{io}^{2019}}{\sum_{o' \in \text{matched}} \text{OEWS}_{io'}^{2019}}, \qquad E_i = \sum_{o \in \text{matched}} s_{io}^{2019} e_o.$$

The score covers 345 industries in the BEA-357 classification, with mean 1.32, standard deviation 0.33, and range $[0.34, 2.31]$. High-exposure industries include food retail, child care, personal services, restaurants, hospitals, accommodation, and residential care. Low-exposure industries include software, data processing, insurance, securities, consulting, accounting, and computer systems design. Regression samples apply the exclusions described in Section 2.

Validation and timing. van der Feltz et al. (2023) validate the Danish JEM panel using occupation-linked infection records for approximately two million workers across three waves during February 2020–December 2021. Its predictive relationship is most evident in the initial wave and attenuates later. Denmark's broad access to testing reduces dependence on symptom-selected test samples. This validates the Danish panel scores that our index uses; it is not a validation of the principal-component weighting itself. The crosswalks and employment weights predate the pandemic. The COVID-specific JEM scores characterize occupational exposure, rather than measuring industries' realized employment or inflation outcomes.

A.6 Detrending Data for Model Calibration

Calibration targets are deviations from chain-level log-linear trends. Gross output and employment use the 2017–2024 window; gross-output deflators and wages use the pre-pandemic 2017–2019 window. The longer quantity window incorporates the realized growth path, whereas the pre-pandemic price and wage trends do not absorb the subsequent inflation surge. An additional normalization sets aggregate detrended employment to zero in 2024. The employment gap is therefore measured relative to this terminal benchmark, not to an extrapolated pre-pandemic employment trend.

Tier-level measurement. Real gross output Y_i is measured by BEA gross output in 2017 dollars, and employment N_i comes from QCEW. For the 2020 employment target, we apply growth from January–February 2020 to January–February 2021 to the 2019 annual-average level. This separates persistent losses from the temporary layoffs of March–April 2020 that were largely reversed by year-end. The rebased series determines the employment target, inherited capacity in 2021, and the calibration of rebuilding costs. Model labor productivity is the ratio of matched output to this employment series. Annual-average employment is retained only when constructing the chain-level productivity trend; it is not a second employment target. The index i denotes a tier and c its chain.

Chain-level trends. We compute one annual log trend for each chain aggregate over the relevant observation window:

$$g^{\text{trend}}_{X,c} \;=\; \tfrac{1}{T}\log\!\left(X^{c}_{2017+T}\big/X^{c}_{2017}\right), \qquad T=7 \text{ for } Y,N; \quad T=2 \text{ for } P_{GO},\, W,\, WN,$$

where the chain aggregate sums the chain's three tiers: for Y and N the raw sum; for P_{GO} the implicit deflator $\sum_i P_i^{GO}(t)\,Y_i(t)/\sum_i Y_i(t)$; for W the ratio of the chain wage bill to chain employment; for WN the sum of tier wage bills; and Y/N is computed as $g^{\text{trend}}_{Y,c} - g^{\text{trend}}_{N,c}$. The three tiers of a chain therefore share a trend rate, and rates differ across chains. Each tier's calibration target for year t is the tier's own annual log growth minus its chain's trend. Multi-year excess uses two- or three-year cumulative log changes minus the corresponding multiple of the annual trend.

Applied chain-level trend rates. Annual rates in percent per year, from the BEA and QCEW vintages used in the paper (N after the 2024 anchor shift):

	Y (GO)	N	Y/N	P_{GO}	W	WN
C_1	+4.36	+0.29	+4.08	+0.99	+3.83	+4.12
C_2	+1.01	+1.16	−0.16	+2.08	+3.17	+4.33
C_3	+1.78	+1.27	+0.51	+1.96	+2.16	+3.43
C_4	−0.16	+1.32	−1.48	+1.45	+2.93	+4.25

Exogenous price paths. The exogenous-block paths are detrended on their own pre-COVID 2017–2019 rate, the same convention applied to endogenous tier prices:

$$\varepsilon_e(t) = \log P_e(t) - \log P_e(t-1) - g^{\text{pre}}_e, \qquad g^{\text{pre}}_e = \tfrac{1}{2}\log\!\big(P_e(2019)/P_e(2017)\big),$$

with $g^{\text{pre}}_{RE} = +2.83\%$, $g^{\text{pre}}_{FG} = +2.81\%$, and $g^{\text{pre}}_{EN} = +1.51\%$ per year, corresponding to the real-estate, finance-and-government, and energy blocks. The per-tier import-price shocks $\varepsilon^{IMP}_{i,t}$ are built the same way from BLS import-price indices aggregated to the tier basis. For $t > 2024$, the growth-rate shocks are set to zero, so each detrended exogenous price remains at its 2024 level during the terminal transition.

Fit to the calibration targets. Figure A2 compares the calibrated model's chain-level paths with the detrended targets constructed above. The model closely matches gross output and the gross-output price deflator; employment and labor productivity deviate from their targets in some years.

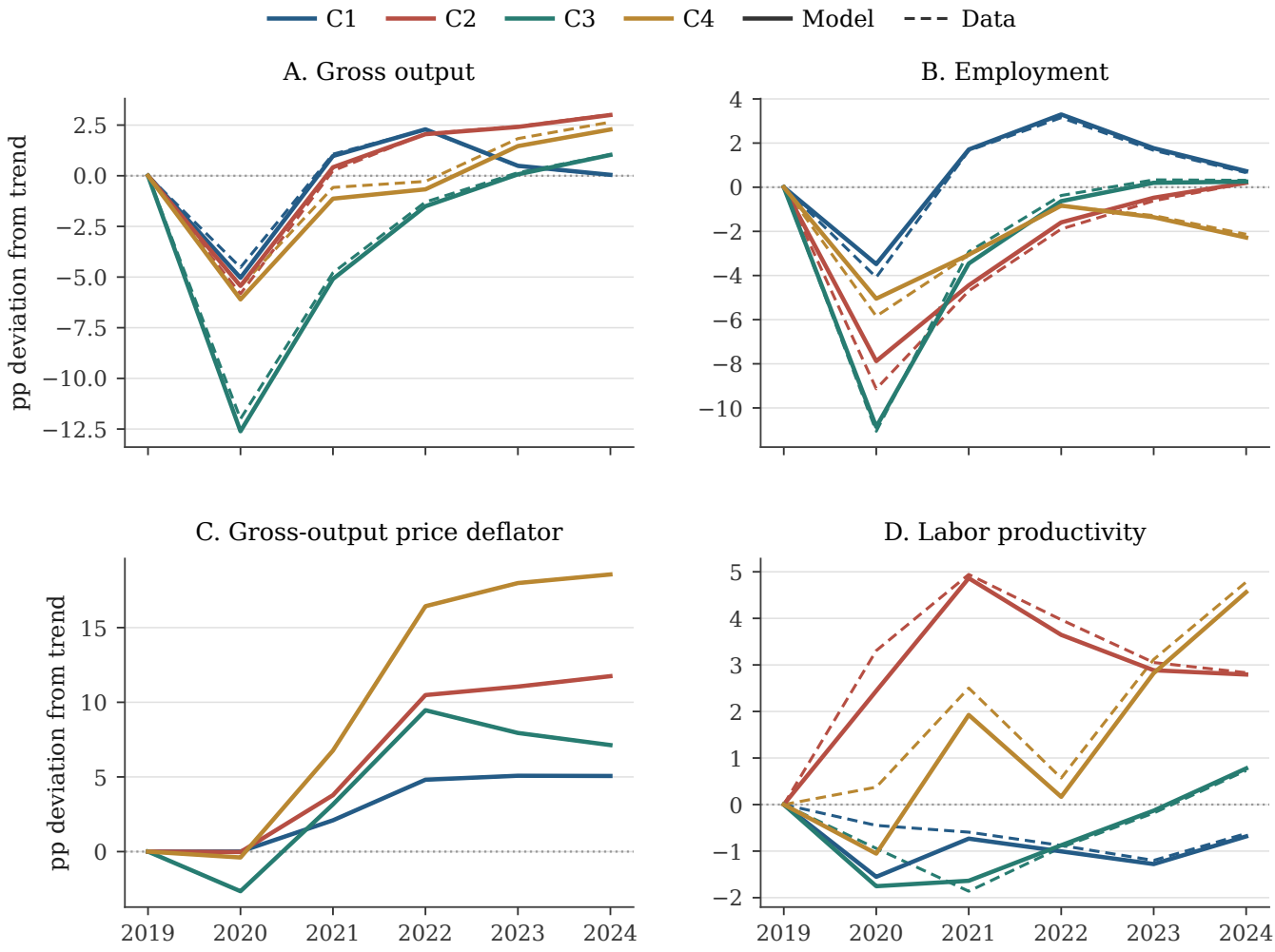

Figure A2: Model fit to the chain-level calibration targets.

Notes: Data (dashed) and model (solid) for chains C_1–C_4 (C1–C4 in the legend), 2019–2024, in pp deviations from trend. Gross output, employment, and labor productivity are detrended over 2017–2024, with employment anchored so that detrended aggregate employment is zero in 2024; the gross-output price deflator is detrended over 2017–2019.

A.7 Price Indices, Input Demands, and Price Setting

This appendix derives the conditional input demands and pricing equation used in Section 3. The index i denotes a chain-by-tier composite, $j \in \{H, S\}$ its hit or safe node, and $t = 1$ the year 2020. Final demand, market clearing, and aggregate prices are defined in the main text.

A.7.1 Price indices and input demands

Cost minimization for the CES tier composite gives its price index and demand for each node's output:

$$P_{i,t} = \left[\sum_{j \in \{H,S\}} s_{ij} P_{ij,t}^{1-\rho} \right]^{1/(1-\rho)}, \qquad \sum_{j} s_{ij} = 1, \tag{A.37}$$

$$Y_{ij,t} = s_{ij} (P_{ij,t} / P_{i,t})^{-\rho} Y_{i,t}. \tag{A.38}$$

Likewise, conditional on the total intermediate-input bundle $m_{ij,t}$, demand for inputs from endogenous supplier tier k and the EXO block is

$$m_{ij,k,t} = \omega_{i,k}(P_{k,t}/p^m_{i,t})^{-\rho} m_{ij,t}, \qquad m^{\text{EXO}}_{ij,t} = \omega^{\text{EXO}}_i (P^{\text{EXO}}_{i,t}/p^m_{i,t})^{-\rho} m_{ij,t}. \tag{A.39}$$

Here $p^m_{i,t}$ is the input price index in equation (9). The weights determine benchmark sourcing, and ρ governs substitution in response to relative prices. The baseline uses the same elasticity for intermediate inputs and for hit and safe output.

A.7.2 Rotemberg pricing

A variety producer $\ell \in [0,1]$ in node (i,j) faces demand

$$y_{ij,t}(\ell) = \left[p_{ij,t}(\ell)/P_{ij,t}\right]^{-\varepsilon_i} Y_{ij,t}, \qquad \Pi_{ij,t}(\ell) = p_{ij,t}(\ell)/p_{ij,t-1}(\ell). \tag{A.40}$$

The elasticity ε_i applies within a node and differs from the across-node elasticity ρ. The price-adjustment cost, measured in node-output units and scaled by node output, is $\Gamma_i(\Pi) Y_{ij,t}$, where

$$\Gamma_i(\Pi) = \tfrac{\bar\phi_i}{2}(\Pi - \bar\Pi)^2 + \tfrac{\lambda_i}{2}[(\Pi - \bar\Pi)^-]^2, \tag{A.41}$$

$$\Gamma_i'(\Pi) = \bar\phi_i(\Pi - \bar\Pi) + \lambda_i(\Pi - \bar\Pi)^-, \qquad x^- \equiv \min\{x, 0\}. \tag{A.42}$$

Let $\mathscr{J}_{ij,t}$ denote the firm's discounted value, distinct from the production composite $V_{ij,t}$. The firm takes the node price $P_{ij,t}$, aggregate node output $Y_{ij,t}$, real marginal cost $MC_{ij,t}$, and pricing wedges as given, and chooses its own price $p_{ij,t}(\ell)$:

$$\begin{aligned}\mathscr{J}_{ij,t}(p_{ij,t-1}(\ell)) = \max_{p_{ij,t}(\ell)} \Big\{ &[p_{ij,t}(\ell)/P_{ij,t} - MC_{ij,t} - \mu^e_{i,t} - \bar\mu^e_i \mathbf{1}\{t=1\}] y_{ij,t}(\ell) \\ &- \Gamma_i(\Pi_{ij,t}(\ell)) Y_{ij,t} + \beta \mathbb{E}_t \mathscr{J}_{ij,t+1}(p_{ij,t}(\ell)) \Big\}.\end{aligned} \tag{A.43}$$

The wedges enter as additive shifts to the pricing incentive. Suppressing the node and variety indices, differentiation uses

$$\frac{\partial y_t}{\partial p_t} = -\varepsilon_i \frac{y_t}{p_t}, \qquad \frac{\partial \Pi_t}{\partial p_t} = \frac{\Pi_t}{p_t}, \qquad \frac{\partial \Pi_{t+1}}{\partial p_t} = -\frac{\Pi_{t+1}}{p_t}.$$

At symmetry, $p_{ij,t}(\ell) = P_{ij,t}$ and $y_{ij,t}(\ell) = Y_{ij,t}$. Multiplying the first-order condition by the current price gives

$$\begin{aligned}0 = &[1 - \varepsilon_i + \varepsilon_i(MC_{ij,t} + \mu^e_{i,t} + \bar\mu^e_i \mathbf{1}\{t=1\})] Y_{ij,t} \\ &- \Gamma_i'(\Pi_{ij,t}) \Pi_{ij,t} Y_{ij,t} + \beta \mathbb{E}_t [\Gamma_i'(\Pi_{ij,t+1}) \Pi_{ij,t+1} Y_{ij,t+1}].\end{aligned} \tag{A.44}$$

Define $\Psi_i(\Pi) = \Pi \Gamma_i'(\Pi)$. Rearranging and dividing by current output yields

$$\begin{aligned}\Psi_i(\Pi_{ij,t}) = \varepsilon_i \left(MC_{ij,t} - \frac{\varepsilon_i - 1}{\varepsilon_i} + \mu^e_{i,t} + \bar\mu^e_i \mathbf{1}\{t=1\} \right) \\ + \beta \mathbb{E}_t \left[\Psi_i(\Pi_{ij,t+1}) \frac{Y_{ij,t+1}}{Y_{ij,t}} \right].\end{aligned} \tag{A.45}$$

This is equation (12). The factor Π arises because firms choose price levels rather than inflation directly. Today's price also changes next period's inflation and hence its adjustment cost, producing the continuation term. Without adjustment costs or wedges, $MC = (\varepsilon_i - 1)/\varepsilon_i$ is the static inverse markup. When $\lambda_i > 0$, local adjustment costs differ on the two sides of the nominal anchor.

A.7.3 Inflation beliefs and quantity forecasts

The baseline combines model-implied future quantities with the aggregate inflation forecast in equation (16). Let $\mathbb{E}_t^s$ denote the subjective pricing operator. With future quantity known along the solved path, it is specified by

$$\mathbb{E}_t^s[\Psi_i(\Pi_{ij,t+1})Y_{ij,t+1}] \equiv \Psi_i(\Pi^e_{t+1|t})Y_{ij,t+1}. \tag{A.46}$$

Dividing by current output gives the operator in equation (15). Firms thus use the same aggregate inflation forecast in each node's pricing equation while retaining node-specific quantity forecasts. Setting $\nu_{\text{forward}} = 1$ makes aggregate inflation perfectly foreseen; it does not make every node's inflation forecast exact unless that node's inflation equals the aggregate forecast.

A.8 Calibration of Model Price Stickiness Parameters

We use the monthly price-change frequencies of Pasten et al. (2020) (PSW) to calibrate the annual Rotemberg parameter $\bar{\phi}$. We first calculate the probability of no price change over a year, then match the local slopes of the Calvo and Rotemberg pricing equations.

To motivate annualization, consider an auxiliary partial-adjustment process in which the desired price moves permanently by one unit and resetting firms immediately choose that target. With monthly reset probability f_m, the aggregate response is $p_t = (1 - f_m)p_{t-1} + f_m$, giving twelve-month adjustment $1 - (1 - f_m)^{12}$. This calculation holds the desired price fixed; it abstracts from the endogenous marginal costs and forward-looking adjustment in the full model.

An annual auxiliary adjustment process with persistence λ_a has first-year adjustment $1 - \lambda_a$. Matching this to the monthly calculation gives the annual non-reset probability

$$\lambda_a = (1 - f_m)^{12}.$$

At zero trend inflation, matching the log-linear Calvo and Rotemberg Phillips-curve slopes maps λ_a to $\bar{\phi}$. Writing the slope as $\kappa = (\varepsilon - 1)/\bar{\phi}$, we obtain

$$\bar{\phi} = (\varepsilon - 1)\,\frac{\lambda_a}{(1 - \lambda_a)\,(1 - \beta\,\lambda_a)}, \qquad \beta = 0.96,\ \varepsilon = 5. \tag{A.47}$$

A larger non-reset probability therefore implies higher adjustment costs and a flatter local price response to marginal cost.

Industry matching. Pasten et al. (2020) report monthly frequencies for 341 industries on the 2007 BEA vintage, whereas our accounts use the 357 industries of the 2017 vintage. We match each 2017 industry to the nearest PSW grouping in six steps: 218 industries match directly on NAICS codes, and 116 are recovered by progressively widening the NAICS or BEA-66 stem (49 within NAICS-4, 34 within NAICS-3, 28 within NAICS-2, 5 within BEA-66), with 2019 QCEW wage-bill weights at every aggregation step. Twenty aggregate or service industries without a PSW counterpart (education and corporate management, repair and personal services, civic and religious organizations, gasoline stations, and the retail, information, construction, and wholesale-and-telecommunications aggregates) are assigned the wage-bill-weighted frequency of a conceptually similar two-digit NAICS sector; the three exogenous government and housing blocks receive a fallback value, which is immaterial because their prices are exogenous. The last column of Table A10 reports, per cell, the number of endogenous industries matched directly.

For each of the model's twelve chain-by-tier cells, we first annualize industry non-reset probabilities and then average them using 2019 QCEW wage-bill shares. In the following equation, c indexes a chain-by-tier cell and s_i is industry i's wage-bill share within that cell:

$$\lambda_a^c = \sum_{i \in c} s_i \, (1 - f_m^i)^{12}. \tag{A.48}$$

Averaging the monthly probabilities before compounding would give a different value, because compounding is nonlinear. Cell $\bar{\phi}^c$ follows from (A.47) evaluated at λ_a^c. Wage-bill shares are the calibration weights; they stand in for the expenditure weights that a price index would strictly require. Table A10 reports per-cell values, with $1 - f_m^c \equiv (\lambda_a^c)^{1/12}$ the effective monthly non-reset probability. The price-stickiness calibration retains an earlier industry-to-cell assignment: 33 industries belong to different cells in the final production-network classification of Appendix A.2. The reported parameters use the retained assignment; changing it would require re-aggregation and a new model solution.

Table A10: Rotemberg adjustment costs from monthly price-change frequencies.

Cell	$1 - f_m^c$	monthly reset freq.	ψ_a	$\bar{\phi} = 4\,\psi_a$	n PSW-exact / total
$C1_h$	0.839	16.1%	0.157	0.63	0/4
$C1_m$	0.906	9.4%	0.629	2.52	10/20
$C1_l$	0.930	7.0%	1.202	4.81	10/19
$C2_h$	0.917	8.3%	0.829	3.32	19/47
$C2_m$	0.877	12.3%	0.324	1.30	5/10
$C2_l$	0.802	19.8%	0.082	0.33	16/20
$C3_h$	0.929	7.1%	1.172	4.69	17/29
$C3_m$	0.906	9.4%	0.629	2.51	16/31
$C3_l$	0.924	7.6%	1.011	4.04	30/41
$C4_h$	0.899	10.2%	0.522	2.09	14/22
$C4_m$	0.880	12.0%	0.348	1.39	52/67
$C4_l$	0.903	9.7%	0.583	2.33	22/31

Notes: Monthly frequencies from Pasten et al. (2020) are mapped by equations (A.48) and (A.47); $\psi_a = \lambda_a^c / [(1 - \lambda_a^c)(1 - \beta\lambda_a^c)]$ and $\bar{\phi} = 4\psi_a$. The model uses the four consumer-facing values and the wage-bill-weighted mean across the eight middle and upstream cells, $\bar{\phi}_{ml} = 2.86$. Industry counts use the classification retained for price-stickiness calibration, described above.

A.9 Inflation Expectations Anchoring Estimates

We use monthly one-year-ahead forecasts from the Cleveland Fed and the Michigan Survey of Consumers to guide the expectations calibration. In this empirical appendix, Π denotes annual inflation in pp, rather than the gross inflation factor used in the model. Let $E_t[\Pi_{t+12}]$ be the observed forecast, Π_t^{past} trailing twelve-month CPI inflation, and Π_{t+12} realized inflation over the following year. We project the forecast on realized future inflation, trailing inflation, and an anchor $\bar{\Pi} = 2\%$, imposing weights that sum to one:

$$E_t[\Pi_{t+12}] = \nu_{\text{forward}}\Pi_{t+12} + \nu_{\text{past}}\Pi_t^{\text{past}} + \nu_{\text{target}}\bar{\Pi} + u_t, \qquad \nu_{\text{forward}} + \nu_{\text{past}} + \nu_{\text{target}} = 1. \tag{A.49}$$

Subtracting the anchor yields the estimated regression,

$$E_t[\Pi_{t+12}] - \bar{\Pi} = \nu_{\text{forward}}(\Pi_{t+12} - \bar{\Pi}) + \nu_{\text{past}}(\Pi_t^{\text{past}} - \bar{\Pi}) + u_t. \tag{A.50}$$

The regression has no intercept. We recover the target coefficient from the adding-up restriction and calculate its standard error using the estimated covariance matrix. Newey–West standard errors with twelve lags allow for overlapping annual observations. The coefficients sum to one but are not restricted to be nonnegative.

The regression uses realized future inflation to summarize how observed forecasts covary with inflation and the anchor. Because future realizations were not known when the forecasts were formed, the coefficients are not structural information weights. CPI is the inflation benchmark because the market inputs to the Cleveland Fed series are CPI based.

Table A11: Inflation-forecast projections with coefficients constrained to sum to one.

Series	Sample	N	$\hat{\nu}_f$	$\hat{\nu}_p$	$\hat{\nu}_t$	R^2	RMSE
Cleveland Fed	**COVID + after (2020–2024)**	59	-0.13	0.28	0.85	0.69	0.47
			(0.03)	(0.02)	(0.02)		
Cleveland Fed	Pre-COVID (2016–2019)	48	-0.04	0.43	0.61	0.12	0.34
			(0.12)	(0.13)	(0.18)		
Cleveland Fed	Full (2003–2024)	263	-0.05	0.25	0.80	0.44	0.50
			(0.04)	(0.03)	(0.04)		
Michigan	COVID + after (2020–2024)	59	0.22	0.45	0.33	0.66	0.56
			(0.04)	(0.04)	(0.04)		
Michigan	Pre-COVID (2016–2019)	48	-0.25	-0.16	1.41	-12.22	0.63
			(0.23)	(0.37)	(0.43)		
Michigan	Full (2003–2024)	263	0.10	0.44	0.46	-0.98	1.04
			(0.09)	(0.10)	(0.10)		
Stability across the surge (splits of the COVID+ window):							
Cleveland Fed	2020-01–2021-12	24	-0.13	0.30	0.83		
			(0.04)	(0.08)	(0.05)		
	2022-01–2024-12	35	-0.22	0.31	0.91		
			(0.14)	(0.04)	(0.10)		
	Δ (late − early)		-0.09	0.01	0.08		
Michigan	2020-01–2021-12	24	0.25	0.30	0.45		
			(0.03)	(0.06)	(0.04)		
	2022-01–2024-12	35	0.27	0.47	0.27		
			(0.20)	(0.04)	(0.16)		
	Δ (late − early)		0.01	0.17	-0.18		

Notes: Adding-up-constrained OLS in equation (A.50), with no intercept, $\bar{\Pi} = 2\%$, and $\hat{\nu}_t = 1 - \hat{\nu}_f - \hat{\nu}_p$. Subscripts f, p, and t denote future inflation, past inflation, and the target; RMSE is the root mean squared error in pp. Parentheses report Newey–West standard errors with 12 lags (or $\min(12, N-2)$ in split samples). Realized inflation is log CPI growth over the previous or following twelve months. The COVID period is split at January 2022. Cleveland Fed forecasts are model-implied (Haubrich et al., 2012); Michigan forecasts are the Survey of Consumers one-year median. CPI source: FRED CPIAUCSL.

Calibration. Table A11 reports the estimates. In the Cleveland Fed post-COVID projection, the coefficient on realized future inflation is negative: $\hat{\nu}_{\text{forward}} = -0.13$ (SE 0.03). The past and target coefficients are 0.28 and 0.85. The full-sample coefficients are −0.05, 0.25, and 0.80, respectively. These estimates motivate an adaptive-anchored approximation, but do not themselves constitute a convex combination. We impose the nonnegative model weights $(0, 0.25, 0.75)$ as a parsimonious calibration, rather than interpreting the projection as evidence that agents disregard information about the future. The alternative anchors $\bar{\Pi} \in \{1.50, 1.75, 2.00, 2.25\}\%$ give past coefficients in $[0.26, 0.33]$; the associated sensitivity outputs are included in the replication package.

Household comparison. The Michigan post-COVID coefficients are 0.22, 0.45, and 0.33. Relative to the Cleveland Fed series, the household projection places less weight on the anchor and more on past and future realized inflation, consistent with differences in expectation formation discussed by Coibion and Gorodnichenko (2012). We use the Cleveland Fed model-implied series for the baseline and the household survey as a comparison. Neither directly measures the expectations of the firms in the production network; the perfect-foresight variant in Appendix A.10.3 assesses a different expectations assumption.

A.10 Quantitative Results: Robustness and Sensitivity

This appendix reports parameter sensitivity, the alternative inflation-expectations regime, and price-dispersion comparisons. Model paths follow one convention throughout. "Model" retains all fitted wedges and the EXO price shocks. "Model $\mu^e = 0$" sets the recovery pricing wedges to zero. "Model $\mu^e = 0$, no EXO" also sets the EXO price shocks to zero. The model floor further sets the rebuilding costs to zero ($\gamma_i = 0$). Every rebuilding (cost-wall) contribution reported here is the difference between "Model $\mu^e = 0$, no EXO" and the model floor, that is, between the wall-on and wall-off paths with the recovery pricing wedges and the EXO price shocks set to zero in both, as in Figure 4.

A.10.1 Parameter sensitivity of the cost-wall contribution

Table A12 reports the cumulative rebuilding contribution through 2021 and its additional contribution over 2021–2023. Each exercise changes a parameter governing substitution, downward price rigidity, rebuilding costs, recalls, or wage indexation. Expectations remain adaptive and anchored. For these exercises, ρ_m denotes substitution between labor and intermediate inputs, ρ_b substitution across intermediate-input composites, and σ_w substitution between hit and safe producers. The baseline sets all three equal to $\rho = 0.39$.

Table A12: Sensitivity of the rebuilding contribution under adaptive expectations.

	Cost wall contribution (pp)	
Experiment	2019–2021	2021–2023 increment
Baseline	+4.11	+0.16
Higher warm-pool floor ($\psi = 0.30$)	+3.20	+0.29
Low cost anchor ($c = 0.10$, $\gamma \times 0.78$)	+3.65	−0.07
All elasticities at 0.5 ($\rho_b = \rho_m = \sigma_w = 0.5$)	+3.57	+0.24
High hit/safe substitution ($\sigma_w = 5$)	+2.10	+0.55
Lower downward rigidity ($\lambda \times 0.5$ per chain)	+3.59	−0.11
High labor–materials substitution ($\rho_m = 0.5$)	+3.92	+0.14
Wage backward indexation off ($\iota_w = 0$)	+4.21	−0.37

Notes: Adaptive-anchored expectations. Entries are differences in cumulative inflation, in pp, between "Model $\mu^e = 0$, no EXO" (wall on) and the model floor (wall off). The second column is the increment over 2021–2023, not the cumulative contribution since 2019. Each row re-solves the model under the indicated parameter change. The high-substitution attribution uses a separately re-fitted economy; Appendix A.10.2 explains this distinction. Other parameters retain their baseline values in Table 3.

Findings. The initial rebuilding contribution is positive in every exercise, but its size varies. Higher recall capacity and a lower hiring-cost target reduce it. In the separately re-fitted high-substitution economy, the contribution through 2021 is approximately half the baseline value. Appendix A.10.2 distinguishes this re-fit from a

change at fixed wedges. Raising all three substitution elasticities to 0.5 has a smaller effect. Lower downward price rigidity also reduces the initial contribution. Removing wage indexation changes the initial contribution little but lowers its subsequent increment. The parameters therefore affect the size and persistence of rebuilding pressure differently.

A.10.2 Unevenness and substitution sensitivity

The importance of uneven capacity also depends on buyers' opportunities to substitute away from constrained producers. We examine two margins: substitution between hit and safe producers within a composite, and substitution across composites in the intermediate-input bundle. Raising across-composite substitution to $\rho_b = 5$, while retaining the baseline's recovered wedges, lowers the rebuilding contribution through 2022 from 4.76 to 3.47 pp. A separately re-fitted economy with higher within-pair substitution, $\sigma_w = 5$, assigns 2.74 pp to rebuilding.[38] These exercises assess sensitivity to the substitution structure. They are not additional components of the unevenness decomposition.

Table A13: Unevenness and substitutability: the cost wall's contribution under alternative configurations.

	Cost-wall contribution (pp)		Share of baseline
	through 2021	through 2022	2022 (%)
Observed losses (baseline)	4.11	4.76	100
Capacity loss even within hit/safe pair	1.83	2.05	43
Higher within-pair substitution ($\sigma_w = 5$)	2.10	2.74	57
Higher across-composite substitution ($\rho_b = 5$)	3.14	3.47	73

Notes: Cumulative rebuilding contributions in pp under adaptive expectations: "Model $\mu^e = 0$, no EXO" (wall on) minus the model floor (wall off), within each economy. The $\sigma_w = 5$ economy is separately re-fitted. The even-capacity and $\rho_b = 5$ experiments retain baseline wedges. The final column divides the 2022 contribution by the baseline value of 4.76 pp. Rows are separate sensitivity exercises, not additive components.

A.10.3 Perfect foresight of aggregate inflation

The baseline uses adaptive-anchored inflation expectations, with weights $(0, 0.25, 0.75)$. The alternative sets $(\nu_{\text{forward}}, \nu_{\text{past}}, \nu_{\text{target}}) = (1, 0, 0)$ in every period, so aggregate inflation is forecast perfectly throughout the transition, including 2020. Other parameters remain at their baseline values, and the structural 2020 and recovery-period pricing wedges are recalibrated to the same targets.

Inflation decomposition. Figure A3 repeats the decomposition of Figure 4 with perfect foresight of aggregate inflation and the baseline recall share $\psi = 0.20$. Rebuilding contributes more in 2021 and less after 2022, while its cumulative contribution through 2022 remains close to the baseline. The model floor is also lower early in the recovery. The same recovered productivity path—about 2% above trend over 2020–2023—reduces costs in both exercises, but forward-looking pricing brings more of this effect into the initial response. The alternative expectation rule thus shifts the response toward the early recovery and reduces subsequent inflation persistence.

[38] The re-fitted economy recovers demand, productivity and pricing wedges anew to match the observed sectoral paths. The fixed-wedge economy is re-solved without recovering those wedges and no longer matches the data. Each reported contribution is the difference between "Model $\mu^e = 0$, no EXO" and the model floor within that economy. At the baseline's wedges, raising σ_w alone does not reduce the contribution, so its reported reduction reflects the re-fit. The even-within-pairs experiment also keeps wedges fixed.

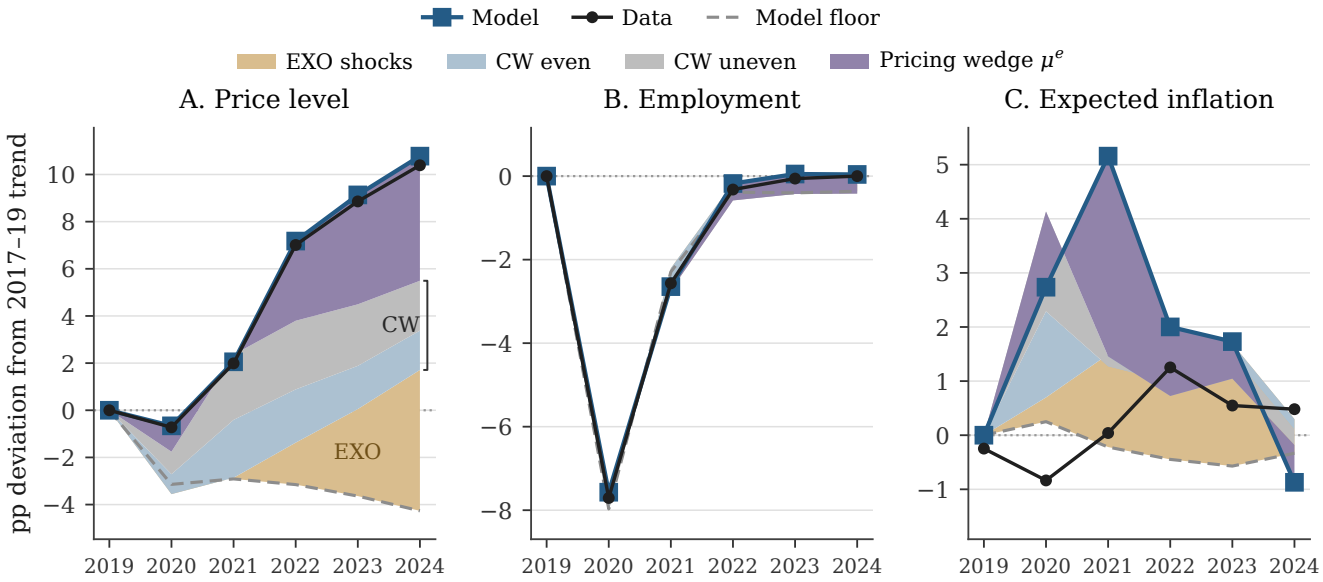

Figure A3: Inflation-by-channel decomposition under perfect foresight (baseline $\psi = 0.20$).

Notes: The variables, detrending, and sequential decomposition are as in Figure 4. Aggregate inflation is forecast perfectly in every period, with $(\nu_{\text{forward}}, \nu_{\text{past}}, \nu_{\text{target}}) = (1, 0, 0)$. The recall share is $\psi = 0.20$ and the rebuilding-cost calibration is unchanged.

A.10.4 Additional price implications

Figure A4 retains the complete demand-shock comparison underlying Panel A of Figure 5. Each point on a curve is the impact response to a separate one-period demand shock from the same steady state, not a successive year of recovery. The observed 2021–2023 points in this supplementary figure are distinct from the model-transition points in the main figure.

Current employment does not determine how far a producer must expand beyond its inherited workforce. A recovery therefore need not follow the impact-response curve obtained from a shock to steady state. The counterfactuals in Section 5.1 evaluate rebuilding along the recovered demand and productivity paths.

Figure A5 compares within-chain price dispersion in two windows. The calibration targets employment-loss dispersion in 2020, not these price variances, although tier prices enter the original accounting fit. In 2019–2021, model dispersion exceeds the data in C_1, is close in C_2, and falls short in C_3 and C_4. In 2021–2023, it exceeds the data in C_1 and falls short in the other chains. The model generates substantial but not uniformly accurate relative-price dispersion.

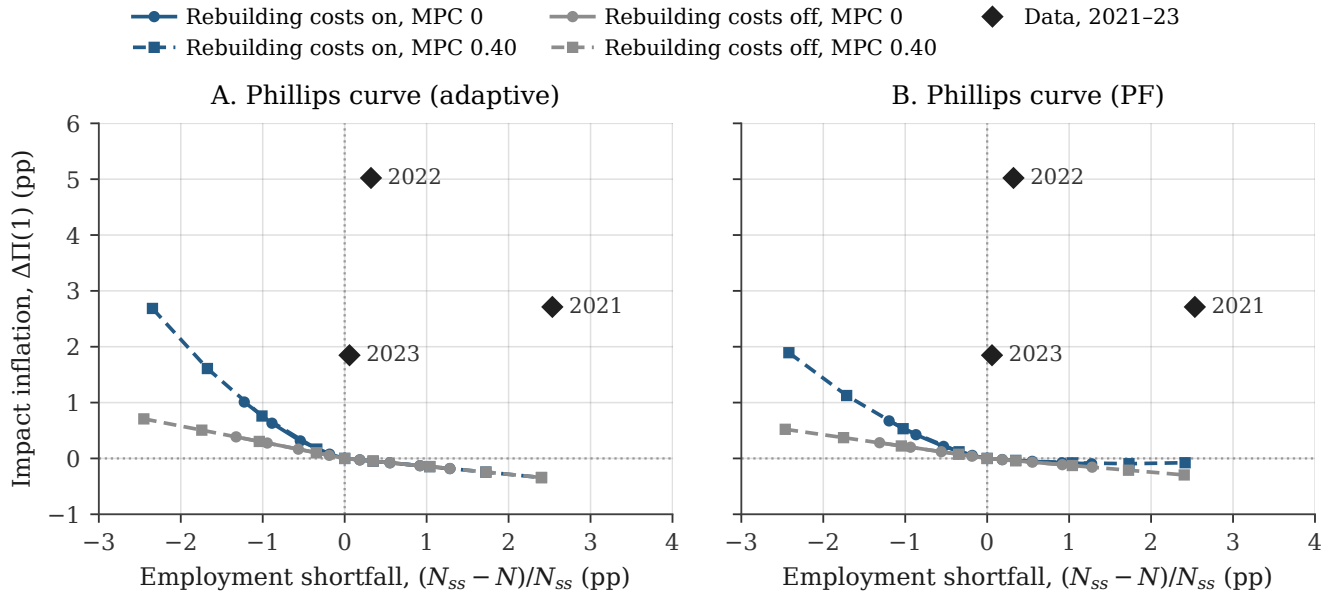

Figure A4: Demand-shock responses under alternative expectations and demand-feedback settings.

Notes: Impact inflation is plotted against the employment shortfall $(N^{ss} - N)/N^{ss}$ in percent. The sweep uses separate pulses $\xi^e \in \{\pm 0.1\%, \pm 0.3\%, \pm 0.5\%, \pm 0.7\%\}$. Blue curves retain rebuilding costs and gray curves set $\gamma_i = 0$. Solid and dashed curves use MPC values of zero and 0.40. The left panel uses adaptive-anchored expectations; the right uses perfect foresight of aggregate inflation. Diamonds are observed 2021–2023 outcomes, not shock-sweep points. The horizontal variable is not an independently identified natural-rate unemployment gap.

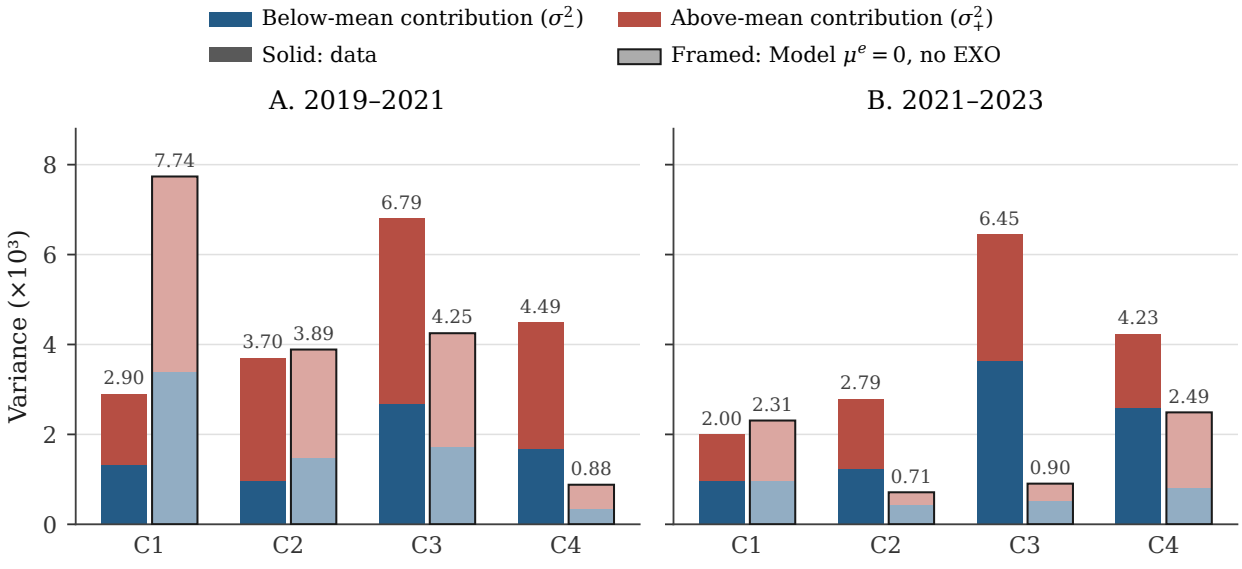

Figure A5: Within-chain price-growth dispersion in two separate windows.

Notes: Variance of cumulative log price changes over 2019–2021 and 2021–2023, multiplied by 10^3 and split into contributions below and above each chain's weighted mean. Data use endogenous BEA detail industries, 2019 nominal gross-output weights, and 1.5-percent winsorization in each tail within chain. The model uses its six nodes per chain on the "Model $\mu^e = 0$, no EXO" path, which sets the recovery-period pricing wedges and the EXO price shocks to zero. Panel A corresponds to the 2019–2021 comparison in Panel C of Figure 5; Panel B reports the separate 2021–2023 window. The two variances are not additive.

A.11 Data Sources

Industry accounts. BEA 2017 producer-price supply–use tables provide benchmark sourcing shares and PCE weights, harmonized to 357 industries. Annual gross-output accounts provide output, value added, and deflators. Price, real-output, and nominal-output changes are calculated from `GO_def`, `GO_index`, and `GO_output`, respectively. Their log changes do not satisfy the price–quantity–value identity exactly. The discrepancy tracks the separate rounding of the source tables, is concentrated in small industries, and is 0.03 pp when weighted by gross output. We retain the supplied series. This source-data discrepancy is distinct from the price–cost decomposition, which adds exactly because its margin component is defined residually. BEA–BLS KLEMS data (63 industries, 1997–2023) supply relative prices and expenditures for estimating ρ. Sources: https://www.bea.gov/industry/input-output-accounts-data, https://www.bea.gov/data/gdp/gdp-by-industry, and https://www.bls.gov/productivity/tables/.

Employment and industry concordances. QCEW employment, payroll, and establishment counts at six-digit NAICS supply the industry employment paths and wage-bill weights: 2017–2024 for the main panel and the model inputs (approximately 1,117 codes) and 2005–2012 for the Great Recession comparison in Online Appendix Figure A7. Census concordances bridge the 2017 and 2022 NAICS classifications. Figure-specific aggregation, matching, timing, and weights are recorded in the list below. Sources: https://www.bls.gov/cew/downloadable-data-files.htm and https://www.census.gov/naics/.

Worker flows. The Census Bureau's Quarterly Workforce Indicators (QWI; LEHD release R2026Q3, schema V4.14.0) supply beginning-of-quarter employment, separations, and recall hires by state and six-digit NAICS industry for private employers (all workers, not seasonally adjusted) for Figure 1. The same release at the four-digit NAICS level, 2017:Q1–2024:Q4, supplies the recall hires and separations used to calibrate ψ in Section 4, and the average monthly earnings of full-quarter jobs (EarnS) and of recent hires that became full-quarter jobs (EarnHirAS) in Online Appendix A.4.3. These four-digit series sum the 48 states and the District of Columbia published in every quarter, which excludes Alaska and Michigan (3.2 percent of 2019 private employment), and are mapped to BEA industries with 2019 private QCEW employment weights. QWI industry codes follow the 2022 NAICS in all years. Recall hires are hires by an employer for which the worker worked in the previous four quarters. Source: https://lehd.ces.census.gov/data/qwi/.

Occupational exposure. The supplementary JEM tabulations of Oude Hengel et al. (2022) supply workplace-exposure scores. BLS ISCO-08/SOC-2010 and SOC-2010/SOC-2018 concordances map them to U.S. occupations; 2019 OEWS employment shares aggregate them to industries. We use the Danish tabulation; Online Appendix A.5 documents the principal-component construction and coverage. Sources: https://www.bls.gov/soc/soccrosswalks.htm and https://www.bls.gov/oes/.

Producer and import prices. Annual-average BLS PPI indices at six-digit NAICS supply dispersion diagnostics and robustness checks. BLS International Price Program indices, mapped through BEA import commodity shares, supply exogenous import prices. Sources: https://www.bls.gov/ppi/databases/ and https://www.bls.gov/mxp/.

Aggregate prices and price adjustment. FRED series `PCEPI`, `PCEPILFE`, `CPIAUCSL`, and `CPILFESL` provide PCE, core PCE, CPI, and core CPI benchmarks (Federal Reserve Bank of St. Louis, FRED; underlying producers BEA and BLS). CPI supplies realized inflation for Appendix A.9. Monthly price-reset frequencies from Pasten et al. (2020) discipline Rotemberg costs; their annualization and industry mapping are in Appendix A.8. Source: https://fred.stlouisfed.org/.

Series used in the figures. The following list records, for each figure that plots data, the underlying series, their identifiers, and the transformations applied. For the model–data comparisons it also records the industry-to-node mapping, weights, employment window, detrending, and model path, which differ across figures. FRED identifiers refer to the Federal Reserve Bank of St. Louis database (https://fred.stlouisfed.org/), which redistributes the BLS, BEA, and Federal Reserve Bank of Cleveland series named below. Monthly series plotted in these figures are converted to quarterly averages.

- *Figure A6 (aggregate inflation, wages, and labor-market indicators).* Panel A: one-year-ahead expected inflation, Federal Reserve Bank of Cleveland model (EXPINF1YR); headline and core CPI, all urban consumers, seasonally adjusted (BLS; CPIAUCSL, CPILFESL), expressed as the inflation rate over the four quarters following the quarter in which the expectation is formed. Panel B: Employment Cost Index, total compensation, all civilian workers (BLS; ECIALLCIV), divided by the CPI, the core CPI, and the core PCE price index (BEA; PCEPILFE), each expressed as the cumulative percent change since 2017Q1. Panel C: prime-age (25–54) employment–population ratio (BLS; LNS12300060), as the percentage-point deviation from its 2019 average, and JOLTS vacancies (JTSJOL) divided by effective searchers, constructed as described below.

- *Figure 1 (employment regained and price dispersion, COVID-19 and the Great Recession).* Panels A and B: QWI state-by-industry cells are summed to national six-digit industries. The sample keeps the 12,926 cells (817 industries in 47 states; about 86 percent of initial employment) that report employment, separations, and recall hires in every quarter of 2005Q1–2012Q1 and 2013Q1–2023Q1 and have positive employment at each initial date; Alaska, the District of Columbia, Massachusetts, and Michigan lack the required coverage. All values used carry QWI status "OK"; suppressed values are excluded. The paper's EXO industries, private households, and the postal service are excluded. Dates: initial 2020Q1 and 2008Q1; the loss window ends at a date fixed one and two years later, 2021Q1 and 2010Q1; the recovery ends at 2023Q1 and 2012Q1. All are first quarters, so no seasonal adjustment is needed. Employment in the sample is lowest in 2020Q3 for COVID-19 and in 2010Q1 for the Great Recession, so the COVID-19 loss is the decline still outstanding at 2021Q1.

  Recall adjustment: for each industry, separations and recall hires are measured in excess of their average in the same calendar quarter of 2018–2019 (2006–2007), and cumulated as running maxima floored at zero, separations through the quarter before the end of the loss window and recalls through the third quarter after it. Their ratio, bounded between zero and one, is the share of excess separations that returned to the same employer. The imputed pool at each date is this share times cumulative excess separations to date less cumulative excess recalls to date, floored at zero; adjusted employment A_{it} is employment plus the pool. The pool is imputed from industry flows, not followed worker by worker. At the end of the loss window it equals 1.0 percent of initial employment for COVID-19 and 0.1 percent for the Great Recession.

  With t_0 the initial date, τ the end of the loss window, T the end of the recovery and $\ell_i = \max(A_{it_0} - A_{i\tau}, 0)$, Panel A is $100 \sum_{i:\ell_i>0}(A_{iT} - A_{i\tau})/\sum_i \ell_i$ in employment counts, so gains beyond an industry's own loss and continued declines both count: 92.5 for COVID-19 and 32.0 for the Great Recession (95.4 and 32.3 without the recall adjustment; 68.9 and 30.7 when each industry's gain is capped at its own loss).

  Panel B: variance across industries of $\log A_{iT} - \log A_{i\tau}$ after 3% winsorization (1.5th and 98.5th unweighted percentiles), split around the weighted mean; weights are the average of each industry's employment shares in 2008Q1, 2016Q1, and 2020Q1. The dashed benchmark applies the same calculation with initial date 2016Q1, loss window ending 2017Q1, and end 2019Q1. Over the loss windows the same variance is 14.7 for COVID-19 and 14.1 for the Great Recession. Paired industry-bootstrap 90 percent intervals (1,000 draws): Panel A difference 60.5 points (45.4–78.1); Panel B ratio 2.52 (1.57–4.05); loss-window variance ratio 1.04 (0.68–1.52).

  Panels C and D: annual log changes in BEA gross-output price indexes for the 341 endogenous industries less a fixed list of 39 commodity-price-linked industries in crop and animal production, meat, dairy, grain and oilseed milling, fertilizers and agricultural chemicals, basic chemicals and petrochemicals, resins and

synthetics, and primary metals (full list in Online Appendix A.2), leaving 302. Weights are nominal gross output in 2019 for every COVID-19 year pair and in 2007 for every Great Recession year pair; each year pair is winsorized at 3% and its variance split around the weighted mean. Each plotted component is the year's component minus its mean over the two annual changes before the episode: 2017–18 and 2018–19 (normal total 0.35) and 2005–06 and 2006–07 (0.67), in the figure's units. Including the commodity-price-linked industries raises the 2020–21 variance from 2.56 to 4.46 and the 2008–09 variance from 1.22 to 3.21.

- *Online Appendix Figure A7 (annual employment and price dispersion, COVID-19 and the Great Recession).* Employment: BLS QCEW national private annual-average employment at six-digit NAICS, 2005–2012 and 2017–2024, weighted by base-year employment (2007 and 2019); year-pairs that cross a NAICS revision keep the industries that map one-to-one in the Census concordances. Prices: BEA detail-level gross-output price indexes (industry accounts), the paper's price variable, for all 341 endogenous detail industries, weighted by base-year nominal gross output. The price sample excludes the paper's EXO industries: selected extractive and refining industries, finance and insurance, real estate, and government. This EXO classification does not include all utilities or every commodity producer. Each bar is the cross-industry variance of annual log changes after 3% winsorization, split into the parts below and above the weighted mean. In Panels C and D, filled bars exclude a fixed list of 39 commodity-price-linked industries, used consistently across the plotted years (5–7% of gross output), and outlines show the all-industry variance. The excluded industries are: crop production (grain, oilseed, vegetable and melon, fruit and tree nut, greenhouse and nursery, and other crop farming; 6 industries), animal production (beef cattle, dairy cattle, poultry and eggs, and other animals; 4), grain and oilseed milling (flour and malt, wet corn, soybean and other oilseed processing, fats and oils, and breakfast cereal; 5), dairy products (fluid milk and butter, cheese, dry and condensed dairy, and ice cream; 4), meat and poultry processing (2), basic chemicals (petrochemicals, industrial gases, dyes and pigments, and other basic organic and inorganic chemicals; 5), resins and synthetic rubber and fibers (2), fertilizer and pesticides (2), and primary metals (iron and steel mills, steel products, aluminum, copper, other nonferrous metals, and foundries; 9).

- *Figure 2 (annual industry inflation accounting).* Annual log growth in BEA gross-output deflators and the four components of equation (2), aggregated with normalized 2017 value-added weights on the 330-industry regression sample. QCEW provides payroll and employment; BEA output supplies labor productivity; benchmark sourcing coefficients and import-price data supply the domestic and imported input contributions. The margin is recovered residually. The components sum to the inflation line before rounding. Exposure regressions use the same industry accounts but compare annualized changes across windows; Appendix A.4.1 reports their timing comparison.

- *Figure A1 (intermediate-input shares).* BEA 2017 supply–use tables at producer prices, aggregated to the chain × tier × hit/safe nodes of Online Appendix A.2.

- *Figure 4 and its appendix variant (Figure A3).* The data paths are the PCE-weighted gross-output price index and employment, built from the BEA detail-level gross-output price indexes and BLS QCEW employment aggregated to the chain × tier nodes and detrended as in Online Appendix A.6; expected inflation is the Federal Reserve Bank of Cleveland one-year-ahead series (EXPINF1YR).

- *Figure 5 (aggregate and relative-price implications).* Panel A reports the adaptive demand-shock responses at MPC = 0.40. Triangles show the model's 2021–2023 transition on the "Model $\mu^e = 0$" path, with the recovery pricing wedges set to zero, not observed data.

  Panel B plots annual inflation and employment shortfalls over 2020–2023 for the data, fitted model, rebuilding path, and model floor. Each path uses its own employment coordinates. Annual inflation is the first difference of the cumulative log price deviation. Data prices are relative to chain-specific 2017–2019 trends; model inflation is relative to the constant-price steady state. The data employment path uses the calibration's detrending and 2024 level normalization, while model employment is relative to its own steady state. The

horizontal axis is therefore a benchmark-relative employment level, not annual employment growth or an independently estimated natural-rate gap. The rebuilding and floor paths retain the structural 2020 pricing wedge; the floor also removes rebuilding costs. The replication files provide coordinates over 2019–2024.

Panel C uses cumulative BEA gross-output price changes from 2019 through 2021. We calculate changes industry by industry, winsorize at the 1.5th and 98.5th unweighted percentiles within each chain, and aggregate using fixed 2019 gross-output weights. Model bars use the six nodes per chain and fixed node PCE weights normalized within chain; model nodes are not winsorized. Both sets of bars split variance around the chain mean, with model bars outlined. Data changes are raw, whereas model prices are relative to steady state. A common chain trend does not affect within-chain variance; industry-specific trend differences in the data are not removed. The three panels depict shock responses, annual trajectories, and cumulative variances, not three estimates of the same Phillips curve.

- *Figure A4 (model Phillips curve).* The 2021–2023 observations use the same aggregate price and employment series as Figure 4, with the employment shortfall measured relative to the steady-state level.
- *Figure A5 (within-chain price dispersion by period, data vs. model).* Data: the BEA detail-level gross-output price indexes of the 341 endogenous industries within each chain (2019 nominal gross-output weights), cumulative log changes over 2019–2021 and 2021–2023, winsorized at 3% within chain. Model: the chain's six nodes on the rebuilding path of Figure 4 with the recovery pricing wedge and the EXO price shocks removed, with the model's node weights. Statistic: the variance of cumulative log changes split around the chain's weighted mean.

Great Recession comparison. Section 5.2.1 uses employment paths mapped to the same four-chain, three-tier, hit/safe structure as the COVID model. The recovery horizons are 2010–2013 and 2021–2024, with 2007 and 2019 as the respective pre-collapse normalizations.

Vacancies per effective searcher. Figure A6 uses the five-group effective-searcher denominator of Heise et al. (2026, Appendix A.3):

$$ES = U_{<27} + 0.48U_{\geq 27} + 0.40N^{\mathrm{MA}} + 0.09\left(N^{\mathrm{NILF}} - N^{\mathrm{MA}}\right) + 0.07N^{\mathrm{emp}}.$$

Here $U_{<27}$ and $U_{\geq 27}$ denote unemployment of less than 27 weeks and at least 27 weeks, N^{MA} denotes marginally attached nonparticipants, N^{NILF} all nonparticipants, and N^{emp} employment. Counts cover persons aged 16 and older. The denominator weights each group by its job-finding rate relative to short-term unemployment; it is the effective-searcher measure, not the paper's fitted wage index. The vacancy numerator uses the JOLTS series rather than the historically spliced vacancy measure in that paper.

We use the FRED vintage of 17 October 2026: UNEMPLOY, UEMP27OV, LNU05026642, LNS15000000, CE16OV, and JTSJOL, in thousands. Short-term unemployment is the published total less long-term unemployment. Most components are seasonally adjusted by their producers. Marginal attachment is adjusted in house using month-of-year ratios to a centered moving average; the quarterly V/ES ratio receives a further quarter-of-year adjustment. Both sets of factors are estimated on 2000–2019 data and applied throughout. Only complete three-month quarters are displayed. The final plotted quarter, 2025Q1, includes an unadjusted CPS population-control break; the break falls after the 2021–2022 reopening period discussed in the text. The series definitions, seasonal factors and break diagnostic are retained in the replication files for Figure A6. This descriptive measure does not replace V/U in the hiring-cost calibration.

A.11.1 Aggregate indicators during the reopening

Figure A6 reports aggregate inflation, compensation, and labor-market indicators. The construction of vacancies per effective searcher is given above. Employment is measured relative to its pre-pandemic level, and the real-compensation series are not adjusted for labor productivity.

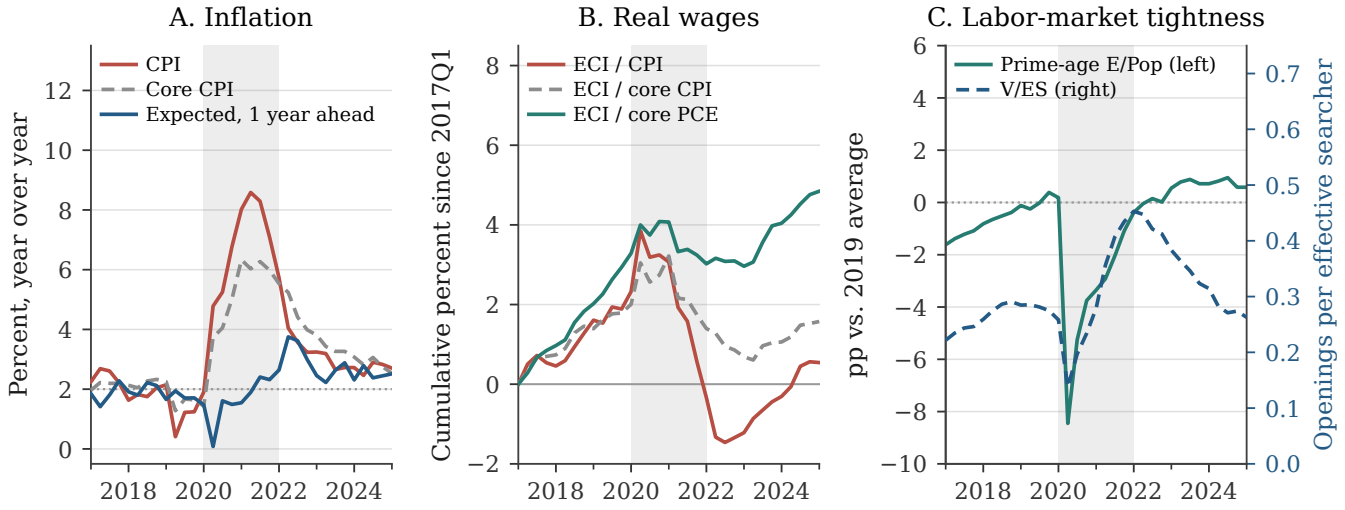

Figure A6: Inflation after COVID.

Notes: Quarterly averages. A: Cleveland Fed one-year-ahead expected inflation and realized headline and core CPI inflation over the following four quarters, dated when the forecast is formed. B: cumulative changes since 2017Q1 in the Employment Cost Index relative to CPI, core CPI, and core PCE. C: prime-age employment–population ratio relative to its 2019 average (left) and JOLTS vacancies per effective searcher, V/ES (right), following Heise et al. (2026, Appendix A.3). Shading marks 2020Q1–2021Q4. The last quarter includes the January 2025 CPS population-control break. Series identifiers, effective-searcher weights, and seasonal adjustment are documented in Appendix A.11. Sources: BLS, BEA, Federal Reserve Bank of Cleveland, and FRED.

Figure A7 reports the cross-industry dispersion of annual employment growth (Panels A and B) and price growth (Panels C and D) around the pandemic and the Great Recession. In Panels C and D, filled bars exclude 39 commodity-price-linked industries and outlines show the variance across all 341 industries. The gap between the outline and the filled bar shows how the measured variance changes when the commodity-price-linked industries are excluded. Outside commodity-price-linked industries, price-growth dispersion in 2020–2021 and 2021–2022 averaged about eight times its 2017–2019 level, whereas it did not rise during the recovery from the Great Recession. These annual QCEW variances differ from the employment measures in Figure 1, which use QWI employment over windows fixed relative to each recession's start (2008Q1 and 2020Q1).

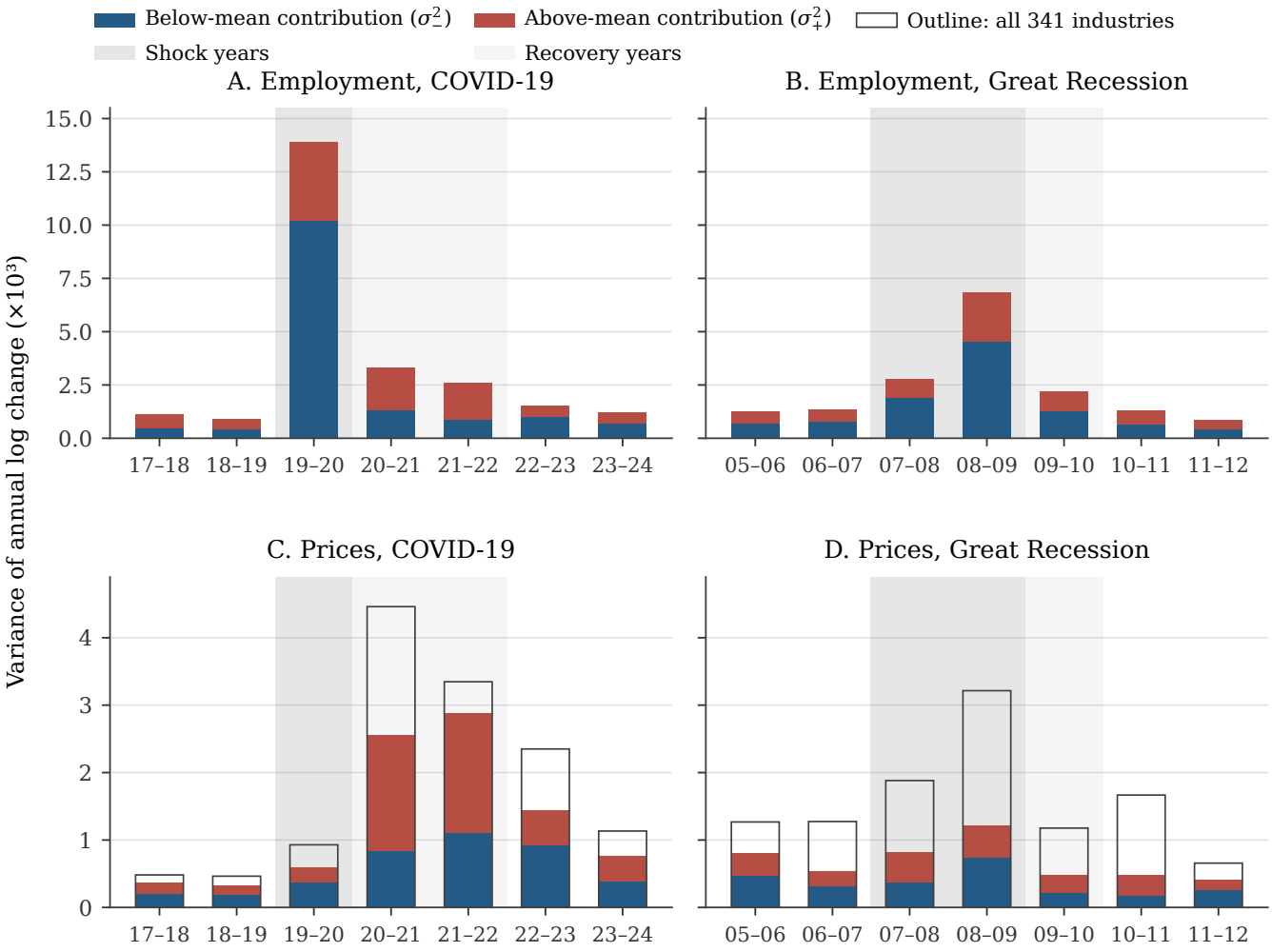

Figure A7: Dispersion of employment growth and price growth: COVID-19 and the Great Recession.

Notes: Bars show the variance of annual log changes across industries, multiplied by 10^3, split into contributions below and above the weighted mean, $\sigma^2 = \sigma^2_- + \sigma^2_+$. Panels A and B use Quarterly Census of Employment and Wages (QCEW) six-digit NAICS-based industry employment, weighted by base-year employment. Panels C and D use BEA's detail-level gross-output price indexes, weighted by base-year gross output, for the 341 industries outside the paper's 16 EXO industries. Filled bars further exclude 39 commodity-price-linked industries (full list in Online Appendix A.2), leaving 302, and outlines show the variance across all 341. Series are winsorized at 3 percent (1.5 percent in each tail). Sources and construction: Online Appendix A.11.